



Pilot Study “ Flash Flood Basins”

Date February 2009

Report Number T23-09-14

Revision Number 1_6_P01

Deliverable Number: D23.3
Due date for deliverable: February 2009
Actual submission date: February 2009
Task Leader: UniPad

FLOODsite is co-funded by the European Community
Sixth Framework Programme for European Research and Technological Development (2002-2006)
FLOODsite is an Integrated Project in the Global Change and Eco-systems Sub-Priority
Start date March 2004, duration 5 Years

Document Dissemination Level

PU Public

PP Restricted to other programme participants (including the Commission Services)

RE Restricted to a group specified by the consortium (including the Commission Services)

CO Confidential, only for members of the consortium (including the Commission Services)

PU

Co-ordinator: HR Wallingford, UK
Project Contract No: GOCE-CT-2004-505420
Project website: www.floodsite.net

DOCUMENT INFORMATION

Title	Pilot study “Flash flood basins”
Lead Author	Marco Borga
Contributors	UniPad, ENPC, WUR, GRAHI-UPC, INPG
Distribution	Public
Document Reference	T23-09-14

DOCUMENT HISTORY

Date	Revision	Prepared by	Organisation	Approved by	Notes
13/05/08	1_0_P23	Marco Borga	UniPad		First draft
05/09/08	1_1_P23	Marco Borga	UniPad		Revised Table of Contents and introduction
06/12/08	1_3_P23	Marco Borga	UniPad	All	Completed first draft
21/01/09	1_4_P23	Marco Borga	UniPad	All	Completed revised draft
20/02/09	1_5_P23	Marco Borga	UniPad		Revised draft ready for Theme leader revision
15/05/09	1_6_P01	J Rance	HR Wallingford		Formatting for publication

ACKNOWLEDGEMENT

The work described in this publication was supported by the European Community’s Sixth Framework Programme through the grant to the budget of the Integrated Project FLOODsite, Contract GOCE-CT-2004-505420.

DISCLAIMER

This document reflects only the authors’ views and not those of the European Community. This work may rely on data from sources external to the members of the FLOODsite project Consortium. Members of the Consortium do not accept liability for loss or damage suffered by any third party as a result of errors or inaccuracies in such data. The information in this document is provided “as is” and no guarantee or warranty is given that the information is fit for any particular purpose. The user thereof uses the information at its sole risk and neither the European Community nor any member of the FLOODsite Consortium is liable for any use that may be made of the information.

© **Members of the FLOODsite Consortium**

SUMMARY

The term "flash flood" identifies a rapid hydrologic response, with water levels reaching a peak within less than one hour to a few hours after the onset of the generating rain event. The time dimension of the flash flood response is linked, on the one hand, to the size of the concerned catchments, which is generally less than a few hundred square kilometres and, on the other to the activation of surface runoff that becomes the prevailing transfer process. Fast surface runoff mainly results from the combination of intense rainfall with steep slopes and/or saturated soils. It also results from anthropogenic forcing such as land use modification, urbanization and fire-induced alteration of the natural drainage system.

The combination of large specific discharges and the short time left for warning, the occurrence at relatively small spatial scale, the local rarity, make the flash flood risk management particularly complex and challenging both in terms of long-term planning and in terms of flood event management. The physical factors which characterise flash floods shape the dimensions of the flash flood vulnerability. This is typically represented by dispersed urbanization, transportation, tourism structures, as well as urbanised areas downstream of small basins (particularly along the Mediterranean coast).

As regards the implementation of risk management measures, the increasing speed of response of a cascade of medium to very small size nested river catchments has two consequences. Firstly, people are exposed individually or in small groups in a diffused manner in space. Second, the more we go to smaller scales, the less they are protected by traditional structural defences aiming to reduce flood volumes and peaks, which are often unsustainable accordingly with the environmental or economic impact. In such circumstances, the only way to protect people is to manage effectively the risk at the event scale. Decision-making about evacuation must be taken before a deadline which becomes progressively shorter when considering smaller catchments. Hence, advancements in hydrometeorological forecasting are absolutely essential to coping with flash floods, particularly as hydrologists, meteorologists, and others strive to increase the accuracy and the lead time of flash flood forecasts. Furthermore, any preparedness measure must be planned well before the event starts, should include knowledge of the local structure of hazard and vulnerability and should incorporate methodologies to learn from past events occurred at the regional scale.

This report focuses on the development and evaluation of a flash flood observational strategy, which aims to provide the basic observational elements for the evaluation (both off line and on line) of the flash flood event risk management proposed by FLOODsite. The flash flood event risk management strategy incorporates the elements developed and evaluated in the Tasks 1, 15 and 16.

Observational flash flood limitations mainly stem from the fact that flash floods develop at space and time scales that conventional observation systems of rain and river discharges are not able to monitor. As these events are locally rare, they are also difficult to capture during classical field-based experimentation, designed to last a few months over a given region. An observational strategy focused on flash flood event is illustrated in this report, considering its two main pillars: the concept of Hydrometeorological Observatory and the methodology for post-event survey.

Flash flood data and observations gathered from the FLOODsite HOs are used to test, both off-line and on-line, the accuracy of flash flood forecasts at ungauged locations offered by the Flash Flood Guidance (FFG) method and a method of model-based threshold runoff computation. This approach requires running the lumped hydrological model to derive flood frequencies at the outlet of the ungauged basin under consideration, and then to derive the threshold runoff from these model-based discharges. This model-based threshold runoff is subsequently used in the forecasting phase when running the model to compute the FFG. The approach provides a pragmatic method to characterize flood severity at ungauged locations. The study examines the potential of this method to account for the hydrologic model uncertainty and for biases originated by lack of model calibration on local conditions.

Finally, geophysical and social flash flood data are used to assess how the current means available for flash-flood monitoring and forecasting can meet the requirements of populations to evaluate the severity of the flood and anticipate its danger. To this end, two well studied flash flood events are examined. The social response time for different social actions in the course of the floods are evaluated, and these are compared to the relevant catchment response time. These afford to reach conclusion pertaining to the characterisation of the social responses according to watershed scale and to the information available, and to the appropriateness of the existing surveillance and forecasting tools to support the social responses identified above.

CONTENTS

Document Information	ii
Document History	ii
Acknowledgement	ii
Disclaimer	ii
Summary	iii
Contents	v
1. Introduction	1
1.1 Structure of the report	2
1.1.1 Part 1: The flash flood observational system	3
1.1.2 Part 2: Validation of the flash flood forecasting platform	3
1.1.3 Part 3: Catchment dynamics and social response during flash floods	4
2. The flash flood observation strategy and the role of the Hydrometeorological Observatories	5
2.1 Introduction	5
2.2 The Cévennes-Vivarais Mediterranean Hydro-meteorological Observatory (OHM-CV), France	6
2.3 The Barcelona Hydrometeorological Observatory, Spain	8
2.4 The north-eastern Italy Hydrometeorological Observatory (LINE)	10
2.5 The Ardenne Hydrometeorological Observatory	12
3. Influence of rainfall spatial resolution on flash flood modelling	13
3.1 Introduction	13
3.2 The Fella 2003 flash flood	15
3.2.1 Post event field campaign	17
3.2.2 Precipitation analyses	18
3.3 Analyses of flood response	19
3.3.1 Analysis of space-time precipitation variability at three catchment scales and at two rainfall resolutions	20
3.4 Influence of rainfall spatial aggregation on peak discharge simulation	23
3.5 Summary and conclusions	26
4. A methodology for post flood field investigations in upland catchments after major flash floods	27
4.1 Introduction	27
4.2 Principles of a methodology	29
4.3 Peak discharge estimation approaches	31
4.4 Discharge estimation checking and validation	32
4.5 Sediment transport or erosion evidences	34
4.6 Illustration of some interpretation results	36
4.6.1 Spatial pattern of peak discharge values: where did the flood generate?	36
4.7 Variability of the rainfall-runoff dynamics: how has the flood been generated?	38
4.8 Conclusions	40
5. Development of a flash food forecasting chain for the Besos catchment in Catalunya	41
5.1 Introduction	41

5.2	Radar rainfall estimation and nowcasting.....	43
5.3	Implications for flood forecasting	46
5.4	Development of a methodology for the redesign of the Catalan raingauge network	47
6.	Flash flood warning in ungauged basins by use of the Flash Flood Guidance and model-based runoff thresholds	50
6.1	Introduction	50
6.2	The Flash Flood Guidance method.....	51
6.3	Description of the hydrological model	51
6.4	FFG computation.....	52
6.5	Threshold flooding conditions.....	52
6.6	Study areas and assessment methodology	52
6.7	Long-term assessment	55
6.7.1	Assessment of the hydrological model	55
6.7.2	FFG assessment	56
6.8	Assessment on three flash flood events	57
6.9	Conclusions and future work.....	62
7.	Catchment dynamics and social response during flash floods: The potential of radar rainfall monitoring for warning procedures	64
7.1	Introduction	64
7.2	Data set used.....	65
7.2.1	Event selection.....	65
7.3	Geophysical parameters.....	65
7.4	Human organisation parameters	66
7.5	Rainfall field variability and catchment dynamics	66
7.6	Characteristics of the social response	68
7.7	Adequateness of monitoring and forecasting techniques at different scales	71
7.8	Conclusions and future research.....	72
7.8.1	Appendix 1:	58
8.	Conclusions and recommendations.....	61
8.1	The flash flood observational system	61
8.1.1	Post event surveys.....	61
8.1.2	Integration of the survey observations by means of hydrological modelling.....	61
8.1.3	Requirements for space-time rainfall observations.....	62
8.2	Assessment of the FFG approach for flash flood forecasting and warning.....	63
8.3	Catchment dynamics and social response during flash floods	64
9.	References	66

Tables

Table 3-1:	Characteristics of the study basins, with catchment area and mean areal cumulated precipitation at four different rainfall resolutions; basin id numbers as reported in Figure 3-1.	23
Table 4-1:	Steps of the proposed data collation and analysis procedures.	29
Table 4-2:	Some examples of maximum peak discharges estimated by the U.S. Geological Survey (Costa, 1987b). Comparison of the unit discharge and of the rainfall intensities	34
Table 6-1:	Main characteristics of the study basins	54
Table 6-2:	Model validation and calibration results on Brenta and Ridanna	55
Table 6-3:	Four-cell contingency table used in the study	56
Table 6-4:	Overall score statistics: threshold runoff computed based on observed data	57

Table 6-5: Overall score statistics: threshold runoff computed based on model simulations	57
Table 6-6: Storm characteristics of the three flash flood events	58
Table 6-7: Flood characteristics of the three flash flood events	58
Table 7-1: Display of the Gard River Case (France). Drainage Area: 2500 km ² . Peak time : 9/09/2002, 18:00 UTC	58
Table 7-2: Display of the Vidourle Case (France). Drainage Area : 620 km ² . Peak Time : 9/09/02, 14:00 UTC	59
Table 7-3: Display of the Valliguières River Case (France). Drainage Area : 93 km ² . Peak Time : 08/09/2002 23:30 UTC	59
Table 7-4: Display of the Fella River Case (Italy). Drainage Area : 20 km ² . Peak time : 29/08/03, 17:00 UTC	60

Figures

Figure 2-1: The network of flash flood pilot areas	6
Figure 2-2: The Cévennes-Vivarais Mediterranean Hydro-meteorological Observatory window.	7
Figure 2-3: The Catalunya Hydro-meteorological Observatory window map showing the deployment of the C-band radar network	9
Figure 2-4: Topographic map of the Barcelona area showing the extension of the Besòs River and its instrumentation	9
Figure 2-5: Radar coverage of the Adige river watershed.	10
Figure 2-6: The Tagliamento river basin.	11
Figure 2-7: The Ardenne Hydro-meteorological Observatory window map	13
Figure 3-1: Location of the OSMER radar and the Fella river basin at Moggio Udinese with topography of North-eastern Italy. The locations of the raingauge stations used in the study are also reported. The dotted line rectangle represents the area used for the analyses of rainfall spatial variability reported in Figure 3-2	16
Figure 3-1: Storm total rainfall (mm) for the August 29, 2003 storm on the Fella river basin at Moggio (basin outlet 10, 623km ²) with the nine study subbasins: Rio degli Uccelli at Pontebba (1, 10.5km ²); Rio Bianco at S. Caterina (2, 17.5km ²); Uque at Ugovizza (3, 24km ²); Aupa at Moggio Udinese (4, 50km ²); Pontebbana at Pontebba (5, 71.2km ²); Fella at S.Caterina (6, 139km ²); Fella at Pontebba (7, 165km ²); Fella at S.Rocco (8, 250km ²) and Fella at Dogna (9, 329km ²).	16
Figure 3-2: Rainfall spatial variability analysis:	17
Figure 3-3: Precipitation analysis for three catchments (Uccelli at Pontebba, 10.5km ² , Fella at S.Caterina, 139 km ² and Fella at Moggio Udinese, 623 km ²), with two different rainfall grid resolutions (1 km and 16 km):	22
mean rainfall intensity [mm h ⁻¹];	22
coverage (for precipitation intensity > 20 mm h ⁻¹);	22
normalized time distance;	22
normalized time dispersion.	22
Figure 3-4: Relationship between the ratio Lr/Lw and a) normalised rainfall error; b) normalised runoff volume error before rainfall volume rescaling; c) normalised runoff volume error after rainfall volume rescaling; d) normalised peak discharge error before rainfall volume rescaling; e) normalised peak discharge error after rainfall volume rescaling.	25
Figure 4-1: Nîmes city (France) on the 3rd of October 1988	27
Figure 4-2: Example of a super-elevation in front of bridge piers located in a river bend and showing a lateral velocity gradient : 0.8 to 1 metre in front of the left bank pile, about 0.5 in front of the central pile and neglectable on the right bank pile. July 2007, Mill Burn, Northumberland, Great-Britain.	33
Figure 4-3: Galeizon tributary reach estimated discharge (45 to 75 m ³ /s) for 3.2 km ² . 1999 floods in the Aude region (France)	35
Figure 4-4: Examples of a shallow slope failure and erosion rills observed on hill slopes after the September 2007 flood on the Selscica Sora basin (Slovenia)	36

Figure 4-5: Estimated specific peak discharges on the Verdoules watershed (300 km ²) after the 1999 floods in the Aude region.	37
Figure 4-6: Specific discharges estimated after the 2002 floods in the Gard region and contour lines of the rainfall amounts (millimetres) received on the 8th and 9th of September 2002.	38
Figure 4-7: Comparison between estimated and simulated discharges for two upstream watersheds in the Aude region after the 1999 floods: (a) Tournissan (10 km ²), (b) Verdoul (18 km ²)	38
Figure 4-8: Comparison between estimated and simulated discharges for two upstream watersheds in the Gard region after the 2000 floods: (a)Crieulon (90 km ²), (b)Vidourle (80 km ²)	39
Figure 5-1: Scheme of the EHIMI warning system	41
Figure 5-2: Comparison of hydrograph results using different rainfall inputs after model calibration (processed radar and raingauge interpolation).	42
Figure 5-3. Comparison of model performances using the DiCHiTop model (left) and the WBrM model (right), after model calibration for multiple events, using different rainfall fields.	42
Figure 5-4. Accumulated rainfall fields during one event registered by the radar of the INM in Barcelona: from 5th of January of 2003 21:30 UTC to 6th of January 07:40 UTC. a) Rainfall field directly obtained from the lowest PPI; b) Rainfall field estimated by applying the proposed VPR correction method; c) Rainfall field obtained by interpolating the data of the rain gauge network. In the legend, “str” refers to stratiform, and “far” refers to further to the predefined 22-km circle from the radar.	44
Figure 5-5. Scattering plots of radar against raingauge accumulated rainfall for the event registered by the radar of the INM in Barcelona: from 5th of January of 2003 21:30 UTC to 6th of January 07:40 UTC. a) Rainfall field directly obtained from the lowest PPI. b) Rainfall field using the proposed VPR correction method; c) Same as (a), but near the radar, where the lowest PPI is below the bright band, the rain rate has been obtained from the lowest PPI. In the legend, “str” refers to stratiform, and “far” refers to further to the predefined 22-km circle from the radar.	45
Figure 5-6. Evolution of the Nash efficiency of the forecasted hydrographs as a function of the anticipation with which hydrographs are simulated (τ). The different lines represent hydrographs simulated with precipitation fields forecasted using different techniques: a) with no forecast; b) by Lagrangian persistence; c) by S-PROG, d) by S-PROG using “updated distributed motion fields”; e) with 2 h of an uniform field with the observed mean areal rainfall, f) with 2 h of actual radar scans.	46
Figure 5-7. Probabilistic rainfall forecasting estimates and its implications in runoff forecasts. Event of 19/07/2001 in the Besos basin. a) Probabilistic rainfall forecasting estimates for 30-min lead time; b) Probabilistic rainfall forecasting estimates for 60-min lead time; c) Probabilistic runoff forecasting estimates for 3 h lead time; d) Evolution of the Nash efficiency of the forecasted hydrographs as a function of the anticipation with which hydrographs are simulated.	47
Figure 5-8. Distributions of the rainfall field error estimation due to different raingauge configurations. a) Independently of the network owner; b) Considering separately the current owner network.	48
Figure 5-9. Final error variance field and regions where installation of new rain gauges is recommended to improve the quality of estimated rainfall fields	49
Figure 6-1: Study basins and their location in Italy	53
Figure 6-2: Storm total rainfall (mm) for the three flash flood events occurred on: a)3-4.10.2006; b)20-21.06.2007; and c)1.11.2004	59
Figure 6-3: Comparison between FFG and rainfall estimates over five rainfall durations (1h, 3h, 6h, 12h and 24h) for four subbasins in the upper Isarco river system and for the two flash flood events occurred on 3-4.10.2006 (a,b,c,d) and on 20-21.06.2007 (e,f,g,h)	61

- Figure 6-4: Comparison between FFG and rainfall estimates over five rainfall durations (1h, 3h, 6h, 12h and 24h) for two subbasins in the upper Brenta river system and for the flash flood event occurred on 1.11.2004 62
- Figure 7-1: Catchment dynamics during the 29 August, 2003 event at three spatial scales: Cucco (0.65 km²), Uqua at Ugovizza (24 km²) and Fella at Pontebba (165 km²). 67
- Figure 7-2: Lag time (in hours) versus drainage area (in km²) for the selected events. The model representing the lower envelop is drawn in dashed line. Gard and Fella events are marked with stars. 68
- Figure 7-3: Representation of 43 elementary human actions in a logarithmic plot of their anticipation time (i.e. time of action before the flow peak) versus the area of the watershed where they occurred. Three types of actions (Fig. 3a) as well as three types of sizes of human groups (Fig. 3b) are distinguished by the shape of each point representing a elementary action. 69
- Figure 7-4: Representation of 43 elementary human actions in a logarithmic plot of their anticipation time versus the area of the watershed where they occurred. Three levels of organisation of the actors are distinguished by the different dot shapes. The bottom line of the shaded area represents the relationship between the catchment lag-time and its drainage area. The upper line is distant of Log 2 from the bottom line and qualitatively indicates the characteristic duration of the generating rain event 71

1. Introduction

The term "flash flood" identifies a rapid hydrologic response, with water levels reaching a peak within less than one hour to a few hours after the onset of the generating rain event (Creutin and Borga (2003); Collier (2007), Younis et al. (2008)). The time dimension of the flash flood response is linked, on the one hand, to the size of the concerned catchments, which is generally less than a few hundred square kilometres and, on the other to the activation of surface runoff that becomes the prevailing transfer process. Fast surface runoff mainly results from the combination of intense rainfall with steep slopes and/or saturated soils. It also results from anthropogenic forcing such as land use modification, urbanization and fire-induced alteration of the natural drainage system.

The combination of large specific discharges and the short time left for warning, the occurrence at relatively small spatial scale, the local rarity, make the flash flood risk management particularly complex and challenging both in terms of long-term planning and in terms of flood event management. The physical factors which characterise flash floods shape the dimensions of the flash flood vulnerability. This is typically represented by dispersed urbanization, transportation, tourism structures, as well as urbanised areas downstream of small basins (particularly along the Mediterranean coast).

As regards the implementation of risk management measures, the increasing speed of response of a cascade of medium to very small size nested river catchments has two consequences. First, people are exposed individually or in small groups in a diffused manner in space (Montz and Grunfest, 2002; Drobot and Parker, 2007). Second, the more we go to smaller scales, the less they are protected by traditional structural defences aiming to reduce flood volumes and peaks, which are often unsustainable accordingly with the environmental or economic impact. Ruin *et al.* (2008) show that, during the September 2002 storm in the Gard region, almost half of the casualties occurred on watersheds of ca. 10 km² and impacted drivers on ill-protected secondary roads and campers. In such circumstances, the only way to protect people is to manage effectively the risk at the event scale. Decision-making about evacuation must be taken before a deadline which becomes progressively shorter when considering smaller catchments. Thus, the warning procedure, that converts perceived or forecasted signals into hazard evaluation and action (Créton-Cazanave *et al.*, 2009), must be completed within a unusually short delay after the onset of the storm (Montz and Grunfest, 2002).

Hence, advancements in hydrometeorological forecasting are absolutely essential to coping with flash floods, particularly as hydrologists, meteorologists, and others strive to increase the accuracy and the lead time of flash flood forecasts. However, a focus on advances in hydrometeorological forecasting alone will not be sufficient to reduce casualties and damages. Because flash flood events usually come as surprises, warning and preparation are essential. However, the time available for communication is very limited and typically there is no time for learning as the flood develops. Therefore, any preparedness measure must be planned well before the event starts, should include knowledge of the local structure of hazard and vulnerability and should incorporate methodologies to learn from past events occurred at the regional scale.

Whereas progress has been made in the last decade in the integration of meteorological forecasts and radar observations in flash flood surveillance, lack of observations hamper advances on understanding the hydrological processes at work during flash floods, and, consequently, on forecasting the stream response to extreme precipitations. Process understanding is required for flash flood forecasting, due to the fact that the small basins prone to flash-floods are rarely gauged and must be modelled without prior calibration. Furthermore, the dominant processes of runoff generation may change with the increase of storm severity, and therefore the understanding based on analysis of moderate flood events may be questioned when applied to forecast the response to extreme storms. In this sense, flash flood forecasting exemplifies the ungauged basin problem under extreme conditions.

Observational limitations mainly stem from the fact that flash floods develop at space and time scales that conventional observation systems of rain and river discharges are not able to monitor. As these events are locally rare, they are also difficult to capture during classical field-based experimentation, designed to last a few months over a given region (e.g., Mesoscale Alpine Programme, MAP). This also explains why a coherent picture of flash flooding in the various European hydroclimatic regimes is still missing.

Due to these limitations, no established verification system exists to check the accuracy of flash flood forecasting techniques; beside this, the existing knowledge on flash flood events across Europe is relatively sparse.

Improvement of flash flood forecasting and warning requires therefore the development of an observation and monitoring strategy capable to provide the essential observational elements to both advance the understanding of the hydrometeorological processes at work during flash floods, and to validate the effectiveness of the flash flood forecasting and warning systems. The roadmap to provide these observations is based on the development of the concept of the Hydrometeorological Observatory and of the methodology for post-event survey, capable to provide high-resolution data on storm and stream/landscape response during flash floods. Synergic to these developments is the identification of the requirements for the effective monitoring of flash flood events.

The Hydrometeorological Observatory (HO) concept identifies a region where flash flood can be observed wherever they occur and not only in places where refined observation system actually exists. To ensure this observational capability, the following characteristics are required: availability of good quality radar data; availability of good quality and relatively dense conventional hydrometeorological data; capability to execute intensive post-event field surveys. To develop the observational strategy, the HO links together hydrometeorological monitoring services, operational forecasting centres and research centres.

On the domain of the Hydrometeorological Observatories, intensive post event campaigns need to be carried out immediately after event and will complement more conventional flash flood data collection. Physical parameters like water levels, velocities, overflowing, and patterns of landsliding/erosion and deposition should be derived from terrain observations, video movies and/or witness observations. The effective execution of intensive post event campaigns requires the development of a comprehensive methodology for organising, executing and summarising the field activities.

This report focuses on the development and evaluation of a flash flood observational strategy, which aims to provide the basic observational elements for the evaluation (both off line and on line) of the flash flood event risk management proposed by FLOODsite. The flash flood event risk management strategy incorporates the elements developed and evaluated in the Tasks 1, 15 and 16.

1.1 Structure of the report

Given the objectives stated in the Introduction, the structure of the report is articulated into three major Parts. The first Part is focused on the structure of the flash flood observational system, which includes the Hydrometeorological observatories and the methodology for post event survey. A subsection is devoted to the analysis of the resolution requirements for flash flood modelling. The second Part is focused on the use of the observations gathered by means of the observational system to investigate the strengths and limitations of the flash flood forecasting and warning platform developed in Tasks 15 and 16, both off line and on line. A final Part is devoted to the analysis of catchment dynamics under flash flood forcing and to the examination of the response social time.

1.1.1 Part 1: The flash flood observational system

Section 2 provides a description and structure of the Hydrometeorological observatories developed in the frame of FLOODsite. The common objective of the HO is to observe flash flood by combining:

- conventional hydrometeorological monitoring;
- weather radar observations;
- complementary information acquired from field surveys executed during the days following the event.

Section 3 illustrates the methodology developed in FLOODsite for the post event survey. Post event field surveys mainly focus on river flood discharges at small scales, compensating the usual lack of runoff data (due to sparsity of the hydrometric network and to its fragility during extreme flood events). Physical parameters like water levels, velocities, overflowing, and patterns of landsliding/erosion and deposition should be derived from terrain observations, video movies and/or witness observations.

Section 4 is focused on the analysis of the required space-time rainfall resolution for effective flash flood analysis. High resolution radar rainfall fields and a distributed hydrologic model are used to evaluate the sensitivity of flash flood simulations to spatial aggregation of rainfall at catchment scales ranging from 10.5 km² to 623 km². The case study focuses on the extreme flash flood occurred on August 29, 2003 on the eastern Italian Alps. Four rainfall spatial resolutions are considered, with grid size equal to 1-, 4-, 8- and 16- km. The influence of rainfall spatial aggregation is examined by using the flow distance as a spatial coordinate, hence emphasising the role of river network in the averaging of space-time rainfall. Effects of rainfall spatial aggregation are quantified by using a dimensionless parameter, represented by the ratio of rainfall resolution (L_r) to the characteristic basin length (L_w), taken as the square root of the watershed area.

1.1.2 Part 2: Validation of the flash flood forecasting platform

Section 5 is devoted to the presentation of a system for distributed flash flood warning developed for a Mediterranean catchment in Spain. The Section reports on three main aspects: 1) Visualization tools, evolving to a more easy-to-use and easy-to-interpret platform; 2) Modularisation of the system, related to the optimisation of the computations in the server, improvements in real-time data acquisition and storage, and operational radar data management and processing; 3) New capabilities and processed information offered to the decision makers, synthesizing spatially distributed warnings over the catchment.

Section 6 investigates the use of the Flash Flood Guidance method and a method of model-based threshold runoff computation to improve the accuracy of flash flood forecasts at ungauged locations. The methodology proposed in this study requires running the lumped hydrological model to derive flood frequencies at the outlet of the ungauged basin under consideration, and then to derive the threshold runoff from these model-based discharges. The study examines the potential of this method to account for the hydrologic model uncertainty and for biases originated by lack of model calibration, which is the typical condition in ungauged basins. Experiments to validate this approach involve the implementation of a semi-distributed continuous rainfall-runoff model and the operation of the FFG method over four basins located in the central-eastern Italian Alps and ranging in size from 75.2 km² to 213.7 km². The model is calibrated on two larger basins and the model parameters are transposed to the other two basins to simulate operations in ungauged basins. The FFG method is applied by using the 2-yr discharge as the threshold runoff. The threshold runoff is derived both by using local discharge statistics and the model-based approach advocated here. Examination of the results obtained by this comparison shows that the use of model-based threshold leads to improvements in both gauged and ungauged situations. Overall, the Critical Success Index (CSI) increases by 12% for gauged basins and by 31% for ungauged basins by using the model-based threshold with respect to use of local data. As expected, the increase of CSI is more remarkable for ungauged basins, due to lack of local model calibration and the greater likelihood of occurrence of a simulation bias in model application over

these basins. This shows that the method of threshold runoff computation provides an inherent bias correction to reduce systematic errors in model applications to ungauged (and gauged) basins.

1.1.3 Part 3: Catchment dynamics and social response during flash floods

Section 7 is the conclusive Section of the Report. The study examines how the current techniques for flash-flood monitoring and forecasting can meet the requirements of the population at risk to evaluate the severity of the flood and anticipate its danger. To this end, the study identifies the social response time for different social actions in the course of two well studied flash flood events which occurred in France and Italy. The study introduces a broad characterization of the event management activities into three types according to their main objective (information, organisation and protection). The activities are also classified into three other types according to the scale and nature of the human group involved (individuals, communities and institutions). The conclusions reached relate to i) the characterisation of the social responses according to watershed scale and to the information available, and ii) to the appropriateness of the existing surveillance and forecasting tools to support the social responses. Study results suggest that representing the dynamics of the social response with just one number representing the average time for warning a population is an oversimplification.

Indications for future works are reported as general conclusion of the report.

2. The flash flood observation strategy and the role of the Hydrometeorological Observatories

2.1 Introduction

The development of a specific '*flash flood observation strategy*' is motivated by the recognition that flash floods develop at space and time scales that conventional observation systems of rain and river discharges are not able to monitor. As these events are locally rare, they are also difficult to capture during classical field-based experimentation, designed to last a few months over a given region (e.g., Mesoscale Alpine Programme, MAP) (Creutin and Borga, 2003).

A fundamental element in the FLOODsite '*flash flood observation strategy*' is the development of the concept of Hydrometeorological Observatories (HOs). These are existing cooperative structures, linking together hydrometeorological monitoring services, operational forecasting centres and research centres. The common objective of the HO is to observe flash flood by combining:

- conventional hydrometeorological monitoring;
- weather radar observations;
- complementary information acquired from field surveys executed during the days following the event.

Post event field surveys mainly focus on river flood discharges at small scales, compensating the usual lack of runoff data (due to sparsity of the hydrometric network and to its fragility during extreme flood events) (Borga et al., 2007). Flash floods being locally rare events, an observation strategy needs to be developed and implemented at the European scale.

The **FLOODsite** network of HOs (called herewith *flash flood pilot areas*) is designed to provide a methodology to develop a database of flash flood events over a variety of hydroclimatic regions across Europe. The network includes the following four HOs, all placed in regions of high flash flood potential:

- Catalunya HO (Spain) (Mediterranean region);
- Cevennes-Vivarais HO (France) (Mediterranean region);
- North-eastern Italy HO (Italy) (Alpine Mediterranean region);
- Ardenne HO (Transnational).

These HOs are characterised by a good density of hydrometeorological stations and by a reliable weather radar coverage. All these observatories are already operational, and incorporate considerable detailed information about flash floods observed in the last decade.

Some key elements of the observational strategy, such as the post event field campaigns and the monitoring programs, have been already tested in the Catalunya HO (e.g. the Barcelona flash flood of October 2005), in the Cevennes-Vivarais HO (e.g. the Gard flash flood of September 2002) and in the North-eastern Italy HO (e.g. the Val Canale flash flood of August 2003). Based on this substantial experience, the observational strategy can be implemented in a fast and efficient way across the HOs network.

Due to the considerable richness in past hydrometeorological data, the HOs network afford to gain essential insight into flash flood hydroclimatology, i.e. to analyse these floods from the perspective of the temporal context of their history of development and variation and the spatial context of the local, regional and global atmospheric and hydrologic processes and circulation patterns from which flash floods develop. This approach is essential when considering the potential effect of future and on-going climate change on flash flood regimes and on flash flood risks.

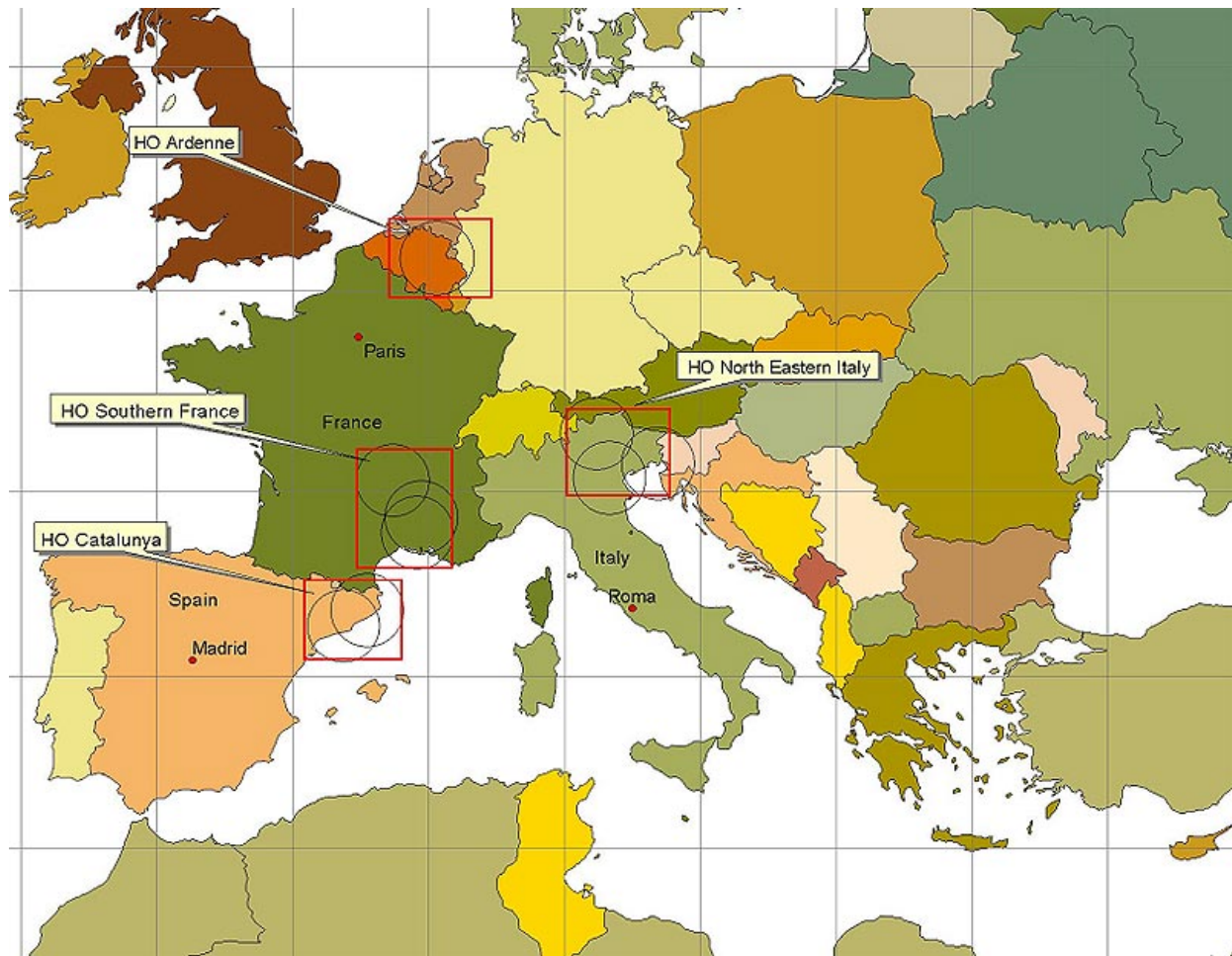


Figure 2-1: The network of flash flood pilot areas

2.2 The Cévennes-Vivarais Mediterranean Hydro-meteorological Observatory (OHM-CV), France

The OHM-CV initiative (<http://www.lthe.hmg.inpg.fr/OHM-CV/index.html>) started in 2000 and has received the label of "Environment Research Observatory" (ORE is the French acronym) from the Ministry of Research in 2002. One of the OHM-CV objectives is to develop a hydrometeorological laboratory in the Cévennes-Vivarais region, described hereafter.

Figure 2-2 presents the general view of the OHM-CV (radar, rain gauges) and a short description of the region (topography, geology) that is regularly prone to flash floods especially in autumn. The Cévennes-Vivarais HO covers an area of 160 x 200 km² in the south-eastern part of the French Massif Central. Many villages and several small to medium-sized towns exist in the region. The main city, Nîmes, has a population of 200 thousand inhabitants.

The area is subject to particularly severe flash flood events. The topography of the area ranges from sea level in the south to a maximum height of 1699 m above sea level at Mount Lozère. The main Cévennes rivers (Cance, Doux, Eyrieux, Ardèche, Cèze, Gard and Vidourle) are right bank tributaries of the Rhône river with a typical Mediterranean hydrological regime (i.e. very low water levels during the summer with floods occurring mainly during the autumn). They are characterised by steep slopes in the head tributaries of the Cévennes Mountains.

In terms of geology, the mountainous part of the region (generally in the north-west of the pilot area) corresponds to the Primary era formations of the Massif Central (granite, schists), while sedimentary

and detrital formations dominate in the Rhône valley region (south-eastern part of the pilot area) with, in places, karstified limestone.

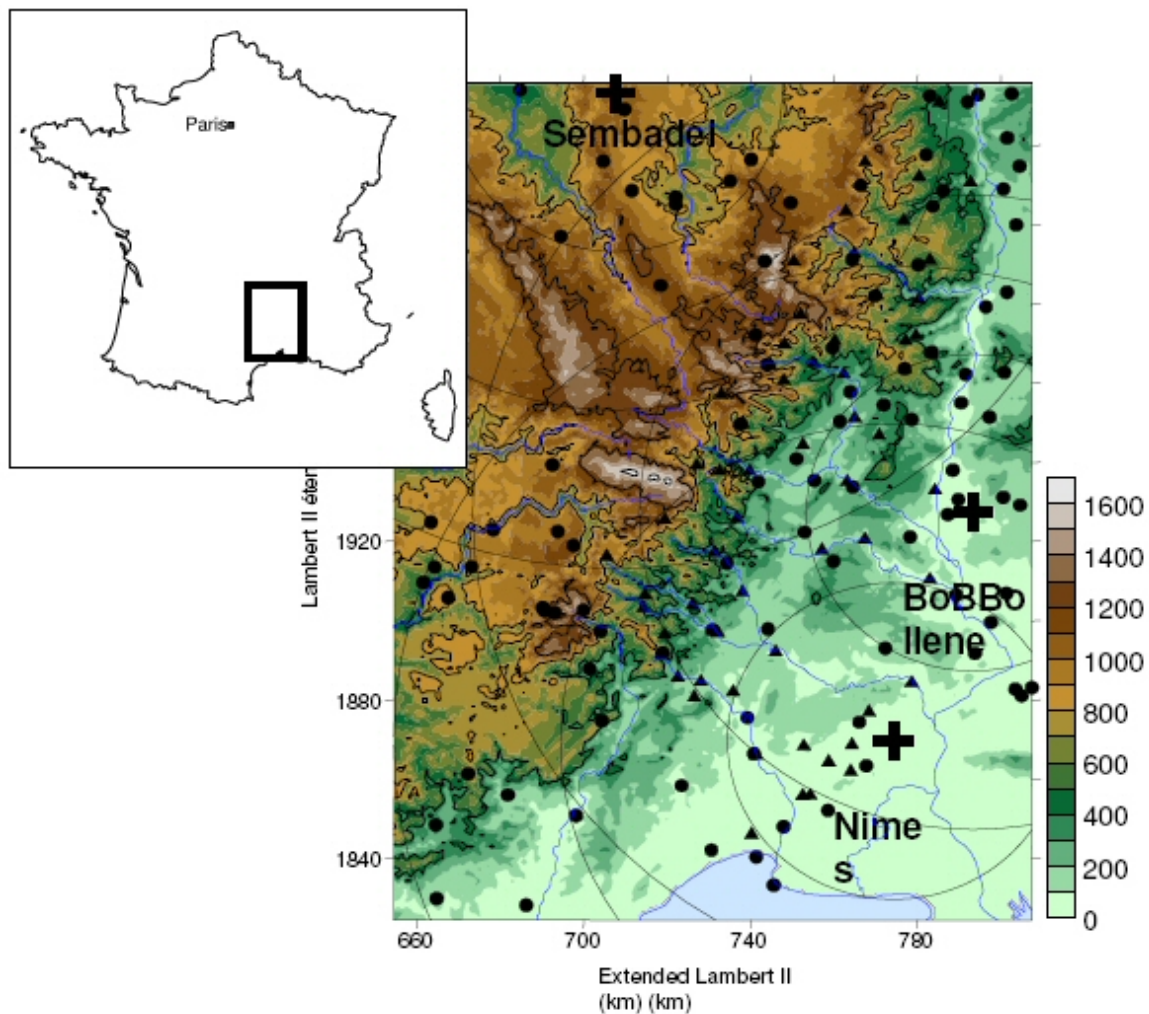


Figure 2-2: The Cévennes-Vivarais Mediterranean Hydro-meteorological Observatory window.

Several historical major floods (Jacq, 1994; Deblaere and Fabry, 1997) can be mentioned: 1858, 1933, September 1958 (Cévennes region), October 1988 (Nîmes), September 1992 (Ardèche area), September 2002 (Gard region), and December 2003 for all the right bank tributaries of the Rhône River.

The punctual 10 year return period rainfall is greater or equal to 50 mm and 200 mm for the hourly and daily time steps, respectively, over most of the region (Bois et al., 1997). Two Cévennes hydrological watersheds (Gardon d'Anduze river at Anduze 550 km² and the Ardèche river at Vogüé 635 km²) were especially studied in the last three decades and may continue to be used as reference basins for detailed research projects. The problem of prediction on un-gauged (or poorly gauged) basins is particularly acute in this region and should be addressed specifically.

This region is already well instrumented with operational observation systems. Nevertheless, the operational instrumentation is managed by several weakly connected meteorological and hydrological services having their own metrological objectives and practices.

Three weather radar sites are indicated in Figure 2-2 and the 40 km range indicators. The black circles and triangles give the locations of the hourly rain gauge network. Within the 160 x 200 km² Cévennes-Vivarais window, the observation system is comprised at the moment of: (i) three weather radars of the Météo-France ARAMIS network located at Nîmes (S-band), Bollène (S-band) and Sembadel (C-band), (ii) two networks of about 400 daily rain gauges and 160 hourly rain gauges and (iii) a network of about 45 water level stations.

2.3 The Barcelona Hydrometeorological Observatory, Spain

The region of Catalunya (Spain) (Figure 2-3) is located in the North-East of the Iberian Peninsula and covers a surface of 32000 km² showing a marked orography characterized by the increasing altitude of the terrain from the sea to the inner regions. Three major mountain chains can be distinguished. The first two are parallel to the coast (rising up to 500 and 1700 m asl), and are located inside a strip of terrain at less than 40 km from the sea. These mountains act as a barrier that induces the convection of humid air coming from the sea, favouring the generation and growth of precipitation. The third mountain chain (the Pyrenees) is located at the North, and exhibits the highest elevations of the region (up to 3400 m).

The mean annual rainfall over the region is about 600 mm. However, one third of the annual precipitation can usually fall in less than 48 hours. In average, two events exceeding 100 mm/day are recorded every year and the return period for events over 200 mm/day somewhere in Catalunya is two years.

This region is drained by a set of coastal rivers. Many of them cross densely urbanised and industrialised zones. Among them, the Besòs River and the Llobregat River pass north and south, respectively, of the conurbation of Barcelona (more than 3 millions of inhabitants). This area and its surroundings is the most vulnerable from the socio-economical point of view. It is also the best covered by the current radar network.

Of special interest is the Besòs watershed (1020 km², Figure 2-4) which was affected in 1962 by a catastrophic flood event that caused about 800 casualties and exceptional economical damages. During last decades, the river bed has been degraded and canalised by means of big concrete protection structures. Considerable EU and Spanish investments have been devoted in recent years to rehabilitate this area into a modern urban sector and create a fluvial park. The city of Barcelona organizes in 2004 an International Forum of the Cultures in a newly urbanised area precisely built in the Besòs river delta.

The radar observation network (Figure 2-3) allows a remarkable coverage of the Barcelona area and its main coastal rivers. The 1962 event made the Besòs watershed to be extensively instrumented and studied in recent years with exceptional hydrological time series compared to the Spanish standards (Figure 2-4). The creation of the fluvial park in Barcellona has motivated the development of a flood forecasting centre operated by CLABSA (the Sewer Management Company of Barcelona City). CLABSA has implemented new instruments (stage record stations) and control structures (inflated dams) along the park. Up to now this system relies on very simple hydrometeorological models, and the warning thresholds are based on conservative assumptions, but research efforts are made to improve this system. An on-line alert system based on hydro-meteorological data and hydrological models is being developed to monitor and forecast the combination of the flows coming from the semi-urbanised Besòs basin and the flows produced by the urban drainage network of the City.

The Hydrometeorological Observatory of Catalunya, and more specifically the Besòs River Project, is supported by CLABSA (Clavegueram de Barcelona, S.A.), the SMC (Servei de Meteorologia de Catalunya) and the ACA (Agència Catalana de l'Aigua).

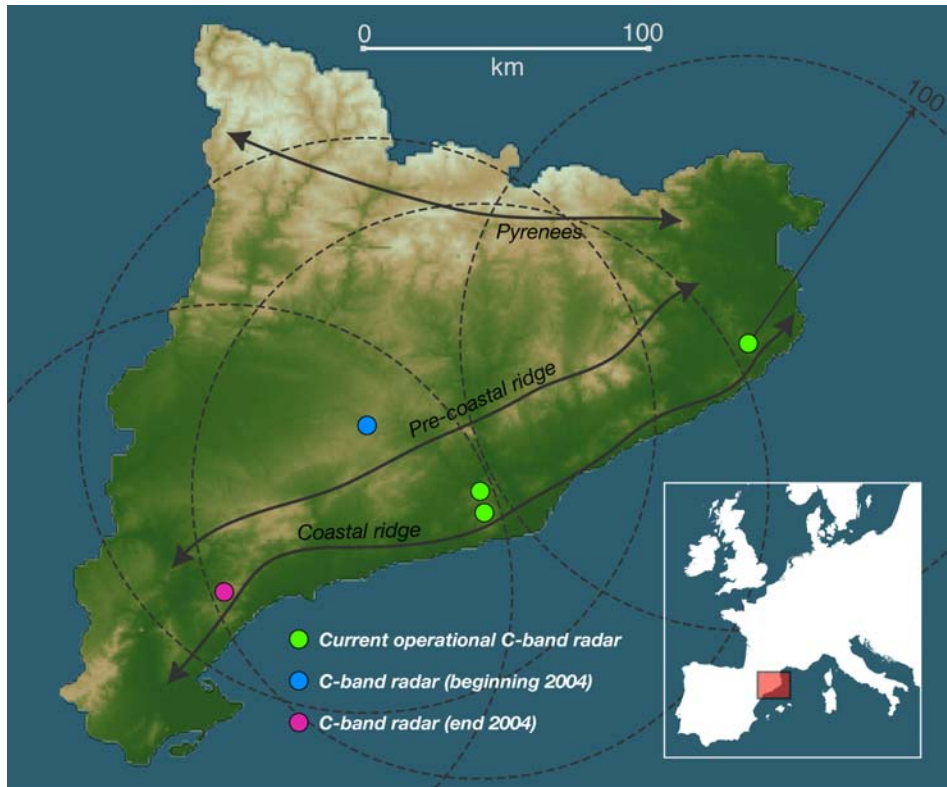


Figure 2-3: The Catalunya Hydro-meteorological Observatory window map showing the deployment of the C-band radar network

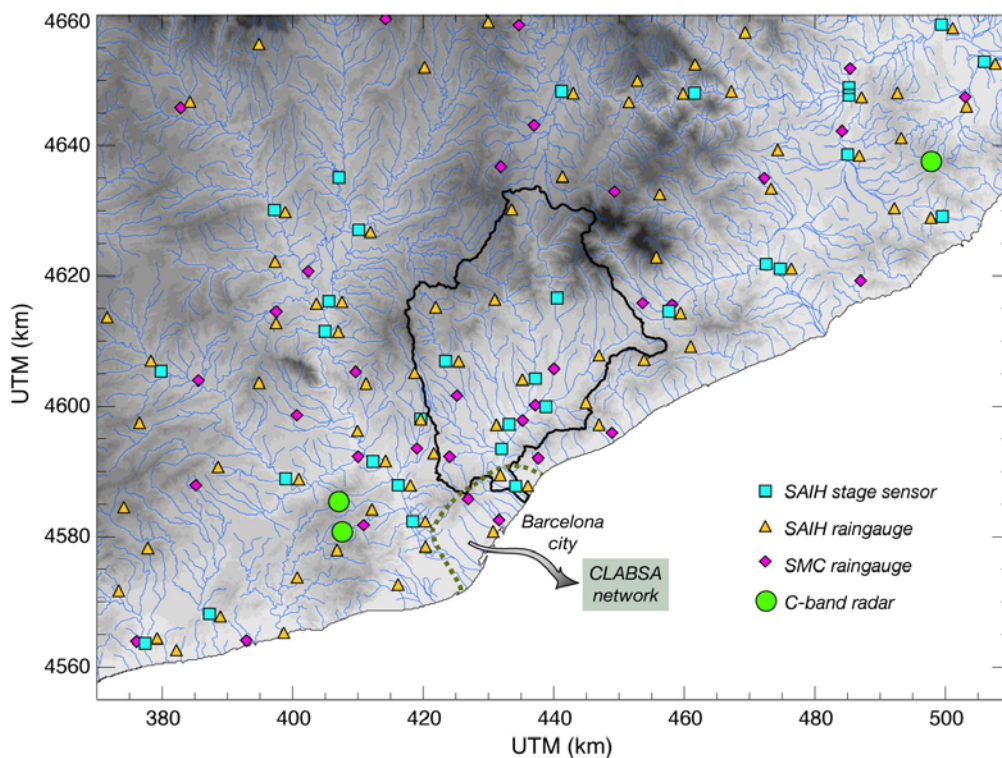


Figure 2-4: Topographic map of the Barcelona area showing the extension of the Besòs River and its instrumentation

2.4 The north-eastern Italy Hydrometeorological Observatory (LINE)

The “north-eastern Italy Hydrometeorological Observatory” (LINE) started in 2000 with focus on the Adige river basin. During 2004, an agreement was reached with the OSMER of the Friuli-Venezia Giulia region to extend the research to the region covered by the Fossilon di Grado weather radar center (with main focus on the Tagliamento river basin). The main objective of LINE is to develop a framework aimed at the effective utilization of radar rainfall estimates for the identification and prediction of flash flood events in a region characterized by rugged topography. Two study regions are considered in this Observatory: the Adige river watershed (Figure 2-5), and the Tagliamento river watershed (Figure 2-6), both in north-eastern Italy.

Most floods in the Adige basin are widespread phenomena generated by frontal precipitation systems. This is the case for the most important floods in 1882, 1965, 1966, and for the floods that occurred from 1998 to 2002. The city of Trento, as well as a large number of towns in the basin, was flooded and heavily hit during the 1966 event. The region, and especially the upper Adige river basin, is frequently hit by flash flood events (Fortezza, July 1999), which trigger important debris flow phenomena.

A number of different agencies are responsible for the operation of the hydrometeorological data gathering and analysis: Ufficio Idrologico in Provincia of Bolzano, METEOTRENTINO in Provincia of Trento, CSIM in the Veneto Region. The Spino d’Adda radar system is managed and maintained by Nuova Telespazio (TELECOM group).

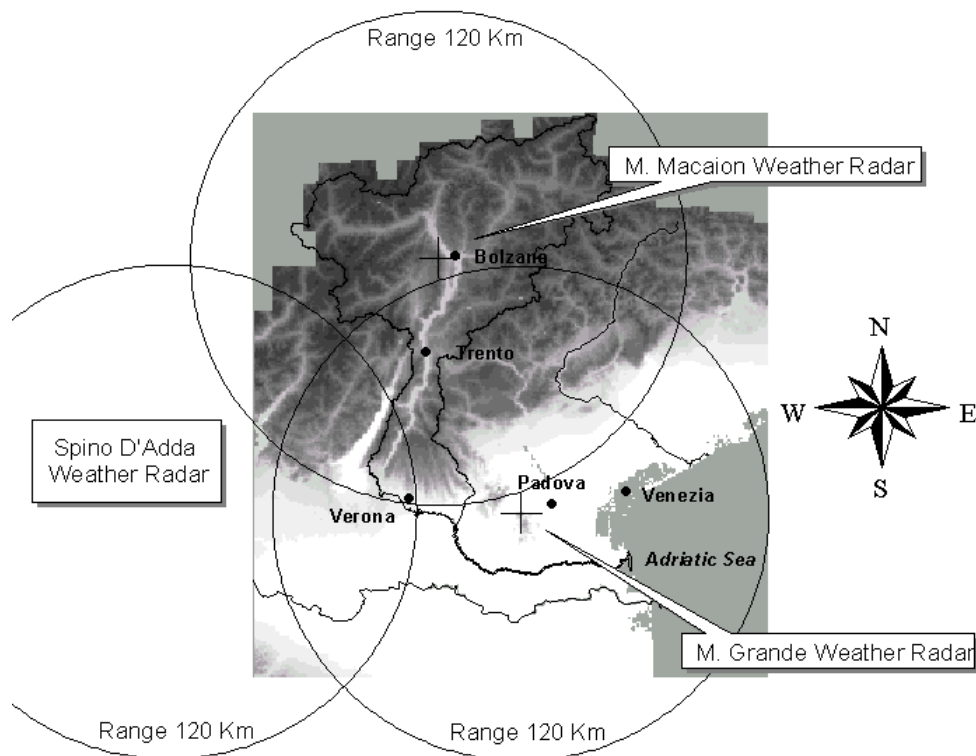


Figure 2-5: Radar coverage of the Adige river watershed.

The Adige river is the second longest river of Italy, 360 km long, rising in the Tyrolean Alps, Northern Italy. It flows south, past Bolzano, Trento, and Verona, to the Po valley where it turns east to flow into the Adriatic Sea. The research is focused on the mountainous part of the basin (12000 km²), which

includes two distinct administrative units: Provincia Autonoma di Bolzano (almost 7000 km²) and Provincia Autonoma di Trento (5000 km²). Altitudes range from 100 m a.s.l. up to 4000 m a.s.l.. The region is located south of the inner alpine province: it ranges between a dry climate (600 mm/yr, due to the dual sheltering effect of the range to both the north and the south) and a wet climate (2500 mm/yr) along the Venetian plains. The southern range experiences showery precipitation with thunderstorm and hail, particularly in summer and autumn.

The operational observation system for the Adige river basin includes:

- (1) A network of three weather radar systems. Two are C-band Doppler weather radars (Mt. Macaion and Mt. Grande) and one is an S-band Doppler radar (Spino d'Adda). They are used for the hydrometeorological surveillance of the region. The Mt. Macaion weather radar (1860 m a.s.l.) has been installed in 1999. The Mt. Grande radar system (420 m a.s.l.) is in operation since 1989 and was recently improved. The S-band weather radar in Spino d'Adda, in the Po valley, has been modified in 1995, enabling coherent (Doppler) measurements. The combination of radar imagery from at least M. Macaion and M. Grande sites allows a good coverage of this region.
- (2) A network of ground-based instruments, including 140 tipping bucket rain gauges and 30 hydrometric stations.



Figure 2-6: The Tagliamento river basin.

The Tagliamento River (with an area of 2871 km²) is the dominant river system of the Friuli region in northeastern Italy (Figure 2-6). From north to south, the Tagliamento traverses four major regions: (i) the Julian and Carnian Alps, (ii) prealps, (iii) the upper and lower Friulian plain, and (iv) the coast. This steep environmental gradient from north to south is associated with climatic differences, e.g., annual precipitation ranges from 3,100 to 1000 mm per year and mean annual temperature from 5 to 14 °C. The southern fringe of the Carnian and Julian Alps frequently receives very intensive rainstorms, resulting in severe erosion, especially in the alpine area. The alpine area of Friuli mainly consists of limestone, with a spatial sequence of Silurian, Devonian, Triassic, Jurassic and Cretaceous formations north to south.

The main tributaries of the upper catchment, the Lumiei, the Degano, the But and the Fella, converge and join the Tagliamento River forming a palmate pattern. Their basins are characterised by steep slopes and lie in one of the wettest regions of Italy, where annual precipitation can reach 3000 mm. Rainfall is concentrated mainly in heavy and erosive showers determining the torrential regime of the river. Furthermore, the mountain basin is seismically active and has a dense distribution of landslides, resulting in much bed load and a braided nature of the river downstream. At Pioverno (2400 km²), the 10 and 100 year floods are estimated to be 2150 m³/s and 4300 m³/s, respectively. The Tagliamento river basin is covered by the Fossalon di Grado weather radar, owned by ARPA Friuli Venezia Giulia (OSMER). The station is located at 25 m a.s.l.. The radar is C-band, Doppler, with dual polarization capability.

2.5 The Ardenne Hydrometeorological Observatory

The Ardennes is an undulating area of moderate relief (maximum elevation of approximately 700 m) and an important natural laboratory to study the hydrometeorology of mountainous catchments. The western part of the Ardennes (France, Belgium, Netherlands) mainly drains to the river Meuse, whereas the eastern part of the region (Luxemburg, Germany) mainly drains to the river Rhine (via the Mosel). Both the Meuse and the Rhine fulfill important functions in the water supply of The Netherlands. These rivers supply water for domestic, industrial and agricultural use and also fulfill important navigational, ecological and recreational functions. It is therefore of significant societal relevance to develop strategies to mitigate the impact of floods and droughts associated with the flow regimes of the rivers Meuse and Rhine. To achieve this objective, the hydrometeorology of the (mostly mountainous) upstream areas, such as the Ardennes, needs to be better understood. The aim of a recently established research collaboration between Wageningen University (WU), the Royal Meteorological Institute of Belgium (RMI) and the Hydrological Service of the Walloon Region of Belgium (MET-SETHY) is to investigate whether an improved assessment of the space-time structure of precipitation, as can be obtained with a newly installed weather radar in the Ardennes, in combination with an innovative approach towards modelling the rainfall-runoff process, will lead to an improved understanding of the hydrometeorology of Ardennes catchments.

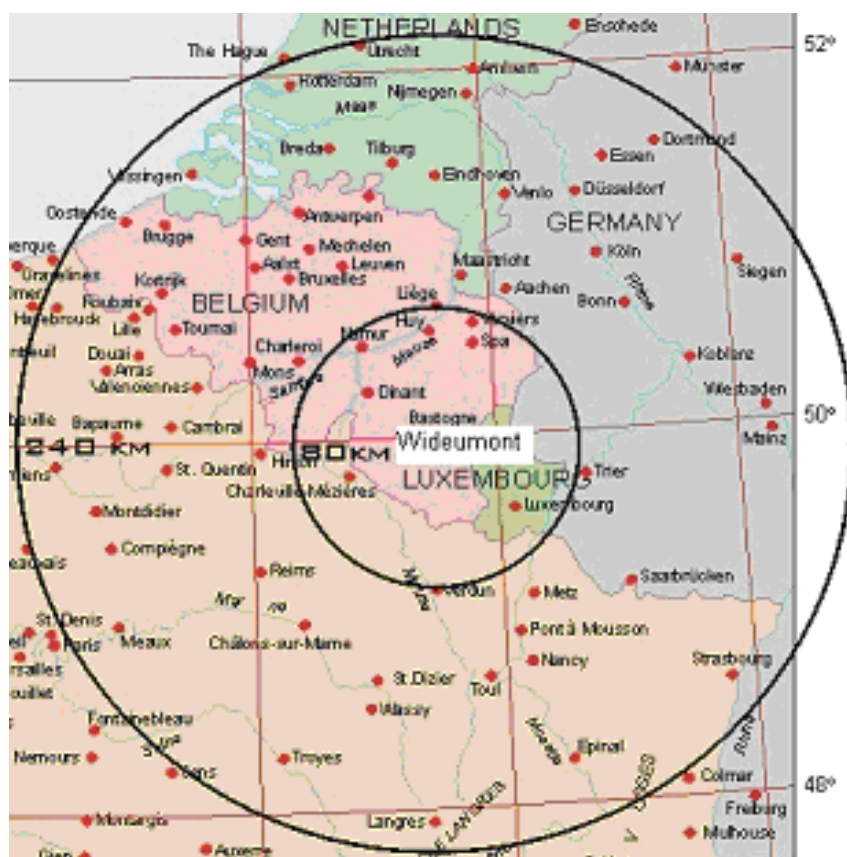


Figure 2-7: The Ardenne Hydro-meteorological Observatory window map

3. Influence of rainfall spatial resolution on flash flood modelling

3.1 Introduction

Rainfall is the primary input to most hydrological systems, and a key issue for hydrological science and practice is to assess the importance of the spatial structure of rainfall and its representation for flood runoff generation. This problem is particularly important for the case of flash flood events, which are characterised by high space-time variability both in the rainfall forcing and in the hydrologic response (Creutin and Borga, 2003). The influence of rainfall representation on the modelling of the hydrologic response is expected to depend on complex interactions between the rainfall space-time variability, the variability of the catchment soil and landscape properties, and the spatial scale (i.e. catchment area) of the problem (Obled et al., 1994; Woods and Sivapalan, 1999; Bell and Moore, 2000; Smith et al., 2004). The literature addressing this problem includes quite heterogeneous approaches in terms of the methodologies adopted and conclusions drawn from the analyses (Nicotina et al., 2008).

In general, when addressing the problem of the sampling scale effect, it is found that the measured (apparent) variability of spatially-continuous fields depends on two terms: extent and support (Blöschl and Sivapalan, 1995). 'Extent' refers to the overall coverage of the data (the watershed scale, given by L_w , root square of the watershed area); 'support' refers to the resolution area (the aggregation length, L_r). Based on theoretical and empirical evidence, it is found that the apparent spatial variability of the rainfall field represented at some aggregation scale decreases with decreasing the 'extent' and with increasing the aggregation length. The first effect is a logical consequence of the existence of spatial correlations: for a given aggregation length, the smaller L_w , the closer the data and, thus, the closer

their values. The second effect arises because dispersion within a fixed domain L_w decreases as the support L_r increases: the rainfall values at 8-km resolution are less dispersed than the rainfall values at 1-km resolution, for a fixed domain.

Increasing the aggregation length leads not only to a reduction of the rainfall apparent spatial variability. It has been found (Ogden and Julien, 1994; Winchell et al., 1998; Segond et al., 2007) that when the ratio L_r/L_w exceeds a certain threshold, the uncertainty in the location of precipitation over the catchment becomes a major source of error in rainfall volume estimation at the catchment scale. Indeed, typical spatially varying rainfall patterns consist of regions of heavier or lighter precipitation outside the immediate boundaries of a catchment. Rainfall values pertaining to areas just outside the catchment may enter the computation of the average rainfall over the basin by increasing the resolution area. As such, this error source leads to a rainfall volume error.

The sensitivity of runoff modelling to both attenuated spatial variability and rainfall volume error depends strongly on the smoothing effect of catchment characteristics (Winchell et al., 1998; Segond et al., 2007). When there is not enough variability in rainfall to overcome the damping effect of the catchment, detailed knowledge of rainfall spatial variability is not required to model the catchment response, although reliable information of catchment-averaged rainfall is important (Naden, 1992; Obled et al., 1994; Woods and Sivapalan, 1999; Smith et al., 2004; Andreassian et al., 2001). However, there is not an agreed approach to quantify the damping effect of a given catchment and the conclusions drawn from the different studies depend heavily on the runoff model, the characteristics of the rainfall forcing and the type of catchment examined.

Focusing the analysis on flash flood events allows one to isolate specific runoff generation mechanisms and catchment properties which are perceived as dominant with this type of events. In particular, the substantial role exerted by Hortonian runoff generation with high intensity rainfall events emphasise the role of surface runoff and river network geometry in the averaging of space-time rainfall (Norbiato et al., 2008). In this case, the concept of flow distance, i.e. the distance along the runoff flow path from a given point to the outlet, may provide a useful metric to examine the influence of rainfall resolution on runoff modelling (Woods and Sivapalan, 1999). The dampening effect arises here because the excess rainfall generated at points placed at equal flow distance will be averaged out in the runoff propagation process, in spite of the rainfall spatial variability. The averaging of space-time rainfall fields across locations with equal flow distance coordinates may be sensitive to the spatial resolution of the rainfall representation and as such it may explain, at least partially, the pattern of runoff model sensitivity to rainfall resolution.

These concepts are examined in this study with reference to the flash flood event which occurred on August 29, 2003 in the Fella river basin (eastern Italian Alps). The regional flood response of the Fella river basin is examined in terms of space-time rainfall variability and heterogeneous land surface properties. A distributed hydrologic model, which includes an empirical infiltration model and a network-based representation of hillslope and channel response, plays a central role in examining the regional flood response. Detailed observations from a weather radar are used to estimate the rainfall forcing (Borga et al., 2007). To elucidate the controls of rainfall spatial aggregation on model error, the distributed hydrologic model is applied over ten different sub basins ranging from 10.5 km² to 623.0 km² and by using four different rainfall resolutions: 1-, 4-, 8- and 16-km. The range of spatial resolution covers the aggregation scales often encountered in flash flood forecasting, from fine-scale radar rainfall estimates to large-scale rainfall forecasts provided by numerical weather forecast models.

The report is organized as follows. Section 2 describes the study region and provides the documentation of the flash flood event used in this investigation. Section 3 illustrates the distributed model used in the study, whereas Section 4 examines its sensitivity to spatial resolution of rainfall over a range of catchment scales. Section 5 completes the report with discussion and conclusions.

3.2 The Fella 2003 flash flood

The flash flood of the Fella catchment on 29 August 2003 (Figure 3-1) occurred at the end of a climatic anomaly of a dry and hot summer and was one of the most devastating flash flood events in North-eastern Italy since starting of systematic observations. The rainfall event started at 10:00 CET (Central European Time) and lasted for 12 hours, focusing on the 705 km²-wide Fella basin (Figure 3-1), which is a major left-hand tributary of the Tagliamento river system. The Fella basin has a mean altitude of 1140 m a.s.l., with an average annual precipitation of 1920 mm. Ten sub-basins of the Fella river system are examined in this study, ranging from 10.5 km² to 623 km².

Extreme rainfall from the August 2003 storm was produced by quasi-stationary convective banded structures. Some of the bands persisted in the same locations for the duration of the event. The steadiness of these rainbands led to highly variable precipitation accumulations and runoff (Borga et al., 2007). The storm total precipitation (Figure 3-1) is characterised by a band of rainfall accumulation exceeding 300 mm localised on the right-hand tributaries of the Fella river. The storm total rainfall distribution reflects south west - north east motion of the storm elements and west-east shift of the tracks of the storms. Rainfall intensity up to 100 mm hr⁻¹ over 15-minutes time step was recorded during the explosive growth phase of the storm (between 14:00 and 18:00 CET) (Norbiato et al., 2007). Rainfall produced by the August 2003 storm resulted in severe flooding throughout the Fella river basin. The storm produced catastrophic flooding at drainage areas up to 80-90 km².

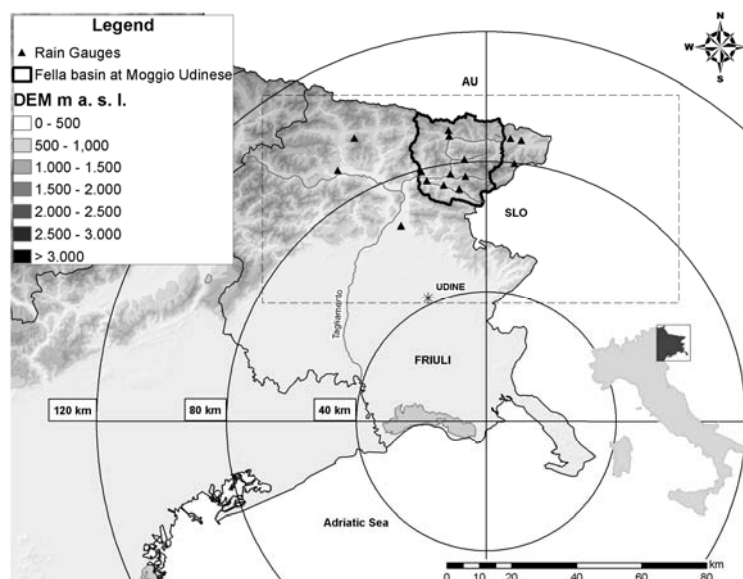


Figure 3-1: Location of the OSMER radar and the Fella river basin at Moggio Udinese with topography of North-eastern Italy. The locations of the raingauge stations used in the study are also reported. The dotted line rectangle represents the area used for the analyses of rainfall spatial variability reported in Figure 3-2

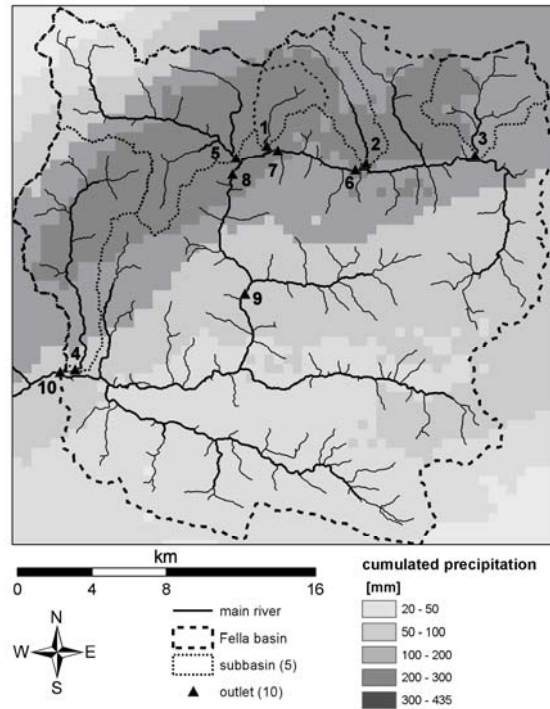


Figure 3-1: Storm total rainfall (mm) for the August 29, 2003 storm on the Fella river basin at Moggio (basin outlet 10, 623km²) with the nine study subbasins: Rio degli Uccelli at Pontebba (1, 10.5km²); Rio Bianco at S. Caterina (2, 17.5km²); Uque at Ugovizza (3, 24km²); Aupa at Moggio Udinese (4, 50km²); Pontebbana at Pontebba (5, 71.2km²); Fella at S.Caterina (6, 139km²); Fella at Pontebba (7, 165km²); Fella at S.Rocco (8, 250km²) and Fella at Dogna (9, 329km²).

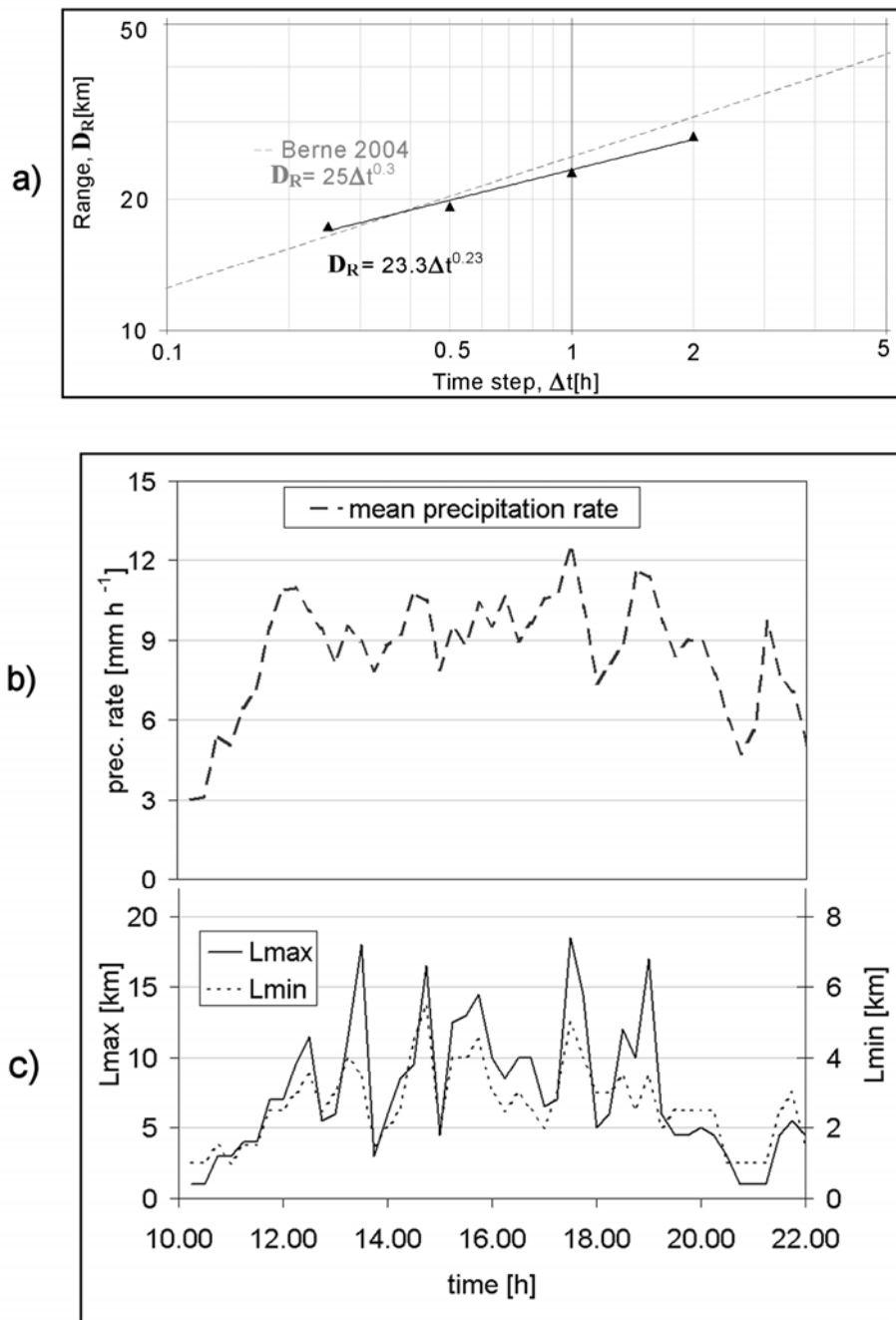


Figure 3-2: Rainfall spatial variability analysis:

- a) Range [km], resulting from spatial climatological variogram analysis, versus time step [h]; results are compared with analysis carried out by Berne et al. [2004] (dashed line);
- b) Mean precipitation of non zero values inside the rectangle area shown in Figure 3-1.
- c) Lengths of maximum and minimum axis for indicator variogram on binary rainfall fields using 20mm h⁻¹ threshold.

3.2.1 Post event field campaign

Flash flood events are difficult to monitor because they develop at space and time scales that conventional measurement networks of rain and river discharges are not able to sample effectively (Borga et al., 2008). This explains why the investigation of flash flood events is by necessity event-based and opportunistic as opposed to driven by observations from carefully designed field campaigns.

Post-event surveys play therefore a critical role in gathering essential observations to implement and verify hydrological models for flash flood analyses.

Following the August 2003 event, post flood surveys were planned. Surveys were concentrated in the upper Fella basin and included: (i) collection of rainfall data, (ii) collection of streamgauge data and execution of indirect peak flood estimation, and (iii) postflood interviews.

Radar and raingauge observations were used to derive rainfall fields for the August 2003 storm. 5-minute raingauge data were collected at 15 raingauges (Figure 3-1), whereas storm total rainfall was available at further six daily raingauges. Volume scan reflectivity data from the Doppler, dual-polarised C-band OSMER radar station, located at Fossalon di Grado (Figure 3-1) (time resolution of 5 min and spatial resolution of 250 m in range by 0.9 degree in azimuth), were used to derive radar rainfall rates. Spatially detailed rainfall estimates were obtained by adjusting radar observation accounting for the physics of the radar sensing and incorporating accumulated values of the available raingauge stations (Borga et al., 2002).

Streamgauge data and observations from post-event surveys, combined with hydraulic modelling, were used to examine the hydrologic response to the storm. Stream gauge data were available at eight sites, generally located either close or at bridge crossing sites, where measurements are taken by means of ultrasound sensors. Hydraulic modelling, combined with surveys of the post-flood river section geometry and data about pre- and post-flood geometry, was used to derive stage-discharge relationships at these river sections (Borga et al., 2007). Furthermore, hydraulic modelling was used to estimate peak discharges based on surveyed high watermarks and postflood channel geometry at another three sites (including the site at the outlet of Uqua basin, Figure 3-1) and to confirm the estimates at the gauged sections. Twenty-two local residents, mostly located close to the Uqua river basin and its fan, were interviewed about the severity of the storm, occurrences of surface flow, timing of rainfall and stage peaks.

3.2.2 Precipitation analyses

The structure of the rainfall spatial variability has been examined by using the climatological variogram (Lebel et al., 1987; Berne et al., 2004). The domain used for this analyses is a 128 km by 64 km region centred on the Fella River basin (Figure 3-1). With the approach based on the climatological variogram, one may take into account information from all the realizations (e.g. rainfall field for successive time steps) assuming the fields to have similar statistical characteristics except for a constant factor. The variogram can therefore be normalised by the respective variance of each field considered and then averaged over all the realizations. Assuming the structure functions have the same shape, the mean normalised variogram obtained (with variance parameter equal to one), also called climatological variogram, is representative of all the realizations. In particular, we have used here a spherical variogram as a reference spatial structure. The main adjustment factor of this function is the variogram shape and particularly its range (i.e., the decorrelation distance). This allowed us to calibrate a relation between the rainfall accumulation time step Δt (hours) and the range D_R (km) (Figure 3-2a), as follows:

$$D_R = 23.3\Delta t^{0.23} \quad (1)$$

Interestingly, this equation is relatively close to the one reported by Berne et al. (2004) for flash flood events observed in France. According to Eq. (1), the range of the variogram of half-hourly rain rates is set equal to 19.5 km.

Space and time generation of runoff is controlled mainly by the spatial distribution of the intense rainfall cells. We characterise this spatial distribution by using the concept of the indicator variogram (Barancourt et al., 1992), i.e. by converting the rainfall field into a corresponding binary process. For this, a binary function denoted $i(x,y)$, called the indicator function by Journel, 1983, is defined by $i(x,y) = I_{P(x,y) > 20 \text{ mm/h}}$, i.e.:

$$i(x,y)=1 \text{ if } P(x,y)>20 \text{ mm/h}$$

$$i(x,y)=0 \text{ otherwise.}$$

The threshold of 20 mm h⁻¹ was selected here to isolate the fraction of the basin hit by flood producing rainfall. We analysed the binary field by using the indicator variogram, which show a significant anisotropy with longer correlations in the N55E direction. To account for anisotropy, we conceptualised the range in space as an elliptical field, quantified by the major and minor axes at each time step. We describe the temporal evolution of the spatial structure of rainfall accumulated at 30-min time step by reporting the time series of max and min lengths (Figure 3-2c). The indicator variogram analyses highlight the high variability of the storm properties with time. During the period of very intense rainfall occurrence (i.e., between 14:00 and 18:00 CET) the major axis length ranges between 7 and 18 km, whereas the minor axis length ranges between 3 and 5 km. This indicates that the shape of the high intense areas is elongated, with the minor axis length equal to 30% of that of the major axis, and points out to the high spatial variability of the high intensity rainfall fields.

3.3 Analyses of flood response

Hydrologic response on the Fella River basin is examined by using a simple spatially distributed hydrologic model (KLEM – Kinematic Local Excess Model; Borga et al., 2007). The distributed model is based on availability of raster information of the landscape topography and of the soil and vegetation properties. In the model, the SCS-Curve Number (SCS-CN) procedure (U.S. Department of Agriculture, 1986) is applied on a grid-by-grid way for the spatially distributed representation of runoff generating processes. A linear transfer function based on a simple description of the drainage system response is used to represent runoff propagation.

The general SCS-CN runoff equation is

$$q = \frac{(P - I_a)^2}{(P - I_a + S)} \quad \text{for } P \geq I_a \quad (2)$$

$$q = 0 \quad \text{for } P < I_a$$

where q (mm) is the direct runoff depth, P (mm) is the event rainfall depth, I_a (mm) is an “initial abstraction” or event rainfall required for the initiation of runoff, and S (mm) is a site storage index defined as the maximum possible difference between P and q as $P \rightarrow \infty$. $P - I_a$ is also called “effective rainfall”, or P_e . The SCS-CN method can be applied by specifying a single parameter called the curve number, CN, which is function of the hydrologic soil-cover complex and ranges in principles from 1 to 100. The value of S for a given soil is related to the curve number as

$$S = C \left(\frac{100}{CN} - 1 \right) \quad (3)$$

where C is a calibration parameter (mm), called infiltration storativity. The use of the parameter C allows one to use the spatial distribution of CN values, which represents an input data in this work, and to simulate correctly, at the same time, the observed flood water balance (Borga et al., 2007).

The distributed runoff propagation procedure is based on the identification of drainage paths, and requires the characterization of hillslope paths and channeled paths. We used a channelization support area (A_s) (km²), which is considered constant at the subbasin scale, to distinguish hillslope elements from channel elements and two parameters (v_h and v_c (m s⁻¹)) as the two time-invariant hillslope and channel velocities, respectively. The model has been implemented at 30-min time step and using a 20-m grid size cell for the description of landscape morphology and soil properties.

The hydrological model used here is based on the rather strong assumption that space-time excess rainfall distribution and drainage network structure provide the most important controls on extreme flood response. However, its parsimonious structure is a favourable characteristic for analysis of flash flood events, which are affected by considerable uncertainty on rainfall and discharge data. As such, this model structure has been used in a number of studies on flash flood events (Zhang et al., 2001; Borga et al., 2007). The accuracy of the model simulations have been examined and discussed by Borga et al. (2007), who showed that the model reproduces peak discharge and the time of peak discharge reasonably well. The model parameters calibrated at 1-km rainfall aggregation length were used for the sensitivity analysis.

3.3.1 Analysis of space-time precipitation variability at three catchment scales and at two rainfall resolutions

To characterize the influence of temporal and spatial variability of rainfall on flood response according to the metric provided by the flow distance concept, we utilized 30-min rainfall fields at two different aggregation lengths to compute the following quantities:

- 1) the mean rainfall rate over the catchment at time t during the storm, $M(t)$;
- 2) the fractional coverage of the basin by rainfall rates exceeding 20 mm h^{-1} , $F(t)$;
- 3) the normalized time-distance of rainfall from the basin outlet, $D(t)$; and
- 4) the normalised dispersion of rainfall, $S_{NOR}(t)$.

Consistently with analyses reported above, the threshold of 20 mm h^{-1} was selected here to isolate the fraction of the basin hit by flood producing rainfall. The mean rainfall rate and fractional coverage time series provide basic information on rainfall mass balance and distribution of rainfall rates over the catchment. They do not provide information on the spatial distribution of rainfall relative to the basin network structure, however. The drainage network, as represented by the routing time $\tau(u)$ from the arbitrary location $u=x,y$ to the outlet of the basin. The routing time $\tau(u)$ is defined as

$$\tau(u) = \frac{L_h(u)}{v_h} + \frac{L_c(u)}{v_c} \quad (4)$$

where $L_h(u)$ is the distance from the generic point u to the channel network following the steepest descent path, $L_c(u)$ is the length of the subsequent drainage path through streams down to the watershed outlet, and v_h and v_c are the two invariant hillslope and channel velocities introduced above. The routing time provides a natural metric for analyzing the spatial distribution of rainfall, as shown previously by Woods and Sivapalan, 1999, Zhang et al., 2001 and Borga et al., 2007. The routing time incorporates both geometric and kinematic properties in its determination.

The normalized time-distance at time t , $D(t)$, is a function of the rainfall field $R(t, u)$ and the routing time $\tau(u)$. It is defined as the ratio of the rainfall-weighted centroid routing time $D_1(t)$ and the mean routing time D_{mean} ,

$$D(t) = \frac{D_1(t)}{D_{mean}} \quad (5)$$

In Eq. (5) the time-distance $D_1(t)$ is given by

$$D_1(t) = |A|^{-1} \int_A w(t, u) \tau(u) du \quad (6)$$

where A is the spatial domain of the drainage basin and the weight function $w(t, u)$ is given by

$$w(t, u) = \frac{R(t, u)}{|A|^{-1} \int_A R(t, u) du} \quad (7)$$

The value D_{mean} is defined as

$$D_{mean} = |A|^{-1} \int_A \tau(u) du \quad (8)$$

Values of $D(t)$ close to 1 reflect a rainfall distribution either concentrated close to the mean time-distance or homogeneous, with values less than one indicating that rainfall is distributed near the basin outlet, and values greater than one indicating that rainfall is distributed towards the periphery of the drainage basin.

The rainfall-weighted flow time-distance dispersion is given by:

$$S(t) = \left\{ \int_A w(t, u) [\tau(u) - D_1(t)]^2 du \right\}^{0.5} \quad (9)$$

The dispersion for uniform rainfall is defined by:

$$S_1 = \left\{ \int_A [\tau(u) - D_{mean}]^2 du \right\}^{0.5} \quad (10)$$

and the normalised dispersion is given by

$$S_{NOR}(t) = \frac{S(t)}{S_1} \quad (11)$$

Values of $S_{NOR}(t)$ close to 1 reflect a uniform-like rainfall distribution, with values less than 1 indicating that rainfall is characterised by a unimodal peak, and values greater than 1 indicating cases of multimodal rainfall peaks close and far from the basin outlet.

Results are reported in Figure 3-3 for three catchments: Rio degli Uccelli (10.5 km²), Fella at S. Caterina (139.0 km²) and Fella at Moggio (623.0 km²) and for rainfall fields aggregated over length scales of 1 and 16 km. Rio degli Uccelli and Fella at Moggio represent the smallest and largest catchment examined in the study, respectively, whereas Fella at S. Caterina represents an intermediate catchment scale. Inspection of the mean rainfall intensity shows that aggregation at 16-km scale has relatively less effects over the larger basin (Fella at Moggio), whereas significant smoothing effects (with reductions up to 50%) are recognised over Rio degli Uccelli, particularly for the period 14:00 to 18:00, with intermediate effects for Fella at S. Caterina.

The dynamics of the fractional coverage is consistent with the information provided by the temporal evolution of the rainfall spatial structure reported in Figure 3-2c. For Rio degli Uccelli, which was located under one of the major convection band during the phase of explosive growth of the storm, the size of the rainfall band is enough to ensure full coverage in the period between 14:00 and 17:30. Interestingly, increasing the rainfall aggregation length induces generally a sharper behaviour in the rainfall coverage, as it is illustrated by the case of the Fella at S. Caterina. Inspection of this last case shows that, even though the ratio of rainfall resolution to the characteristic basin length (L_r/L_w) is larger than one for the 16-km resolution, the rainfall is far from being spatially uniform, being the

catchment located between two or more rainfall cells. This needs to be accounted for in the discussion below.

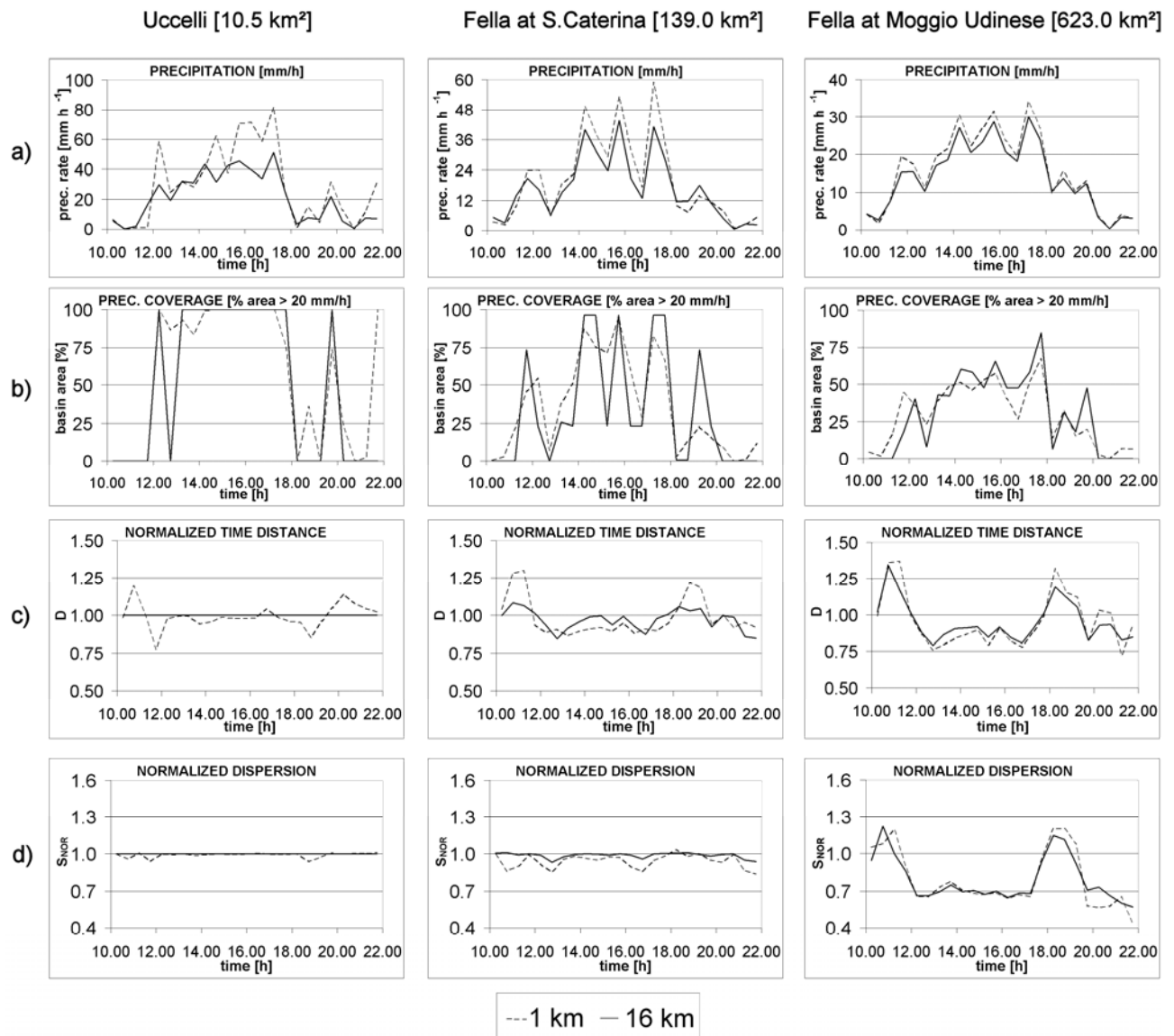


Figure 3-3: Precipitation analysis for three catchments (Uccelli at Pontebba, 10.5km², Fella at S.Caterina, 139 km² and Fella at Moggio Udinese, 623 km²), with two different rainfall grid resolutions (1 km and 16 km):

mean rainfall intensity [mm h^{-1}];

coverage (for precipitation intensity $> 20 \text{ mm h}^{-1}$);

normalized time distance;

normalized time dispersion.

Examination of normalised distance highlights different behaviours across the various catchments. Analysis of normalised dispersion over the period of heavy rainfall and at 1-km resolution shows that rainfall concentration translates from the lower portion of the basin to the upper portion and that the dynamics of the normalised distance increases with catchment scale, as expected. Aggregation over 16-km length scale has generally the effect to reduce the dynamics of the normalised distance and has a different impact according to catchment scale. For Rio degli Uccelli, aggregation over 16-km averages out any dynamics, as expected since the rainfall field provided to the catchment at this resolution is completely uniform.

A similar pattern can be recognised for the normalised dispersion, with precipitation exhibiting a unimodal peak for Moggio (at least during the period of extreme precipitation) and a more uniform distribution for the case of Rio degli Uccelli, with S. Caterina being in an intermediate position.

3.4 Influence of rainfall spatial aggregation on peak discharge simulation

Effects of rainfall spatial aggregation on flood response modelling are examined here with reference to the ratio of rainfall resolution to the characteristic basin length (L_r/L_w), taken as the square root of the watershed area. To elucidate the controls of rainfall aggregation on model error, the KLEM model was applied over ten different sub-basins ranging from 10.5 km² to 623 km² (Table 3-1 and Figure 3-1) and by using four different rainfall resolutions: 1-, 4-, 8- and 16-km. This provides 40 different combinations of watershed characteristic lengths and rainfall aggregations.

Table 3-1: Characteristics of the study basins, with catchment area and mean areal cumulated precipitation at four different rainfall resolutions; basin id numbers as reported in Figure 3-1.

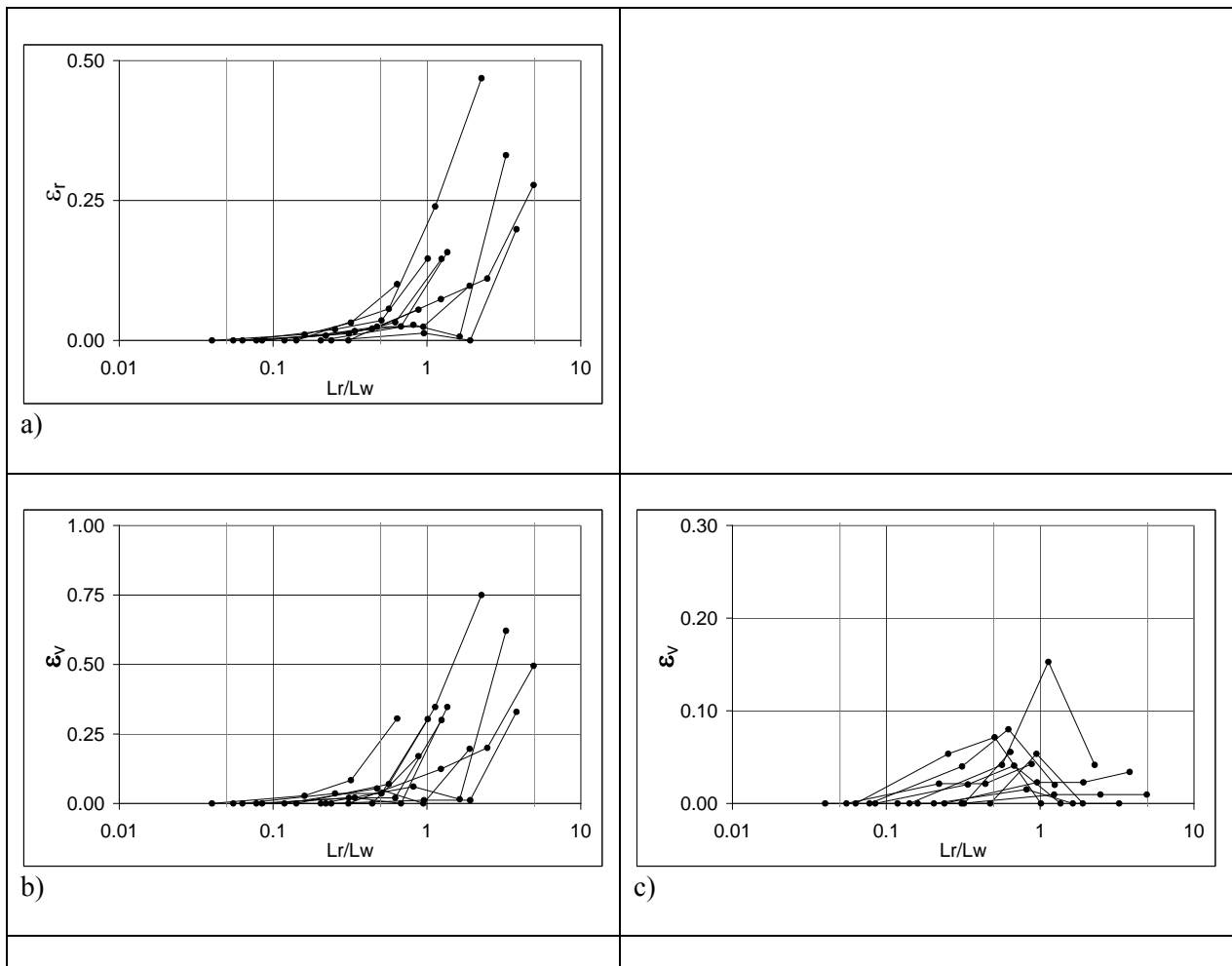
Basin id number	Area [km ²]	Mean areal precipitation [mm] using resolution			
		1km	4km	8km	16km
1	10.5	353	327	314	255
2	17.5	307	303	307	246
3	24	287	279	285	192
4	50	301	284	229	160
5	71.2	246	240	240	222
6	139	241	237	235	203
7	165	247	244	239	211
8	250	253	248	244	216
9	329	237	235	232	224
10	623	189	187	183	170

As shown above, varying the spatial rainfall resolution induces rainfall volume errors, a reduction of the rainfall apparent spatial variability and a distortion of the rainfall geometry with respect to the flow distance metric. In order to separately address the first two effects we performed numerical experiments in which rainfall depths are rescaled and forced to be exactly preserved at each time step over the range of rainfall resolutions and catchment scales examined.

The error analysis was carried out for rainfall and runoff volumes and for peak discharges, by comparing results obtained by using a given input resolution with those obtained from 1-km grid size, considered here as the reference resolution. The error statistics ‘normalised rainfall volume error’ ε_r , ‘normalised runoff volume error’ ε_v and ‘normalised peak discharge error’ ε_q were computed for rainfall volume, runoff volume and peak discharge, respectively, as follows:

$$\begin{aligned} \varepsilon_r &= \frac{|P_{Lr} - P_l|}{P_l}, \\ \varepsilon_v &= \frac{|V_{Lr} - V_l|}{V_l}, \\ \varepsilon_q &= \frac{|Q_{pLr} - Q_{pl}|}{Q_{pl}}, \end{aligned} \tag{12}$$

where P_{Lr} and P_l , V_{Lr} and V_l , and Q_{pLr} and Q_{pl} , represent the rainfall volume, the runoff volume and the peak discharge resulting from aggregation over L_r - and l - km length, respectively. The error statistics were computed before and after rescaling the rainfall fields at different resolution to preserve rainfall volumes.



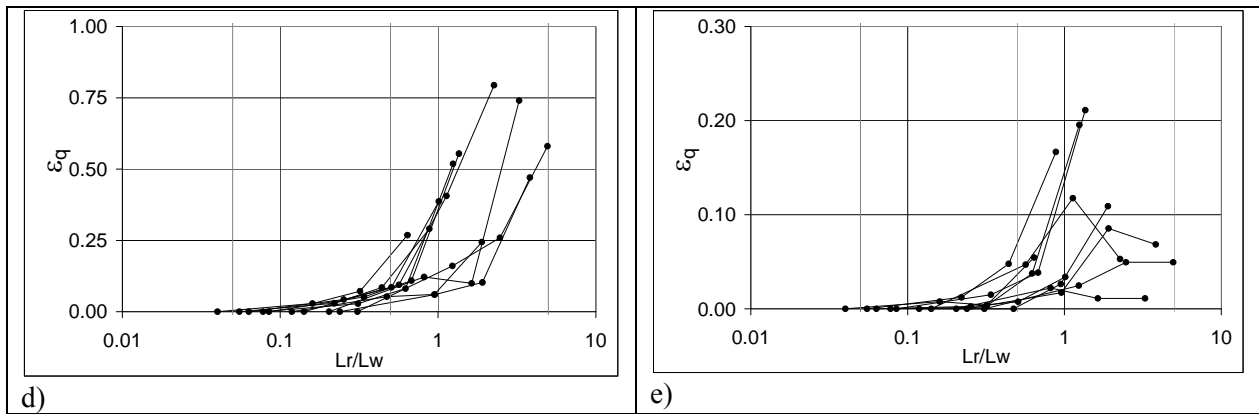


Figure 3-4: Relationship between the ratio L_r/L_w and a) normalised rainfall error; b) normalised runoff volume error before rainfall volume rescaling; c) normalised runoff volume error after rainfall volume rescaling; d) normalised peak discharge error before rainfall volume rescaling; e) normalised peak discharge error after rainfall volume rescaling.

Examination of the normalised rainfall volume errors (Figure 3-4a) highlights the impact of the error caused by incorrectly smoothing the rainfall volume either into or out of the watershed; this generally corresponds to negative errors – i.e. underestimation of the true rainfall volumes (Table 3-1). These results generalise those reported at the previous Section for the catchments of Rio degli Uccelli and Fella at Moggio and examined by using grid resolutions equal to 1 and 16 km. A large rainfall volume error was found for grid size equal to 16 km for the Rio degli Uccelli. This corresponds to L_r/L_w equal to 5.1, for which the normalised rainfall volume error amounts to 27%. On the contrary, the error for the Fella basin at Moggio, for which L_r/L_w is equal to 0.64, amounts to 9%. For the Fella at S. Caterina ($L_r/L_w = 1.37$), the error amounts to 15%. The figure shows that use of the ratio L_r/L_w is capable to filter out quite effectively the effect of the catchment size on the rainfall volume error. Inspection of the maximum values of the errors shows that the error is up to 0.1 for L_r/L_w equal to 0.4, and then increases to 0.2 for L_r/L_w equal to 1.0 and to 0.5 for L_r/L_w equal to 2.5.

Results are reported in Figure 3-4b,c and 5d,e for the volume and peak errors, respectively. Large runoff volume errors are shown in Figure 3-4b, particularly for the 2005 event, which is characterised by a peak value around 0.75 for a value of L_r/L_w slightly exceeding two. The figure shows that the general pattern of rainfall volume errors is transmitted to the volume errors and that the rainfall volume errors generally magnify through the rainfall-runoff modelling, as it is expected after examining the structure of the SCS-CN runoff model.

The impact of reduced rainfall variability alone on runoff volume errors is illustrated by Figure 3-4c, where errors are reported after rainfall volume rescaling. The figure shows that errors are sharply reduced, and generally below 10%. For one case (Aupa at Moggio) the runoff volume error slightly exceeds 0.15.

The relationship between the normalised peak discharge error and L_r/L_w , before rainfall volume rescaling, is reported in Figure 3-4d. The pattern of peak discharge errors reported in this figure is consistent with that of runoff volume errors, as expected. The error may reach values up to 0.75 for L_r/L_w slightly exceeding two. Peak discharge errors after rainfall volume rescaling are reported in Figure 3-4e. This figure reveals that runoff volume errors explains the peak discharge errors in a number of cases, but not always. In three cases the peak discharge errors are comprised between 0.15 and 0.22, and are not related to the corresponding volume errors, which are less than 0.05. Inspection of the simulated hydrographs for these cases (not reported here for the sake of brevity) indicates that errors are related to differences in the peak timing. This observation indicates that increasing the rainfall aggregation length produces, in some cases, a large distortion of the rainfall spatial distribution with respect to the river network, hence resulting in considerable errors in the shape of the

simulated hydrographs (including peak values and timing). This is not unexpected, because errors in the representation of the concentration of rainfall distribution in terms of flow distance translate into a distorted timing distribution of the simulated runoff.

3.5 Summary and conclusions

This report focuses on the analysis of the effects of spatial rainfall resolution on runoff simulation for an extreme flash flood event. The increasing availability of radar observations at different spatial resolutions requires examination of the impact of using different aggregation lengths on hydrologic modelling, with specific focus on highly variable flash flood-generating storms. Focus on extreme flash flood events leads, by necessity, to an event-based and opportunistic approach, as opposed to driven by observations from carefully designed field campaigns in experimental watersheds. Extreme, flood-producing storms are spatially and temporally rare and are seldom represented in the observations from experimental watersheds. Accurate post event analyses played an essential role in providing the data required for the present study.

Our evaluations are based on combining fine space-time rainfall observations with a distributed hydrologic modelling based on an empirical infiltration model and a network-based representation of hillslope and channel flow. Radar observations and model analyses are used to evaluate the sensitivity of model results to spatial aggregation of rainfall at various catchment scales ranging from 10.5 km² to 623 km². Four rainfall spatial resolutions are considered, with grid size equal to 1-, 4-, 8- and 16- km. A dimensionless parameter given by the ratio between length resolution and the square root of the watershed area (L_r/L_w) is used to describe the sensitivity of runoff model.

The analyses are focused on sensitivity of the simulated peak discharges to three different issues: i) rainfall spatial resolution; ii) rainfall volume errors and biased rainfall spatial variability; iii) distortion of rainfall spatial variability with respect to the river network. The principal conclusions of the study are summarized below.

1. Increasing the L_r/L_w parameter induces large errors on the simulated peak discharge. Maximum values of the peak discharge error are up to 0.2 for L_r/L_w equal to 0.5 and to 0.33 for L_r/L_w equal to 1.0. The error may reach values up to 0.75 for L_r/L_w exceeding 2.0. All these errors are negative – i.e. the simulated peak discharge decreases by increasing the L_r/L_w parameter.
2. An important error source related to spatial rainfall aggregation is the rainfall volume error caused by incorrectly "smoothing rainfall volume" either into or out of the watershed. For $L_r/L_w < 1.0$, around 50% of the peak discharge error is due to the rainfall volume error. The remaining error is significantly controlled by the interaction between the attenuated and geometrically biased rainfall spatial variability and the smoothing effects of catchment characteristics.
3. We examined the role of river network geometry in the averaging of space-time rainfall and on simulated peak discharges after rescaling the rainfall fields to preserve rainfall volumes. Increasing the resolution length may lead to a distorted geometry of the rainfall field with respect to the river network. This is an important control on peak discharge error – when rainfall volumes are preserved.

Further work might determine whether the results obtained in this investigation apply to other model formulations. The present investigation has obtained illustrative examples of how rainfall variability, as filtered by using different spatial aggregation lengths, feeds through to variability in modelled runoff response at the catchment scale. More extensive investigations would strengthen this understanding and provide additional guidance on the design of radar/raingauge networks for flow forecasting and the spatial resolution requirements for rainfall at different catchment scales.

4. A methodology for post flood field investigations in upland catchments after major flash floods

4.1 Introduction

Are field investigations conducted after major flash flood events really useful and what for? The question formulated in that manner may appear a little surprising. In fact, flash-floods, sudden floods with high peak discharges produced by severe thunderstorms that are generally of limited areal extent (IAHS, 1974), rank as the most destructive process among weather-related hazards in many parts of the world. Forgoing studying these extreme events, because no measured data are directly to hand, or because data that does exist are not considered as sufficiently accurate, or even because it is time consuming and limiting the hydrological analyses to moderate events on gauged watersheds, would be focussing on the trivial while skipping the essential.

Post-flood surveys appear clearly as a necessity to increase the existing knowledge on such events to provide adapted methods of analysis and technical solutions for flood prevention and control.



Figure 4-1: Nîmes city (France) on the 3rd of October 1988

The questions are rather how to proceed, what type of data can and should be collected for what type of analysis and what questions should be explored.

Past experience show that two main types of post-flood investigations can be distinguished which differ by their objectives and context. The first type is generally commissioned by the local or national authorities after a major catastrophe. The main objective is to answer questions raised by the public and local stakeholders on the causes of the floods, the possible human impacts on the flood magnitude and frequency, but also on the management of the crisis, the efficiency of the flood mitigation measures and the solutions to recover from the flood and to limit the future risks (Huet, 2005). Typical examples are the investigations conducted after the major 1987 floods in Switzerland (Bundesamt für Wasserwirtschaft, 1991) or more recently in France (Huet et al., 2003; Lefrou et al. 2000). The purposes of such investigations are well defined and limited to the raised questions. Scientists are generally involved either to conduct studies on some specific questions or to take part to scientific support groups. Research activities may be conducted during such investigations, but it is then a by-

product. The objective is mainly to draw the lessons of the event at the local scale and not to increase the overall scientific and technical knowledge.

A second type of post-flood investigations is conducted more systematically by technical services like the U.S. Geological Survey (Carter et al., 2002; Winston and Criss, 2002; Juracek et al., 2001; Bowers, 2001), the IRPI in Italy (Istituto di Ricerca per la Protezione Idrogeologica) for instance or by research institutions (Gilard and Mesnil, 1995; Hemain and Dourlens, 1989). The aim is then to document the extreme events. Most of the past works have been limited to a description of the event through the available measured data (rain gauge or river gauge measurements) and some field observations as cross-section surveys and corresponding peak discharge estimates generally for one single selected river reach (Rico et al., 2001; House and Pearthree, 1995; Gutknecht, 1994; Costa, 1987a; Jarrett, 1987). Sometimes the description of the sediment transfer processes, of their localisation and the estimation of the transferred volumes is provided (Alcoverro et al. 1999; Cariedo et al., 1998). A detailed rainfall-runoff analysis including the identification of the major runoff producing areas on the affected watersheds and the study of the relation between the time sequences of the floods and of the rainfalls is rarely done due to the lack of measured rainfall and discharge data. The inventory of extreme events and of their peak discharge values is of course important to define the range of the possibilities, to build envelope curves and to study the regional patterns of the river flood extreme peak discharges (O'Connor and Costa, 2003; Perry, 2000, Parde, 1958), or to reduce the uncertainties in flood frequency analyses (Payraastre et al., 2005).

But the recent developments of the measurement networks, especially Weather radar networks, open new perspectives for the analysis of flash-floods. Weather radar provides rainfall estimates at appropriate space and time resolutions. It seems therefore now possible to undertake an analysis of the rainfall-runoff dynamics (Borga *et al.*, 2007; Delrieu et al., 2005; Sächsisches Landesamt für Umwelt und Geologie, 2004; Gaume et al., 2004; Gaume et al., 2003a; Gaume et al., 2003b; Belmonte and Beltran, 2001; Ogden et al., 2000, Smith et al., 1996). This opens the possibility to answer questions such as:

- What are the rainfall-runoff dynamics during a flash-flood, and what is the influence of the watershed characteristics, of the initial soil moisture or ground water recharge conditions on this dynamics?
- As a subsidiary question, what type of watershed characteristics (slopes, land use, geology, soil types...) should be considered in a regional flood frequency analysis?
- What are the dominant flood generating processes during a flash-flood?
- Is the answer to this question dependent on the land-use and geo-morphological properties of the watershed?
- What part of the catastrophe can be attributed to anthropogenic factors (change in land use, deforestation, agricultural drainage, imperviousness, road network, river management)?
- Are the dominant processes the same during flash-flood events and medium flood events, and is it possible to extrapolate tendencies observed on medium flood events (flood frequency distributions, rainfall-runoff models)?
- What is the influence of "artificial" processes such as blockages and their breaking ups, or of the sediment load (i.e. mainly water flood versus hyper-concentrated or even debris flow) on the peak discharge and the shape of the rising limb of flood hydrographs?
- How do the existing flood forecasting models perform on such events?

Due to the time-space characteristic scale of flash-flooding, the majority of the upstream catchments affected by these floods are not gauged. In addition, the peak discharges can be spatially highly heterogeneous, even within small catchments: cross-section surveys and peak discharge estimates are also useful to map the discharges on gauged watersheds. A detailed flash-flood study should not be limited to the few gauged river cross-sections if some exist. Flash-floods are by definition rare events. If an intensive research activity is to be set up on these hydrological events, which seems to be the case according to the recent European research calls for proposals, it is necessary to develop specific

methods to collect and analyse the existing information about the floods when and where they occur and not to limit the analysis to the few events affecting gauged watersheds.

This report, based on past experience of post-flood studies, is a first attempt to propose some guidelines on how to identify, collect and analyse data available after a major flash-flood event. Three main types of data will be considered.

- Indicators of the peak discharge values: mainly cross-section surveys based on flood marks but also clues of flow velocities (video movies, witness observations, water super-elevations in river bends or in front of obstacles). The report presents and criticizes various indirect post-flood peak discharge estimation methods and puts the emphasis on validation procedures.
- Indicators of the time sequence of the flood: mainly eyewitness accounts where no stream gauge measurements are available. Accounts from eyewitnesses are occasionally cited in flash-flood studies, they have seldom been, to our knowledge, systematically collected and analysed.
- Sediment transfer processes (erosion and deposition on slopes and in river beds, hyper-concentrated, mud or debris flow) as the main focus of the post-flood investigation but also as an indication of the local runoff generation processes and flow energy and velocity.

Information on socio-economic aspects can also be collected such as geo- and time- references of accidents, qualitative description of public behaviour, and effectiveness of warning broadcasts, nature and extension of the damages caused to bridges, roads and buildings, but will not be discussed herein.

This report is based on illustrations of the hydrological valuations of the collected data. This, we hope, will convince the readers that the conclusions that can be drawn from post-flood investigations are worth the time spent to collect and analyse the data. Our common knowledge on flash-floods will only grow through the multiplication of post-flood field surveys for two main reasons. The conclusions drawn on one single event, based on inaccurate and partial data may be questionable and will be consolidated on the basis of repeated post-flood analyses. Various case studies are needed to determine whether the hydrological behaviour described for one flash-flood is a general pattern for the considered region or type of watershed or is an outcome of spatial and temporal specific circumstances (i.e. rainfall pattern, wetness state of the soils, soil types, geology of the watersheds...).

The report is structured into two parts: i) the presentation of a proposed post flood investigation methodology and ii) illustration of post flood hydrological analyses. We hope that the guidelines presented herein will contribute to the systematization of post flash-flood field investigations.

4.2 Principles of a methodology

The proposed methodology is presented in detail in a research report published within the European research project FLOODsite (Gaume, 2006). This report can be downloaded on the Floodsite Web site or directly obtained from the authors of the present report.

Table 4-1: Steps of the proposed data collation and analysis procedures.

Data collation process	Data analysis process
<p>Phase 1: Just after the flood Collect the data on the rainfall event (rain gauge measurements, radar images) to locate the affected areas If possible, first reconnaissance visit of the affected areas, pictures (flood marks, large debris, river bed state) can be taken, but no survey work can generally</p>	<p>Step 1: peak discharges estimation and mapping Based on the cross-sections surveyed, peak discharges and specific discharges can be estimated at various locations of the considered river and of its tributaries and reported on a map. Test of the spatial consistency of the estimates and comparison with rainfall data to get a first idea of</p>

<p>be conducted during the crisis time.</p> <p>Phase 2: A few weeks after the flood The cross-section surveys can begin as well as some interviews of witnesses depending on the local atmosphere.</p> <p>Phase 3: A few months after the flood It is certainly the best period for the survey work especially for the interviews. The area is fully accessible and the stress has fallen again. The river beds and marks may have been cleaned out, this is why the pictures taken in phase 1 or 2 are important. Collect additional data useful for the analysis (river gauge measurements, digital terrain model, soil, land-use, geological map, soil moisture measurements, satellite or pictures taken by plane, flood marks inventories...) Preparation of the rainfall-runoff simulations to support the interpretations.</p> <p>Phase 4: The year after the flood Due to the inaccuracy of the available data, a post flood investigation has some similarities with police inquiries. It is a long lasting work, requiring cross-checking and possibly returns to the phase 3.</p>	<p>possible runoff rates. A comparison with rainfall, geological, land use maps gives some first idea of the possible factors affecting the flood magnitude.</p> <p>Step 2: rainfall-runoff dynamics Where radar quantitative precipitation estimates appear reliable and where complete or partial flood hydrographs can be retrieved from measured data or accounts or documents (dated pictures) from the witnesses, they can be compared to simple rainfall-runoff (RR) simulations to get a better idea about the RR dynamics, especially about the evolution of runoff rates during the flood.</p> <p>Step 3: comparison with previous floods If step two could be performed, the same RR simulations can be conducted for previous large floods that occurred on the same catchment if it is gauged or on nearby similar gauged catchments.</p> <p>Step 4: Accompanying processes When the runoff is described, accompanying processes such as erosion intensity on hill slopes, sediment transport or local flow characteristics can be studied.</p>
---	---

Table 4-1 summarizes the proposed procedures for the collation and the analysis of the field data. We will here shortly add some additional comments about post-flood investigations and develop on some specific aspects of peak discharge estimation methods and of the use of sediment transfer and erosion evidences.

Three important ingredients are needed for an efficient field survey to be conducted. Firstly, the survey must be well prepared. This preparation includes organizational aspects but also the collation and criticism of the available data (geology, hydrogeology, soils types, measured rainfall rates and discharges, previous conducted hydrological studies on the area...) previously to the field work. The field survey must rely on knowledge of the analyzed watersheds and some initial questions concerning their hydrological behaviour. Therefore, a field survey campaign can hardly be conducted immediately after the flood event. Nevertheless, it is preferable to make a first round tour of the area just after the flood and take pictures to locate flood marks that can rapidly be removed and to have a clear reference state of the river system since river beds are generally rapidly cleaned up after a major flood event.

The second important aspect is the standardization of the type of data collected and of their storage formats and analysis procedures. This facilitates inter-comparisons and data archiving. Moreover, it is important to store all the raw data for an *a posteriori* criticism and discussion of their interpretation. The exact location of the surveyed cross-sections, or interviews should be clearly indicated, pictures taken and stored showing the local environment and specific reference points mentioned by interviewed people or hydraulic singularities which could have influenced the water levels, the surveyed values as well as the details of peak discharge computations and the accompanying hypotheses should be included, as the name of the persons who produced the document. Standard cross-section survey and interview summary forms have been therefore proposed and are presented in the appendix.

Finally, a post-flood field survey can never be an automatic application of a recipe. Each case study has its own specificities. Like in any inquiry on complex situations, it is necessary to develop a terrain observation skill for the selection of the most suited cross-sections for peak discharge estimations and for the detection and the valuation of any possible clue: flood marks, erosion evidences on hill slopes

or in the river beds, films and pictures... Also discharge estimation validation, consistency testing and the search for additional information to confirm the first guesses or conclusions should be a constant concern in post event field surveys. The two following examples illustrate this principle.

4.3 Peak discharge estimation approaches

Peak discharges can be estimated in ungauged sites after a major flood event on the basis of flood marks and surveyed river cross sections. Without direct current meter measurements, these estimates rely on hydraulic modelling and on sound engineering judgment. The sources of uncertainties and errors are numerous: choice of the appropriate surveyed river reaches that must not have been too much modified by sediment movements (erosion or deposition) and not affected by mud or debris flow or blockages, estimate of water levels or water longitudinal profiles through flood marks, choice of the roughness coefficient values.

Flood marks for instance may either indicate the water level in still water areas or the total hydraulic head on obstacles located in the flow. Flood marks in vegetation on river banks or in the flood plain where the flow velocity is reduced should be preferred. Moreover, marks may have been deposited on vegetation temporarily bent by the flow, may have slid down a smooth support, or be the result of water projections. To reduce uncertainties, as many as possible flood marks should be surveyed in a given cross section. Concerning the roughness coefficient, tabulated values (Benson and Dalrymple, 1967) and empirical equations (Chow, 1959) exist. But they were established in cases of moderate floods and low-gradient streams and it seems that the apparent roughness of a stream has to be significantly increased for extreme floods to obtain realistic discharge estimates (Gaume et al., 2004; Jarrett, 1990; Jarrett, 1987).

For all these reasons, it is necessary to seek for various sources of information to enable a cross-checking and to reduce uncertainties and avoid significant errors: select more than one cross-section for each river reach with significantly different cross-sectional shapes and areas, test the upstream-downstream consistency of the estimated discharges on a watershed, and also evaluate directly the possible flow velocity ranges on films and pictures, use sediment transport and erosion indicators, and test the rainfall-runoff consistency. Some examples of discharge estimation checking and validation are presented in the next section.

Field surveys provide cross-sectional wetted areas which accuracies depend on the accuracy of the flood marks. Velocity profiles or average velocities must be determined to evaluate the corresponding discharge values. This is mainly where the hydraulic models are needed. In rivers with shallow slopes – typically 1/1000 or less – one-dimensional hydraulic models are necessary owing to the distance over which backwater effects propagate (see Naullet (2002) for an illustration): i.e. most generally the flow is subcritical even during extreme flood events except in some specific cross-sections (Jarrett, 1987). Note that the definition of the downstream boundary condition is in this case an additional source of uncertainty. In complex cross-section shapes, in the surroundings of bridges or in urban areas, two-dimensional hydraulic models may be needed to capture the complex pattern of transversal and longitudinal velocity profiles (see Denlinger et al. (2001) for an illustration).

In the case of relatively steep river channels in headwater catchments affected by flash floods – slopes typically larger than 0.5% - a uniform flow assumption may provide fair velocity estimates if compared to 1-D hydraulic models, provided that the selected section is sufficiently far (some hundred meters) upstream or downstream an obstacle or change of shape or slope of the channel. Moreover, the cross-sectional shape of these headwater streams is generally simple: a trapezoidal main channel with floodplain of limited extent. The flow is basically one-dimensional.

For these reasons, the most commonly used method to evaluate peak-discharge values after major flash flood events in headwater catchments is the so-called slope conveyance method or the slope area method which is an extension of the former (Webb and Jarrett, 2002; Costa, 1987). It is based on the

application of the Manning-Strickler empirical formula, with an assumption of uniform flow (friction slope S_f equal to the river bed slope S).

$$V = Q / A = KR^{2/3} S_f^{1/2} \quad (1)$$

Where V is the so-called average velocity (m/s), Q is the discharge in (m³/s), A is the wetted cross section (m²), R is the hydraulic radius ($R=A/P$, with P the wetted perimeter in m), and K known as the Manning-Strickler roughness coefficient depending on the river cross-section characteristics which generally takes its values between 5 and 100. The parameter $n=1/K$ is also often used in the technical and scientific literature.

In cases where the flow is not confined in the main river channel but covers also a flood plain, the section has to be subdivided into a main channel area and a right and left overbank flow area, and the discharge calculated separately for each of the sub-areas (Chow, 1959).

The slope conveyance method has also the great advantage to be rapid and enables the evaluation of a large number of peak discharge values for a single flood event and hence the mapping of the flood flows over the area of the affected watershed and reveal the spatial heterogeneities of the runoff which is one of the objectives of post event surveys.

Independently on the hydraulic model chosen, it is important to keep in mind that the data collected are necessarily incomplete and affected by uncertainties, that some local flow characteristics (backwater effect, obstacles limiting the flow in the flood plain...) may be missed out during the field survey, that the method used, especially the Manning-Strickler formula are empirical approximations which may not be extrapolated reliably to the extreme flow conditions encountered during extreme flash flood events (high velocities, significant sediment concentrations). Therefore, peak discharge estimates after flash flood events can not be only based on a single site and single method approach. It is absolutely necessary to search for additional information to check and validate the proposed peak discharge estimates. The next two sections give some examples of how this additional information can be evaluated.

Finally, even after a thorough validation, it is the opinion of the authors that an uncertainty bound of at least 30 to 50% should be added to the estimated peak discharges estimated after flash flood events occurred on headwater catchments. According to the magnitude of the observed flows during such events and to the important spatial and temporal gradients, this large uncertainty does nevertheless not prevent further analyses.

4.4 Discharge estimation checking and validation

Among the possible sources of additional information available for discharge estimation checking, pictures and films taken by eyewitnesses are now often available after major flood events. On these images, super-elevations in front of obstacles located in the flow as trees or piers of bridges may be visible (Figure 4-2). This super-elevation is linked to the flow velocity. The application of the Bernoulli formula gives the range of possible values for the flow velocity in the vicinity of the obstacles, a value that can be compared to the estimated average flow velocity Q/A computed for nearby cross-sections.

$$y_1 + \frac{V_1^2}{2g} = y_2 \Rightarrow V_1 = \sqrt{2g(y_2 - y_1)} \quad (2)$$

With y_1 and V_1 the water depth and mean velocity in the area surrounding the obstacle, and y_2 the water depth in front of the obstacle.

This method has the great advantage to be non-parametric unlike the Manning-Strickler formula and the super-elevation is relatively sensitive to the velocity. It makes it possible to distinguish between moderate velocities, less than 2 m/s and super-elevation lower than 20 cm, high velocities, 3 to 4 m/s corresponding to super-elevations between 40 and 80 cm, and extremely high velocities, more than 1 m of super-elevation. On Figure 4-2, the super-elevation in front of piers of a bridge can be seen. They indicate that the flow velocity may have exceeded 4 m/s on the outside bank of the river bend in front of the bridge and that the average velocity must have been close to 3m/s under the bridge, about 50 cm super-elevation in front of the central pile and almost no velocity on the inside bank of the bend (pictures taken just after the flood peak).



Figure 4-2: Example of a super-elevation in front of bridge piers located in a river bend and showing a lateral velocity gradient : 0.8 to 1 metre in front of the left bank pile, about 0.5 in front of the central pile and neglectable on the right bank pile. July 2007, Mill Burn, Northumberland, Great-Britain.

Image tracking methods can also be used to assess water surface velocities and hence discharges on films (Fourquet, 2003). But their application on films taken by eyewitnesses with a generally moving camera requires a preparation survey of the filmed river reach and the identification of the viewpoints of the camera. To our knowledge, this method has only been applied on controlled cross-sections with fixed cameras for the moment (Creutin et al., 2003).

Likewise, when possible, a consistency test of the estimated peak discharges and of the measured rainfall rates available on the watersheds upstream of the considered river cross-sections should also be conducted. It can at least reveal peak discharge over-estimations: except if an important dam breach occurred during the flood event, the comparison of peak discharges and rainfall intensities should not lead to runoff rates significantly greater than 1. Two methods can be used to test this consistency: (i) application of the so-called “rational method” and comparison of the specific peak discharge (in mm/h) and the event maximum rainfall intensity over a time period close to the estimated time of concentration of the considered watershed, (ii) rainfall-runoff simulation with a constant runoff rate value taken equal to 1 (see Figure 4-7 and Figure 4-8).

Table 4-1 presents some data produced by the U.S. Geological Survey concerning extreme flash-floods that occurred in the United States (taken from Costa, 1987b). In each case, the application of the rational method reveals that the estimated discharges are dubious when compared to the reported measured rainfall intensities. The time of concentration of the Bronco creek is for instance comprised between 1 and 2 hours according to its area. The estimated discharge value would require an average

spatial rainfall intensity at least twice as high as the maximum reported point rainfall intensity over 0.75 hours. This is of course not impossible, the watershed may have been affected by much more intense rainfall not captured by the rain gauge network, but very unlikely. The possible over-estimation of the peak discharge value has been confirmed by other studies for this specific flood event (House and Pearthree, 1995).

Table 4-2: Some examples of maximum peak discharges estimated by the U.S. Geological Survey (Costa, 1987b). Comparison of the unit discharge and of the rainfall intensities

Location	Date	Drainage area (km ²)	Discharge (m ³ /s)	Unit discharge (mm/h)	Measured rainfall intensity
Humbolt river tributary near Rye Patch (Nevada)	31.05.1973	2.2	251	410	127 mm/1h
Meyers canyon near Mitchell (Oregon)	26.7.1965	32.9	1540	169	102 mm/2h
Bronco creek near Wikieup (Arizona)	18.01.1971	49.2	2080	152	89mm/0.75 h
Jimmy camp creek near Fontain (Colorado)	17.06.1965	141	3510	90	203 mm/ 6 h

Likewise, the same procedure leads to some doubts concerning the three other peak discharge estimates. In each case, the estimated peak discharges require that the majority of the measured rainfall amount has fallen homogeneously in space over the watersheds during a reduced duration corresponding to the time of concentration of the watershed: 70 mm over 10 minutes for the Humbolt river tributary, 85 mm over 30 minutes for the Meyers canyon and 180 mm over 2 hours for the Jimmy camp creek. Such rainfall rates are really exceptional, especially in the conterminous United States (Costa, 1987) and particularly if they represent spatial mean rainfall rates rather than point rainfall intensities.

4.5 Sediment transport or erosion evidences

Sediment transport phenomena may be a central topic of a post flood field survey. They may also reveal active hydrological processes or local flow characteristics. In river reaches where clear evidences of bed load sediment transport exist and the sediment size is homogeneous, it is possible to use the Shields relation between the characteristics of the flow, critical shear stress and characteristics (diameter) of the particles of the river, to assess the possible range of a critical flow velocity that can have led to the displacement of these particles. Of course, there is a risk of under-estimation since the river bed deposits visible after the flood event may not be representative of the flood peak, but may have been deposited during the decreasing limb of the flood. Moreover, this approach is highly uncertain. It must not be used to deliver a first guess of peak discharge value in a river reach but as one possible approach to check discharge values estimated otherwise.

It is admitted that significant bed load is induced when the Shields parameter exceeds 0.047 (Eq. 3).

$$\tau^* = \frac{\gamma_w R S_f}{(\gamma_s - \gamma_w) d} > 0.047 \quad (3)$$

With d the diameter of the particles, $(\gamma_w - \gamma_s) / \gamma_w$ the ratio between the volumetric weights of the water and the solid particles, generally close to 1.6 for mineral particles.

Combining Eq. 3 and the Manning-Strickler formula (Eq. 1) with the hypothesis that the river bed and banks' roughness is determined by the size of the particles, i.e. the river bed is flat, with $K=21/d^{1/6}$ (Degoutte, 2006), leads to the empirical Eq. 4.

$$V = 5.8 R^{1/6} d^{1/3} \quad (4)$$



Figure 4-3: Galeizon tributary reach estimated discharge (45 to 75 m³/s) for 3.2 km². 1999 floods in the Aude region (France)

In the example presented on Figure 4-3, the river bed material has undoubtedly been deposited during the flood event. The river gravel diameters are relatively homogeneous, sign that no bigger particles were transported during the flood. The water depth during the peak of the flood was approximately equal to 2.5 metres according to the flood marks (R=1.25 metres). The diameter of the river bed material is comprised between 10 and 20 cm which leads to a flow velocity estimation using Eq.4 of 3 to 3.5 m/s, consistent with the slope conveyance estimation.

Moreover, erosion processes on hill slopes may reveal active hydrological processes and particularly the saturation of the soil necessary to induce slope failures and subsurface flows. As an example, the analysis of the data collected during the recent post flood investigation conducted after the September 2007 flood on the Selscica Sora river in Slovenia has revealed low runoff rates and conversely high infiltration rates into the soils of the watershed as well as a rapid release of a significant part of these infiltrated volumes after the storm, sign of an efficient drainage of the hill slopes. Such a hydrological response is surprising for a mountainous watershed with steep slopes, shallow soils and a bed rock mostly composed of schist stones.



Figure 4-4: Examples of a shallow slope failure and erosion rills observed on hill slopes after the September 2007 flood on the Selscica Sora basin (Slovenia)

As illustrated on Figure 4-4, the storm event induced shallow slope failures and erosion rills on almost every hill slope of the watershed. They confirm that the soil and weathered bed rock covering the hill slopes have been saturated during the storm event. The erosion rills also reveal an active subsurface flow in fractures of the bed rock. The drainage of the hill slope through these fractures may explain the observed rapid release of one part of the infiltrated water volumes just after the flood event.

The two previous illustrations concerning peak discharge estimates and sediment transport and erosion evidence valuations have shown the variety of information sources that can be mobilized after a major flash flood event. The next section presents some examples of the type of hydrological lessons that can be drawn from post flood investigations.

4.6 Illustration of some interpretation results

The data analysis illustrations will be mainly based on two flash-flood examples well known by the authors: the 2002 floods in the Gard region and the 1999 floods in the Aude region, both major events that occurred in the south of France. These are the floods on which the post-flood investigation methodology presented herein has been developed and tested. To our knowledge, among the published works on flash-floods, these two case studies led to the most detailed rainfall-runoff interpretations. The majority of the data and analyses presented hereafter have already been published (Delrieu et al., 2005; Gaume et al., 2004; Gaume and Bouvier, 2004; Gaume et al., 2003b). Our aim here is to show what type of knowledge can be acquired based on post-flood investigations. The focus will be put on two main questions: a) what does the spatial pattern of peak discharge values reveal about the rainfall-runoff processes and b) what is the rainfall-runoff dynamics and its variability during extreme floods? More recently, other post-flood field investigations have been conducted in Italy (Borga *et al.*, 2007) and in Slovenia within the European research project HYDRATE. These two case studies will be referred to in the conclusions of this report. They reveal significantly different reactions of south Alpine watersheds to extreme rainfall events.

4.6.1 Spatial pattern of peak discharge values: where did the flood generate?

The estimated peak discharge values can be used to identify the relative contributions of the various sub-areas of watersheds affected by flash-floods. A first example is given in Figure 4-5 for a 300 km²

watershed affected by the 1999 storm events in the Aude region in France. In this case, the mapped peak specific discharges clearly show a high spatial heterogeneity of the runoff contributions. The estimated peak discharge is about 50 times higher downstream Tuchan than upstream of Padern (9 versus 0.2 m³/s/km²) for similar watershed areas and while the two locations are separated by less than 10 kilometres. This peak discharge distribution is consistent with the observed rainfall amount repartition. The western part of the watershed received about 200 millimetres of rainfall within 24 hours while the north-eastern received more than 400 millimetres. A desk-top application of the “rational method” with estimated time of concentration of the watersheds indicates that the runoff rate has probably remained lower than 10% upstream of Padern and must have been close to 100% around Tuchan to explain the estimated discharges. The observed high spatial heterogeneity of the peak discharges reveals the non-linearity of the rainfall-runoff reaction of these watersheds, linked, as we will be able to see in the next section, to the high initial infiltration and storage capacities of their soils and sub soils.

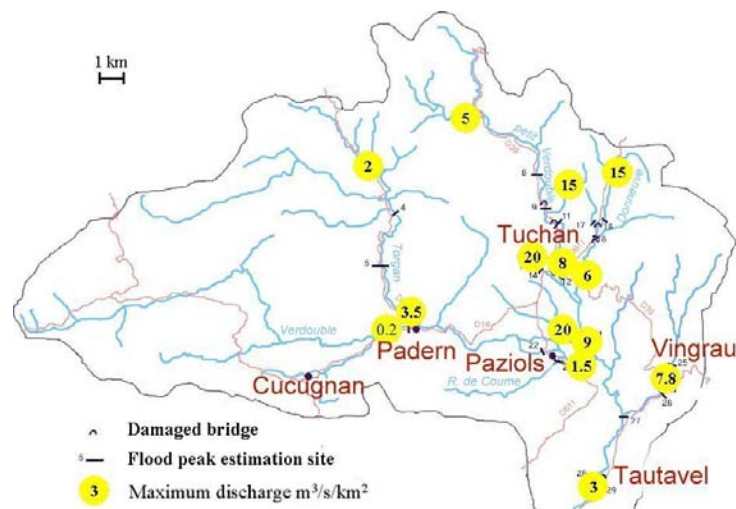


Figure 4-5: Estimated specific peak discharges on the Verdoubie watershed (300 km²) after the 1999 floods in the Aude region.

A second example of a peak discharge map is given in Figure 4-6 for the three main river systems of the Gard region affected by the 2002 storm event. The spatial pattern appears here much more homogeneous but with at least two exceptions. In the north-east, the peak discharge of the upper Alzon river (number 16 on Figure 4-6) appears as significantly lower as the ones of the surrounding watersheds. This area is highly karstified, and the karstic aquifer feeds a perennial source located a few kilometres upstream the surveyed cross sections. This Fontaine d’Eure source is one of the most important of the region and had therefore been harnessed by the Romans to supply the Nîmes city with drinking water through the famous Pont du Gard aqueduct. The mapped results appear to show that this extended karstic system has had a significant attenuating effect on the flood of this watershed. Another outlying watershed appears in the south of the considered area on the Vere stream (number 2 on Figure 4-6). After exchanges with local geologists, it was apparent that this stream has been fed by the overflow of the karstic aquifer which covers a large area located in the north of this watershed. Pictures taken on the Vere watershed indicate that some karstic resurgence appeared during the 2002 flood and were still active a few days after the storm event.

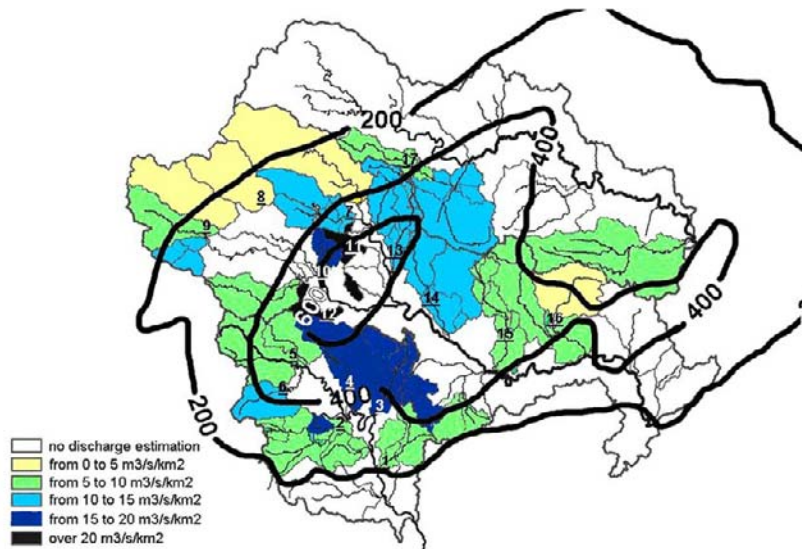


Figure 4-6: Specific discharges estimated after the 2002 floods in the Gard region and contour lines of the rainfall amounts (millimetres) received on the 8th and 9th of September 2002.

These two examples illustrate how spatial heterogeneities as a sign of differentiated hydrological processes, can be revealed through a detailed mapping of peak discharge values.

4.7 Variability of the rainfall-runoff dynamics: how has the flood been generated?

In some cross-sections, it is possible to identify various water levels referenced in time, owing to the number of witnesses and the level of detail of their accounts: typically the time of the river bank overflow, of a bridge overflow, the time of the various flood peaks. These points of reference can be compared to the outputs of very simple rainfall-runoff models fed with radar quantitative precipitation estimates to evaluate the range of possible runoff rates over the flood event. One example is shown in Figure 4-7. The information gathered through interviews appears as bars. The vertical range represents the uncertainty in the discharge estimates – relatively large – and the horizontal span, the uncertainty in time evaluated after validation of witnesses’ accounts (Gaume *et al.*, 2004) (+/- 15 minutes with regard to the time indicated by the witnesses). The rainfall-runoff model is a distributed model combining a SCS-CN (Soil Conservation Service – Curve Number) production function (Soil Conservation Service, 1973) and a kinematic wave transfer function (Gaume *et al.*, 2004). The main adjustment parameter is the so-called curve number CN, taken homogeneous over the watershed area and representing a water storage capacity S on the watershed: $CN=100$ means $S=0$ mm, $CN=70$ means $S \approx 100$ mm and $CN=50$ means $S \approx 250$ mm.

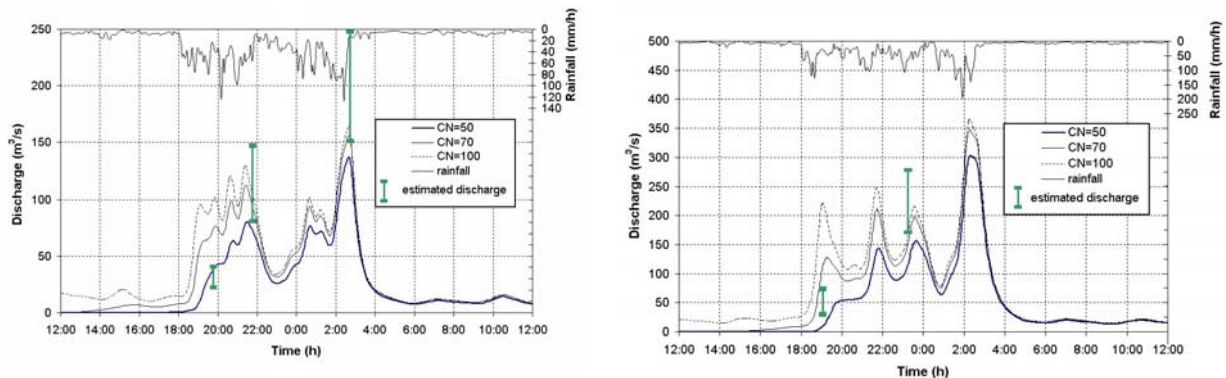


Figure 4-7: Comparison between estimated and simulated discharges for two upstream watersheds in the Aude region after the 1999 floods: (a) Tournissan (10 km^2), (b) Verdoul (18 km^2)

The comparison of the points of reference and of simulated flood hydrographs for two headwaters affected by the 1999 storm in the Aude regions reveals two main characteristics of the flash-floods. First, over bank flow, first bar on the two graphics, occurs late in the storm event and reveals that despite the high rainfall intensities, a large proportion of the initial rainfall volumes did not produce significant runoff and were stored on both watersheds, probably infiltrated in the soils and sub-soils. The adjusted CN value leads to an evaluation of the runoff deficit of about 250 millimetres (CN=50). This value is relatively high but confirmed by other data collected on the Aude flood (Gaume et al., 2004) and in accordance with values estimated for other flash-floods (Borga *et al.*, 2007; Belmonte and Beltran, 2001; Cosandey, 1993). On these watersheds, high intensity rainfall rates seem not to be sufficient to trigger a flash-flood, but a rainfall accumulation (i.e. a certain level of saturation) is necessary. Despite the relatively high rainfall intensities (more than 50 mm/h), the 1999 flash-floods producing processes seem not to be of the hortonian type. Second, the Tournissan and Verdoul watersheds have the same type of bedrock but while 50% of the Tournissan watershed area is covered by vineyards, the Verdoul watershed is essentially covered by forest and scrub. According to the level of accuracy of the available data it is not possible to reveal a clear difference in the rainfall-runoff dynamics of both watersheds. The land use type may have an influence on the rainfall-runoff response, but it is not a first order effect for this specific flash flood.

Figure 4-8 shows another example of rainfall-runoff analysis for two headwaters affected by the 2002 floods in the Gard region. In these cases, the complete flood hydrographs could be relatively accurately reconstructed using existing water level measurements in flood control dam spillways. The comparison with the same simple rainfall-runoff model leads to significantly different conclusions, illustrating the variability of the rainfall-runoff responses depending on the watersheds. The adjusted CN value for the Crieulon stream (70) indicates a moderate water retention capacity of the soils and sub soils, about 100 millimetres, much lower as in the Aude case study. Moreover, the rainfall-runoff model is not able to reproduce the flood hydrograph of the Vidourle watershed. Its runoff coefficient never seems to exceed 50%: the watershed still has some rainfall water retention capacities even during the peak of the flood. Moreover, unlike what is observed on the Crieulon, a relatively high discharge, not simulated by the rainfall-runoff model, remains after the rain event has ceased indicating that a part of the temporary stored rainwater is rapidly returned to the stream after the event. About one third of the flood volume is released during the few days after the flood event in the case of the Vidourle river. Taking into account this late released volume, the retention capacity of the Vidourle watershed appears also to be about 100 millimetres.

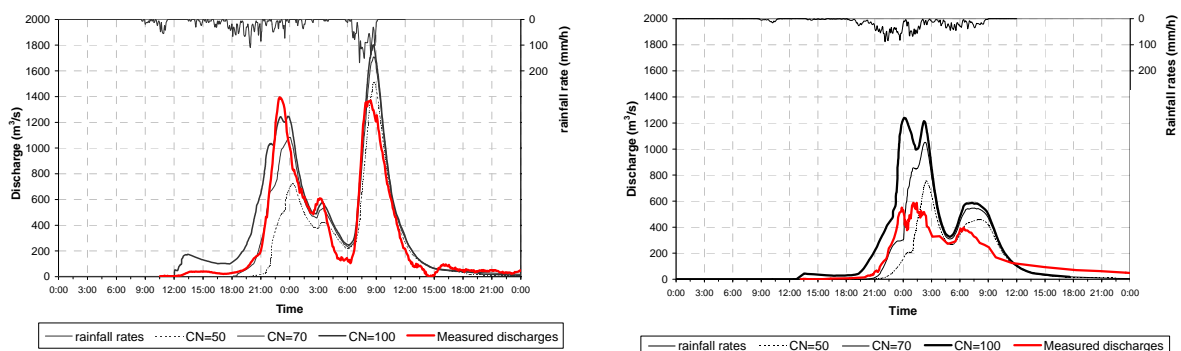


Figure 4-8: Comparison between estimated and simulated discharges for two upstream watersheds in the Gard region after the 2000 floods: (a) Crieulon (90 km²), (b) Vidourle (80 km²)

The geology and the corresponding soil types can be put forward to explain those clear differences in the rainfall-runoff reactions of both watersheds. The Vidourle watershed is mainly composed karstified limestone which may explain its large retention capacities during the flood but also the rapid release of one part of the water stored in the karst after the flood. As for the Crieulon catchment, it is

mainly composed of marls. The analysis of data collected on other headwaters revealed a reaction similar to that of the Crieulon for all the watersheds on marls, highly variable dynamics of karstic areas and a surprise. The watersheds located in the mountainous part of the Gard region with steep hillslopes and bedrocks composed of granite or schists reacted in a way very similar to karstic areas: high infiltration and retention capacities during the storm event and rapid release of one part of the stored water volumes of the flood. Further field investigations and infiltration tests have revealed that the upper schist and granite layers are highly fractured and weathered and have confirmed the very high retention volume and permeability of this layer (Ayrál, 2005). This is consistent with the conclusions of recent post flood studies conducted in the Adige region in Italy (Borga et al., 2007) and Slovenia that revealed huge infiltration and storage capacities on south alpine watersheds with limestone but also schist bedrocks. Steep slopes and *a priori* impervious plutonic or metamorphic bedrocks are not necessarily associated with rapid runoff during high intensity rainfall events! Such counter-intuitive results reveal the gaps in the hydrological knowledge and the need for further post-flood analyses.

4.8 Conclusions

We hope that these few examples have convinced the readers of the usefulness of post flash-flood surveys. It is a tedious and difficult task. We have shown here that recent surveys have revealed important and sometimes unexpected aspects of flash-floods: the importance of the geology and soil types, counter-intuitive behaviours of some areas, limited impact of the land use type, limited contribution of hortonian runoff processes in vegetated catchment even during intense rainfall events. These observations may also lead to a better understanding of the underlying flood generating processes.

A post-flood survey procedure has been suggested herein as well as some analysis methods. It is a first proposal which certainly will be amended. But beyond the procedure and methods, it is important to keep in mind the general philosophy: the data collected are necessarily inaccurate, no method is perfect and the very first concern must be to verify, cross-check, verify and cross-check again. It is the only way to limit the risks of errors on peak discharge estimates for instance as illustrated herein. Moreover, a written methodology is a necessary condition for efficient post flood surveys. The outcome of such investigations depends also highly on the observational skill of the involved hydrologists, on their ability to depict indices and clues (flood and erosion marks) in the landscape, to ask the right questions to the eyewitnesses and technical services. Finally, field surveys are also an excellent exercise for young or even senior hydrologists to maintain and extend their expertise.

5. Development of a flash food forecasting chain for the Besos catchment in Catalunya

5.1 Introduction

This study describes the characteristics of a new generation of software tools that have been designed in order to fit the requirements of flash flood risk management in the area of Barcellona (Catalunya, Spain). Three main aspects of this system are described: 1) Visualization tools, evolving to a more easy-to-use and easy-to-interpret platform; 2) Modularisation of the system, related to the optimisation of the computations in the server, improvements in real-time data acquisition and storage, and operational radar data management and processing; 3) New capabilities and processed information offered to the decision makers, synthesizing spatially distributed warnings over the land.

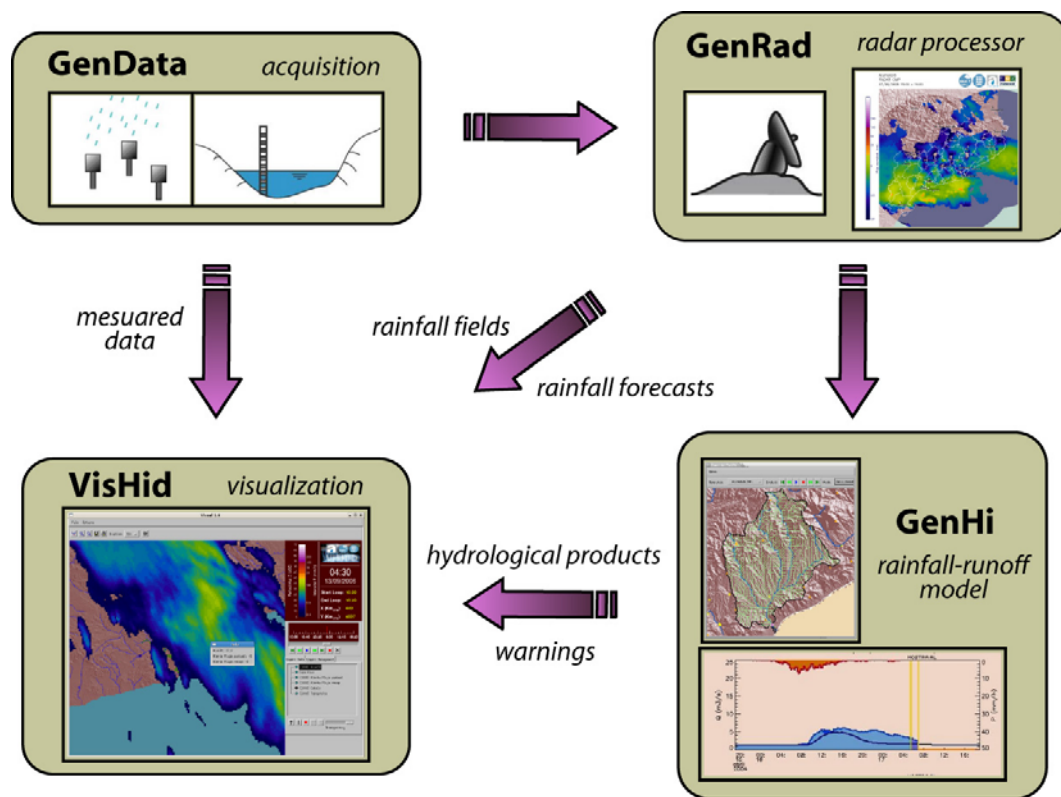


Figure 5-1: Scheme of the EHIMI warning system

It is relevant to illustrate the background of this initiative. The first hydrological studies focused in flash floods in this area were based on the systematic comparison between radar and rainfall estimates from a hydrological perspective (Corral et al, 2005). Both processed radar and rainfall estimates using the splines technique were introduced as input to the DiCHiT hydrological model in different events (with the classical separation between the calibration set and the validation one). In general, results from the radar experiment were worst (in terms of the objective function and also by eye inspection), and there were some special cases where the bad radar performances could be related to problems in the effective current processing of radar data.

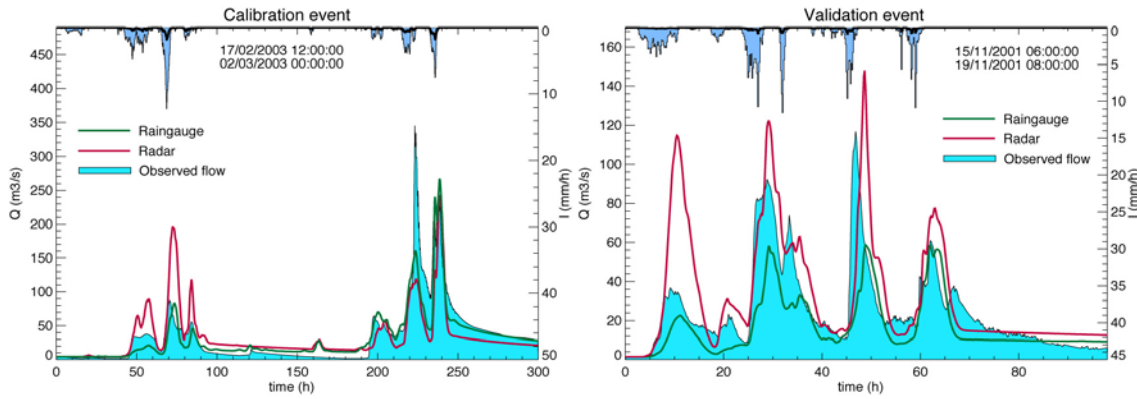


Figure 5-2: Comparison of hydrograph results using different rainfall inputs after model calibration (processed radar and raingauge interpolation).

In parallel to radar processing, improvements have been made in radar-raingauge merging, proposing a methodology based on the Kriging with External Drift (Velasco et al, 2007a). GRAHI-UPC has continued the study of analysing the effects of rainfall inputs to the hydrological model performances. In addition to this, it was interesting to analyse the effects observed in the simulated discharges induced by changes in the structure of the rainfall-runoff model (Velasco et al, 2007d). Two distributed models have been applied and compared on the Besos basin: 1) DiCHiTop, based on a coupled Topmodel-SCS approach; 2) WBrM, consisting of a piecewise linear approximation of non-linear soil moisture processes based on conceptual approaches.

Different types of estimated rainfall fields have been used to assess the sensitivity of hydrographs to rainfall spatial structure. Observed discharges are therefore compared with simulated discharges obtained using only raingauge data (Ordinary Kriging), its basin averaged rainfall, radar information (processed radar images), and finally merged radar-raingauge rainfall fields (Kriging with External Drift). The parameter set of each model was calibrated independently for each type of rainfall field over the same set of events.

The results have shown that discharge simulations using rainfall fields taking into account the spatial variability of rainfall (i.e., radar, or merged radar-rain gauge fields) provide the highest performances in both calibration and validation events (in terms of Nash Efficiency). Regarding the model structure, WBrM model gave highest performances in the calibration events, but in contrast, its performance fell behind DiCHiTop simulations in the validation set.

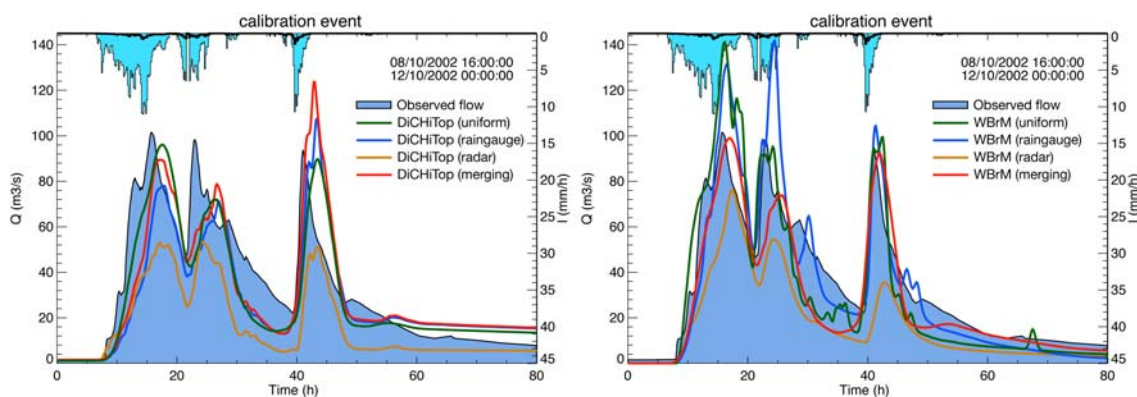


Figure 5-3. Comparison of model performances using the DiCHiTop model (left) and the WBrM model (right), after model calibration for multiple events, using different rainfall fields.

In accordance to FLOODsite objectives, the final purpose of this study is to relate economic efforts needed to implement efficient flood warning systems with the expected reduction of damages, in zones prone to be affected by flash-floods. This project involves the application of three distributed rainfall-runoff models in two different basins (the Besos basin in Catalunya, Spain, and the Traisen basin, in Austria). One of the objectives is a model intercomparison, with the aim to recognise similarities and differences in hydrological modelling from different structures, and to evaluate performances in different climates (Mediterranean and Alpine).

5.2 Radar rainfall estimation and nowcasting

From the results obtained in these previous studies, the effort was led to correct some of the main errors in radar rainfall, particularly the VPR correction (Franco et al, 2007) and the identification of non-precipitating echoes related to anomalous propagation (Berenguer et al, 2006).

Related to the VPR correction, a new method has been proposed, consisting of several steps: 1) Partitioning the radar volume in zones with different types of precipitation (identification of the bright band, detection of convective cells using the algorithm proposed by Franco et al., 2006); 2) Obtaining a representative stratiform VPR (spatial and temporal averaging of the observed stratiform VPRs near the radar); 3) Extrapolation of the radar reflectivity measurements to the ground level (in stratiform zones the representative stratiform VPR is applied; in convective zones the lowest PPI values are used); 4) Obtaining rain intensity from the estimated reflectivity at ground (a specific Z-R relationship is applied depending on the precipitation type (Sempere-Torres et al., 1999). A comparison of these PVR corrected estimates against accumulated raingauge measurements has been used to validate the methodology in the Hydrological Observatory of Catalunya. It is shown that this methodology improves considerably the rainfall estimates when the lowest PPI is affected by the bright band (in general associated to stratiform events), but some problems remain in case of convective precipitation and in zones located far away from the radar (usually between 60 and 100 km in the Spanish environment). In addition, it is shown that near the radar an adequate substitution by the lowest PPI is a good choice instead of the VPR correction (also for stratiform rainfall).

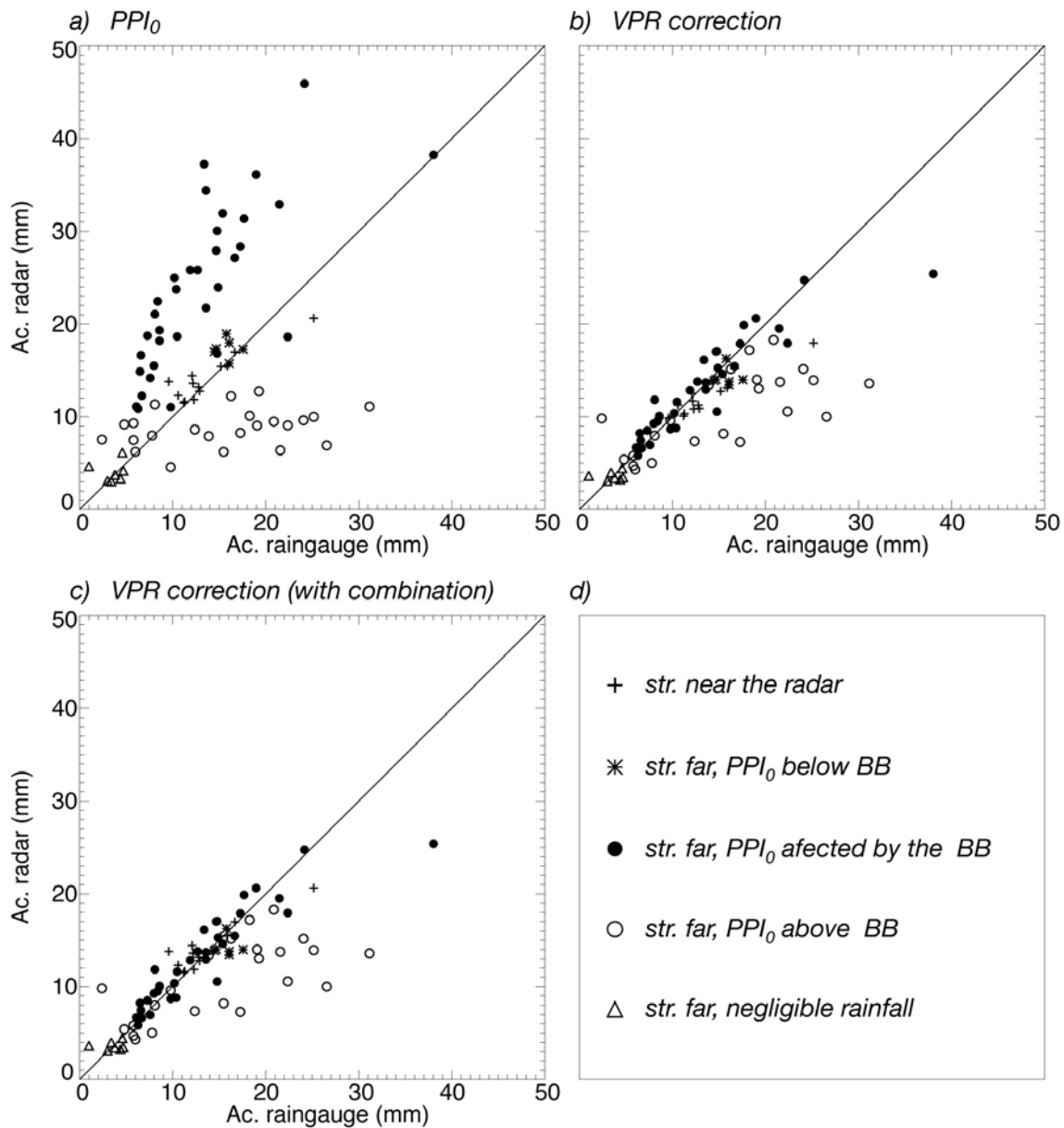


Figure 5-5. Scattering plots of radar against raingauge accumulated rainfall for the event registered by the radar of the INM in Barcelona: from 5th of January of 2003 21:30 UTC to 6th of January 07:40 UTC. a) Rainfall field directly obtained from the lowest PPI. b) Rainfall field using the proposed VPR correction method; c) Same as (a), but near the radar, where the lowest PPI is below the bright band, the rain rate has been obtained from the lowest PPI. In the legend, "str" refers to stratiform, and "far" refers to further to the predefined 22-km circle from the radar.

A radar based rainfall forecasting technique is operationally implemented in the EHIMI system. The selection of this algorithm was made after the comparison between a sophisticated technique (S-PROG) and a reference technique (Lagrangian persistence), from two different perspectives (Berenguer et al, 2005): a) comparing forecasted precipitation fields against radar measurements; b) by means of a distributed rainfall-runoff model, comparing hydrographs simulated with a hydrological model using forecasted rainfall fields against hydrographs generated with the model using the entire series of radar measurements. Using the multiple step ahead methodology (in different subcatchments of the Besos basin), and taking the Nash Efficiency parameter to evaluate the performance, the main conclusions of the study were: 1) The use of a radar-based nowcasting technique can increase the lead

time of a warning system between 20 and 80 minutes (depending of the event), added to the response time of the catchment; 2) The crucial factor to improve the quality of forecasted flows is the quality of the forecasted mean areal rainfall over the basin; 3) Although in rainfall terms the S-PROG can be considered superior to Lagrangian persistence, in terms of simulated hydrographs the S-PROG filtering of higher intensities produces inadequate results, and it is not recommended for hydrological purposes in its current version.

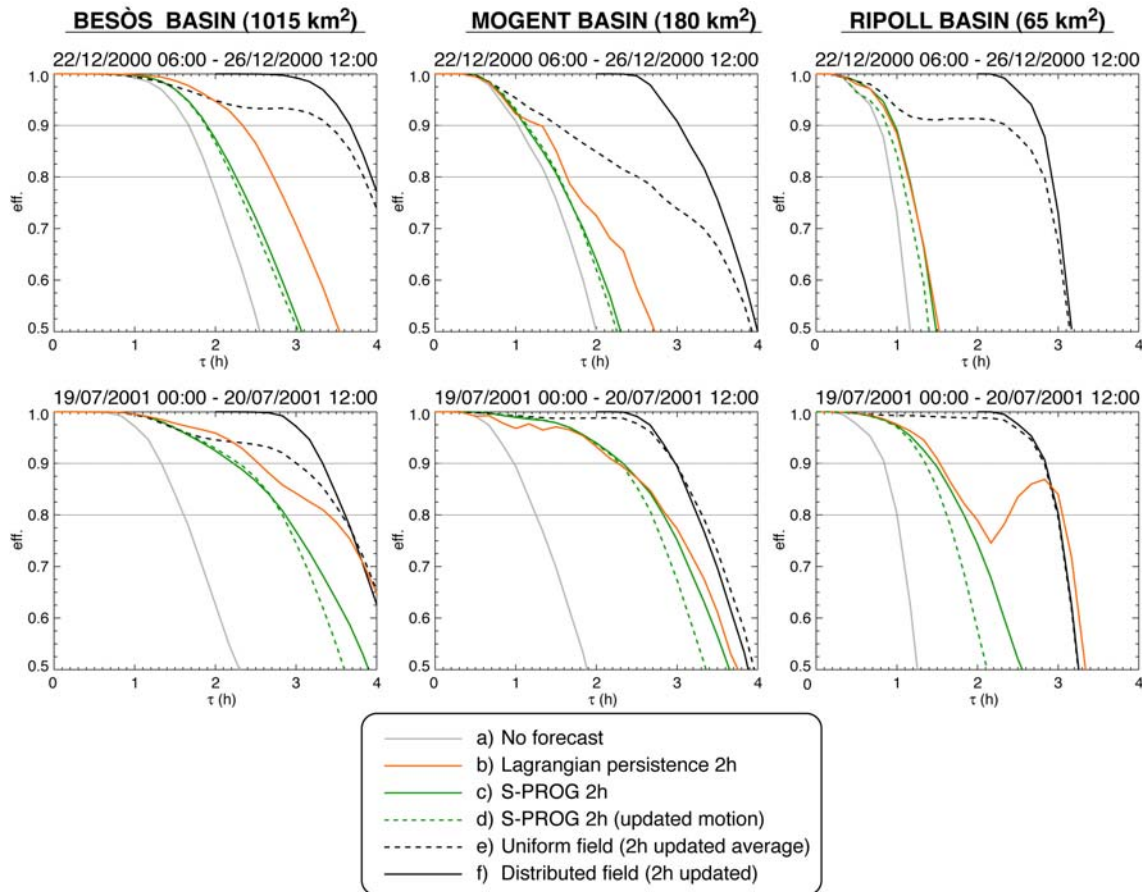


Figure 5-6. Evolution of the Nash efficiency of the forecasted hydrographs as a function of the anticipation with which hydrographs are simulated (τ). The different lines represent hydrographs simulated with precipitation fields forecasted using different techniques: a) with no forecast; b) by Lagrangian persistence; c) by S-PROG, d) by S-PROG using “updated distributed motion fields”; e) with 2 h of a uniform field with the observed mean areal rainfall, f) with 2 h of actual radar scans.

5.3 Implications for flood forecasting

An extension of the analysis with different nowcasting techniques is based on a sophistication of the Lagrangian persistence technique, accounting for the uncertainty due to the growth and decay of rainfall intensities, by the implementation of the String of Beads model (Pegram and Clothier, 2001). The methodology mixes an auto-regressive model in the temporal scale, and a power-law spectrum decomposition in the spatial scale. This technique allows the analysis of the rainfall forecasting and its implications in runoff forecasts in a probabilistic way, assuming the error is related to the rainfall structure error. Results of a first approach show that: 1) Mean areal rainfall over the basin can differ by an order of 3 in relation to the reference rainfall (confidence range of 70%); 2) The non-linearity of

the system (hydrological model) does not always translates to a strengthening of the confidence range of probabilistic runoff forecasts; 3) The anticipation with which hydrographs are well simulated (in terms of Nash Efficiency) ranges from the response time of the catchment (around 2 h in the Besos), to just a few minutes more than that obtained using the deterministic Lagrangian persistence forecast.

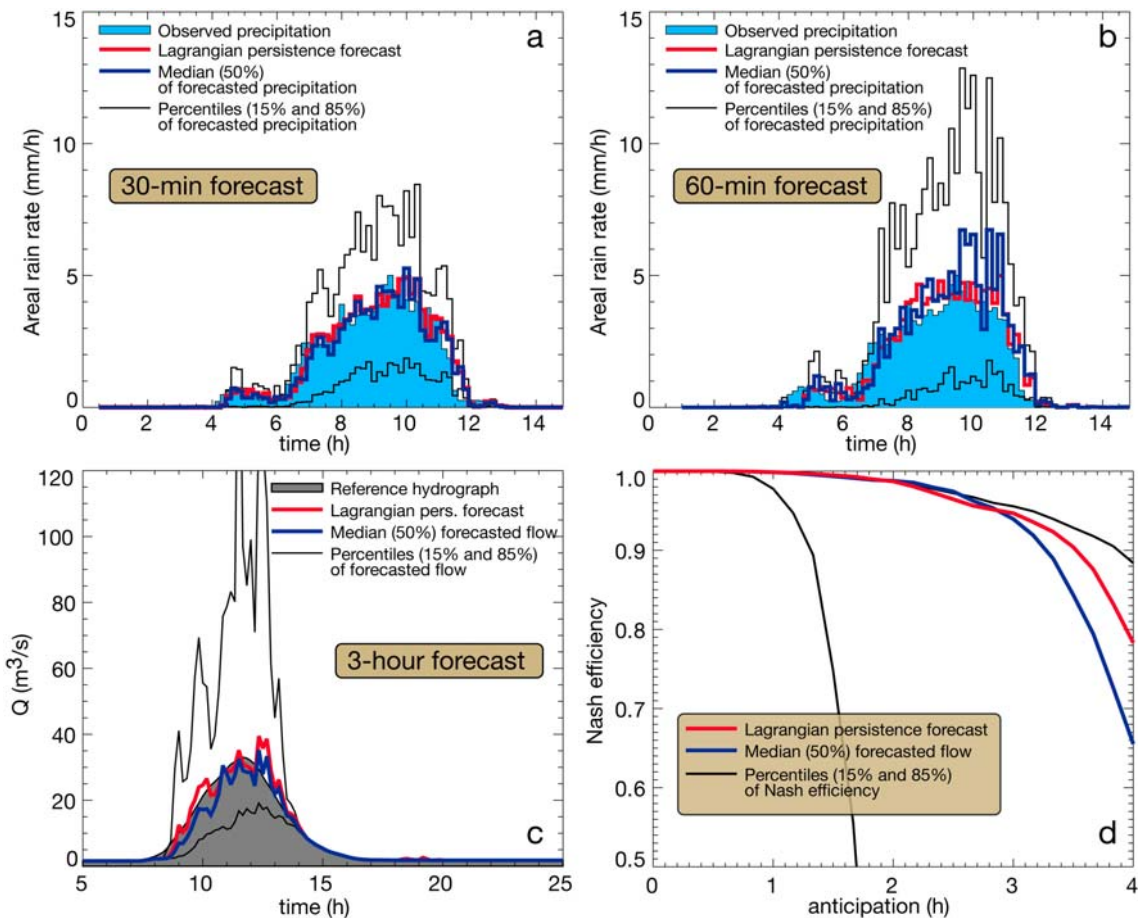


Figure 5-7. Probabilistic rainfall forecasting estimates and its implications in runoff forecasts. Event of 19/07/2001 in the Besos basin. a) Probabilistic rainfall forecasting estimates for 30-min lead time; b) Probabilistic rainfall forecasting estimates for 60-min lead time; c) Probabilistic runoff forecasting estimates for 3 h lead time; d) Evolution of the Nash efficiency of the forecasted hydrographs as a function of the anticipation with which hydrographs are simulated.

5.4 Development of a methodology for the redesign of the Catalan raingauge network

As part of the permanent monitoring process of the behaviour of the EHIMI warning system in the Hydrometeorological Observatory of Catalunya, an activity of smart redesigning of the raingauge network managed by the Catalan Water Agency (ACA) was made. The problem was conditioned to the next criteria: 1) Both radar and raingauge information is useful for the estimation of rainfall fields; 2) Reduce the number of raingauges at least to the middle; 3) There is the possibility to include some new raingauges in places where enough technical facilities exists; 4) Raingauges of the current network could be preserved if they agreed with previous criteria and if its current sites agreed with UNE 500520:2002 standards.

A dense weather radar network exists in Catalunya. Additionally, three governmental entities manage real-time telemetric raingauge networks inside the region. The ACA manages a 125 rain gauge

network, the SMC runs a 149 raingauge network and finally the Ebro Hydrological Confederation (CHE) is in charge of additional 75 raingauges. The approximated average density of the total network is around one raingauge each 90 km². Unfortunately this density is not uniform, and the maintenance induces a huge economic cost for these entities.

The redesign process can be summarized as follows. Ordinary Kriging technique was selected to estimate rainfall field merging radar and raingauge data. This technique allows quantifying the error variance of estimations in the region. Therefore, if all possible combinations of raingauge networks were evaluated, the optimal network of raingauges would be identified selecting the network with the lowest value of error variance. Due to the great number of possibilities, the simulated annealing technique was used to define iteratively the optimal number and locations of the new ACA network. A total of 200 rainfall fields of 1-hour accumulations from the SMC radar composites were used in this study to take into account the spatial and temporal variability of rainfall.

An analysis of the error estimation of the estimated rainfall fields related to different combinations of raingauge networks was made. In principle, the better network will be that minimizing the error estimation variance. But the selection of the final locations of the new ACA raingauge network was based on a multi-criteria decision analysis (adding other technical and economic factors). After the optimal redesign of this raingauge network, the ACA was able to reduce significantly its annual maintenance budget without reduction in the quality of the estimated rainfall fields. These budget reductions open a clear possibility to the addition of new instrumentation (as disdrometers, vertical profilers or microradars) that will improve in the future the rainfall field estimates in the region.

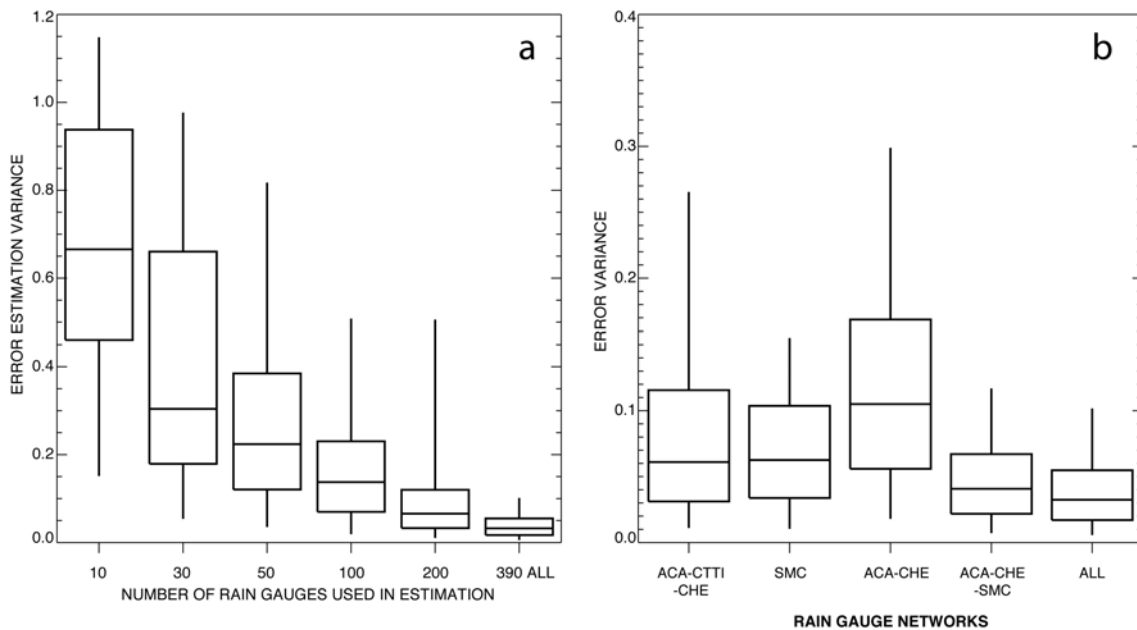


Figure 5-8. Distributions of the rainfall field error estimation due to different raingauge configurations. a) Independently of the network owner; b) Considering separately the current owner network.

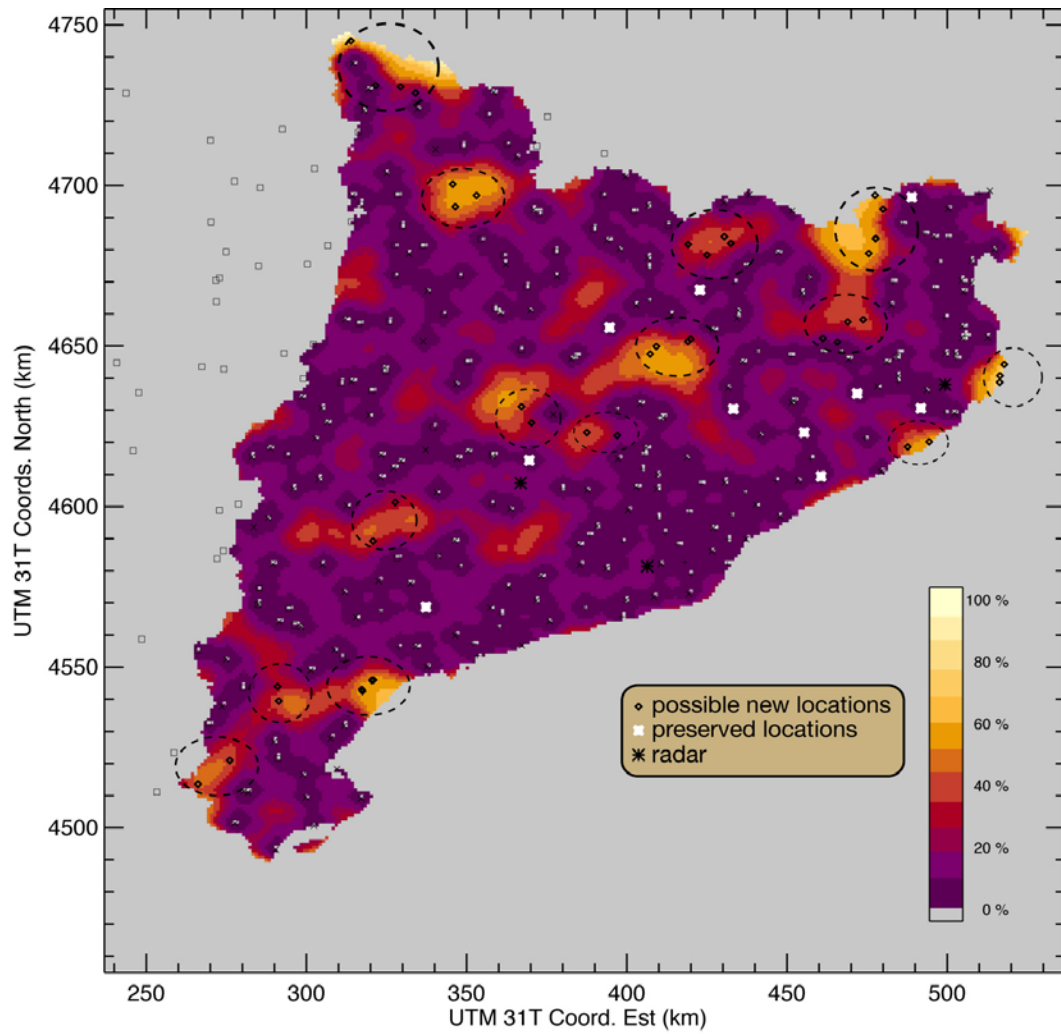


Figure 5-9. Final error variance field and regions where installation of new rain gauges is recommended to improve the quality of estimated rainfall fields

6. Flash flood warning in ungauged basins by use of the Flash Flood Guidance and model-based runoff thresholds

6.1 Introduction

Methods for flash flood warning relying on rainfall thresholds and assessment of local soil moisture status have a quite long tradition in hydrology (Martina et al., 2006; Collier, 2007; Norbiato et al., 2008). One of these procedures is the Flash Flood Guidance method (FFG, hereinafter) (Mogil et al., 1978). According to Georgakakos, 2006, the US National Weather Service relies routinely on Flash Flood Guidance (FFG, hereinafter) computations to produce flash flood watches and warnings. FFG is the depth of rain of a given duration, taken as uniform in space and time on a certain basin, necessary to cause minor flooding (e.g. 2-yr return time flow) at the outlet of the considered basin. This rainfall depth, which is computed by running in inverse mode a lumped continuous hydrological model (typically, a conceptual one), is compared to either real time-observed or forecasted rainfall of the same duration and on the same basin. If the nowcasted or forecasted rainfall depth is greater than the FFG, then flooding in the basin is considered likely. As such, the FFG is not a forecast quantity; rather, it is a diagnostic quantity (Georgakakos, 2004). The assessment of the susceptibility to flash flood, by taking initial soil moisture status into account, is a critical step to anticipate the locations of the river system which may be hit by the flood. Even though the occurrence, location and (or) timing of the flash flood is still uncertain, this information may provide enough lead time so that flash flood mitigation measures can be planned and managed in an anticipatory rather than responsive manner. Use of the FFG for the development of watches and warnings requires assessment of a present or imminent flash flood-inducing rainfall accumulation. The main objective with the FFG is the correct assessment of the flood threshold exceedance, while the correct timing forecast is left to the monitoring activity triggered by the flash flood alert (Georgakakos, 1992).

The key advantages of the FFG are that the method promotes close collaboration between hydrologists and meteorologists by simplifying communication about the hydrological status of basins and allows the forecaster to readily ingest local precipitation information and to update warnings without the need to run complex hydrometeorological forecasting chains. The limitations of the method stems from the need to operate a conceptual hydrological model at the small space scales of flash flood occurrence, where generally no flow data area available to calibrate the model. The performances of the method decrease sharply when applied to ungauged basins by using simple parameter transfer procedures, as reported by Norbiato et al (2008) for an application to North eastern Italy and France. Degradation of performance in ungauged basins is generally due i) to the simulation bias which arise when the hydrological model parameter cannot be calibrated (Bloeschl, 2005), and ii) to the uncertainties in specifying the flow threshold leading to small flooding in the concerned basin (Ntelekos et al., 2006). In this report we propose an alternative way for the application of the FFG to ungauged basins, which has the potential to inherently correct for simulation model biases and to filter out a portion of the hydrological model prediction uncertainty. Our approach requires running the lumped hydrological model to derive flood probability at the outlet of the ungauged basin under consideration, and then to compute the flow threshold based on model-derived simulations. This model-based threshold flow is subsequently used in the forecasting phase when running the model to compute the FFG. In this manner, the Flash Flood Guidance derived from the model-based flow threshold may account for the hydrologic model uncertainty and for biases originated by lack of model calibration on local conditions.

The objective of this report is to test the FFG method with model-based threshold flows under different conditions of data availability. More specifically, we evaluate the efficiency of the method both i) when data are available for model calibration and ii) when the model simulation parameters cannot be calibrated but must be transposed from either parent or nearby gauged basins to ungauged basins. The model used in this study to compute the FFG is a semi-distributed conceptual rainfall-

runoff model, following the structure of the PDM (Probability Distributed Moisture) model (Moore, 1985; Norbiato et al., 2008). We provide an assessment of this approach based on data from a number of catchments in the central-eastern Italian Alps, where both long-term data and data concerning specific flash flood events are available.

6.2 The Flash Flood Guidance method

The FFG is the depth of rain of a given duration, taken as uniform in space and time on a certain basin, necessary to cause minor flooding at the outlet of the considered basin. FFG is estimated each day over a region to diagnose flash flood susceptibility during the following 1-24 hours. FFG is conditional to the soil moisture conditions computed by using a continuous soil moisture accounting hydrological model. To support flash flood computations and using these initial conditions, the model runs off-line in 'what if' scenario runs with increasing amounts of rainfall input of a given duration. FFG for different durations are then compared to either real time-observed or forecasted rainfall of the same duration and on the same basin. The warning is issued based on the comparison between the FFG and the either real time-observed or forecasted rainfall. If the nowcasted or forecasted rainfall depth is greater than the FFG, then flooding in the basin is considered likely. It is important to recognise that the FFG technique does not predict flash flood timing, but only that a flood threat is imminent.

Three elements are therefore included in the FFG method: i) the continuous soil moisture accounting model, ii) the computations of the FFG, and iii) the flood threshold conditions. These elements are described in the next sections.

6.3 Description of the hydrological model

The continuous hydrological model used in this report is a semi-distributed conceptual rainfall-runoff model. The model is described in detail in Norbiato et al. (2008); hence, only a summary description is reported here.

The model runs on a hourly time step and consists of a snow routine, a soil moisture routine and a flow routing routine. The snow routine represents snow accumulation and melt by using a distribution function approach based on a combined radiation index degree-day concept (Cazorzi and Dalla Fontana, 1986). Potential evapotranspiration is estimated by using the Hargreaves method (Hargreaves and Samani, 1982).

The soil moisture routine uses a probability distribution function to describe the spatial variation of water storage capacity across a basin (Moore, 1985). Saturation excess runoff generated at any point in the basin is integrated over the basin to give the total direct runoff entering the fast response pathways to the basin outlet. Drainage from the soil enters slow response pathways. Storage representations of the fast and slow response pathways yield a fast and slow response at the basin outlet which, when summed, gives the total basin flow.

Losses due to evaporation are calculated as a function of potential evaporation and the status of the soil moisture store. Drainage to the slow flow path is represented by a function of basin moisture storage and the slow or base flow component of the total runoff is assumed to be routed through an exponential store. Direct runoff from the proportion of the basin where storage capacity has been exceeded is routed by means of a geomorphology-based distributed unit hydrograph using a geomorphologic filter based on a threshold drainage area (Da Ros and Borga, 1997).

The model application requires specification of 14 parameters: three for the snow accumulation and melt module, 8 for the PDM module and three for the runoff propagation module.

6.4 FFG computation

Five rainfall durations are considered for computing the FFG: one, three, six, twelve and twenty four hours. The model is run continuously in time, and five values of FFG are computed each day (at 12:00) for each considered basin. Selection of the time during the day when the FFG is computed has been shown to have negligible impact on final results. For the considered day, the FFG values are compared with the maximum estimated areal precipitation over the corresponding five durations. The technique predicts the exceedance of the threshold flooding (i.e., a flash flood warning would be issued) when estimated precipitation exceeds the FFG for at least one precipitation duration.

6.5 Threshold flooding conditions

A number of alternatives are available in the literature to determine the threshold flooding conditions (Carpenter et al., 1999). Generally, these are based on regional analysis of observed flow data. Carpenter et al., 1999, suggest that a 2-year flood is a reasonable threshold to use for flood warnings given that the flood flow associated with damage or hazard is often a little higher than bankfull flow.

Recently, Reed et al. (2007) proposed use of threshold frequencies in conjunction with a distributed model to improve the accuracy of flash flood forecasts at ungauged locations. In this report, we use a methodology similar to that proposed by Reed et al. (2007), by computing the threshold flooding condition based on the flood frequency analysis of discharge values simulated by the model. This method requires the post-processing of the historical model simulations to convert flow to frequency. In this report, we used a threshold frequency corresponding to a 2-year return period.

A key assumption of the frequency-based approach is that the hydrologic model has skill in ranking events even if the simulated peak flows are biased relative to the observed data. If this is true, then forecasters can effectively use the model-based threshold flow to derive the FFG.

The skill and consistency of historical simulations in ranking events depends on the consistency of the model chain, and most importantly on the consistency of the rainfall input.

Use of this definition led to identification of 28 flood events exceeding the basin-specific thresholds, over the whole archive of streamflow data. However, use of this definition may give rise to sampling problems, due to the small number of local flood events. Owing to this reason, we used also a lower threshold, characterised by a return time around 0.5 year, corresponding to 94 flood events exceeding the threshold.

6.6 Study areas and assessment methodology

Data from six catchments located in the central-eastern Italian Alps are used for assessment of the method. Figure 6-1 shows the location of the basins, which are clustered into two river systems (upper Isarco river system and upper Brenta river system), together with the position of two weather radar stations used for rainfall estimation.

Table 6-1 provides more detailed basin information, including information on the length period with hourly data available. For the basins of Ridanna at Vipiteno, Fleres, Brenta at Borgo and Brenta at Levico the length of the hourly record of streamflow, precipitation and temperature data ranges from 11 to 13 years, with a total of 48 years. The data were quality controlled and as a results part of the record was set to missing. Basin-averaged precipitation estimates were obtained based on rain gauge stations by using a Thiessen technique, with densities ranging from 1 station per 15 km² (Brenta river

basin) to 1 station per 40 km² (Ridanna river system). Only flood event data were available for the catchments of Racines and Piana.

Catchment drainage area ranges between 14.4 km² and 213.7 km². The topography is rather complex with altitudes ranging from 360 m asl (lowest altitude of Brenta at Borgo) to 3600 m asl (highest elevation of the Ridanna basin). Measured runoff represents the natural runoff variability well, since management activities, such as artificial reservoirs and diversions, do not alter the river regime. However, the upper Brenta basins are heavily influenced by the presence of natural lakes, which drains as much as 77 km².

Metamorphic rock units prevail in the region of the upper Isarco. The most common metamorphic rocks cropping out in the study catchments are gneiss (in the varieties of orthogneiss and paragneiss), phyllites and micaschists. Calc-schists, prasinites and serpentinites are also found, although to a lesser extent. These rock types are characterized by a low to very low permeability. The upper Brenta catchments are characterized by both metamorphic and sedimentary rock units. Left-hand tributaries are significantly affected by karst processes.

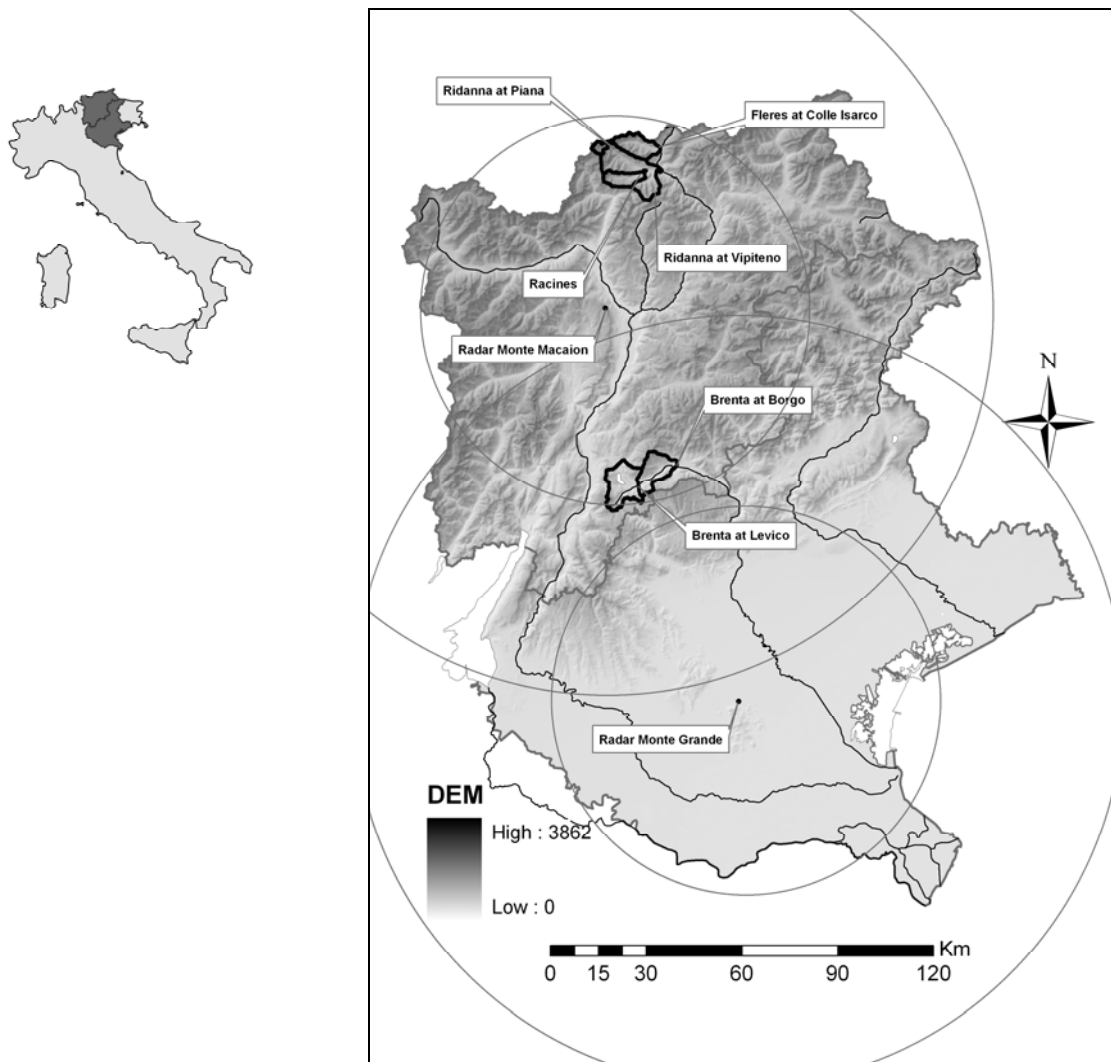


Figure 6-1: Study basins and their location in Italy

Table 6-1: Main characteristics of the study basins

Catchment number	Station name (river system)	Area (km ²)	Elevation range (m asl)	Periods with hourly data available
1	Ridanna at Vipiteno (upper Isarco)	210.2	940-3600	1/10/1992 - 1/10/2007
2	Racines (upper Isarco)	47.6	970-2760	only flood event data
3	Rio Piana (upper Isarco)	14.4	2165-3420	only flood event data
4	Fleres (upper Isarco)	75.2	1069-3107	1/10/1992 - 1/10/2007
5	Brenta at Borgo (upper Brenta)	213.7	380-2400	1/10/1994 - 1/10/2005
6	Brenta at Levico (upper Brenta)	113.0	435-2000	1/10/1994 - 1/10/2005

Mean annual precipitation is lower for the upper Brenta basins (around 1080 mm), due to the sheltering effect of the mountainous ranges to the southerly winds, and higher for the upper Isarco basins (around 1270 mm) which are exposed to the stau effect. However, high intensity events are generally more frequent for the Brenta basins, owing to their position closer to the Adriatic sea. At Vipiteno, a raingauge station representative for the upper Isarco basins, 50-yr return time rainfall quantiles for 1 hour and 3 hours durations amount to 36.5 and 48.9 mm, respectively. At Levico, which can be considered representative for the upper Brenta basins, the quantiles increase to 47.8mm and 68mm, respectively (Borga et al, 2005).

As a consequence of the moderate rainfall regime, peak discharges are relatively low. The largest recorded peak discharge at Vipiteno amounts to 158 m³/s, whereas it is around 60 m³/s for the Brenta at Borgo, due to combined effect of lakes and karst aquifer. Hence, the flash flood events in these areas are generally characterized by limited spatial extent.

Two different evaluation methodologies are used here: i) long-term assessment, and ii) evaluation based on three specific flash flood events.

With the long-term assessment, we evaluate the efficiency of the method both when data are available for model calibration and when the model simulation parameters cannot be calibrated but must be transposed from either parent or nearby gauged basins to ungauged basins. The model is first calibrated on Ridanna at Vipiteno (for the upper Isarco river system) and on the Brenta at Borgo (for the upper Brenta river system), hence the model parameters are transferred to the other basins of the corresponding river system.

With the evaluation based on specific events, the method is assessed on three flash flood events occurred on 3-4.10.2006 and 20-21.06.2007 for the upper Isarco river system and on 01.11.2004 for the upper Brenta river system.

6.7 Long-term assessment

6.7.1 Assessment of the hydrological model

With the long term assessment, the hydrological model was calibrated over Ridanna at Vipiteno (for the upper Isarco river system) and on the Brenta at Borgo (for the upper Brenta river system), with the objective of adjusting the model’s parameters to decrease the difference between observed and simulated streamflow values. In this study, the Shuffled Complex Evolution-University of Arizona (SCE-UA, Duan et al., 1992) global optimization algorithm was used for calibration of the hydrological model parameters. The following objective functions were used during the optimization process for this study:

1: the Nash and Sutcliffe, 1970, coefficient of efficiency defined as:

$$E_{NS} = 1 - \frac{\sum_{i=1}^n (O_i - S_i)^2}{\sum_{i=1}^n (O_i - O_{ave})^2} \quad (1)$$

where O_i is the hourly i -th observed discharge, S_i is the simulated discharge, and O_{ave} is the mean value of the observed discharges. The coefficient of efficiency was selected because it is dimensionless and is easily interpreted. If the model predicts observed streamflow with perfection then $E_{NS}=1$. If $E_{NS}<0$ then the model’s predictive power is worse than simply using the average of the observed values.

2: the relative bias (RB) defined as:

$$RB = \frac{\sum_{i=1}^n (S_i - O_i)}{\sum_{i=1}^n O_i} \quad (2)$$

RB is a measure of total volume difference between observed and simulated streamflows, and is important in the evaluation of simulations from continuous hydrologic models.

A simple split sample test (Klemes, 1986) was considered for calibration and validation of the hydrological model. The test involves dividing the available data into two sets, one used for parameter estimation (calibration period) and the other for validation (validation period).

Results from the calibration and validation of the model are reported in Table 6-2, which reports both the coefficient of efficiency (E_{NS}) and the relative bias (RB) for the calibration and validation period, as well as for the whole data period. These results show on one hand the difficulties related with the application of the model to the Brenta river, where the poor model accuracy is due to the combined influence of lake storage and karstified aquifer, and a non-negligible bias remains even after calibration. On the other hand, validation results show that the model describes quite well the behaviour of the Ridanna at Vipiteno.

Table 6-2: Model validation and calibration results on Brenta and Ridanna

	Calibration period		Validation period		Whole simulation period	
	NS	BIAS (%)	NS	BIAS (%)	NS	BIAS (%)
Brenta at Borgo						
Calibration: 10.94-09.01	0.71	2.6	0.5	8.7	0.64	5.0
Validation: 10.01-09.05						
Ridanna at Vipiteno						
Calibration: 10.92-09.97	0.80	1.4	0.79	-2.6	0.79	3.4
Validation: 10.97-09.07						

6.7.2 FFG assessment

Assessment of the quality of flash flood warnings based on FFG estimates is obtained by using contingency tables. Contingency tables are highly flexible methods that can be used to estimate the quality of a deterministic forecast system and, in their simplest form, indicate its ability to anticipate correctly the occurrence or non occurrence of predefined events. A four-cell contingency table can be constructed which depicts the relationship between the forecasts and the events. Consider a set of forecasts that can have only two alternatives (e.g., yes, no) (Table 6-3).

Table 6-3: Four-cell contingency table used in the study

EVENTS	FORECASTS	
	YES	NO
YES	X	Y
NO	Z	W

Let: X denote the number of positive forecasts (estimated rainfall exceeds the FFG) that correspond to an occurrence of the event (the flow at the basin outlet exceeds the threshold runoff) (hits) Y denote the number of events (the flow at the basin outlet exceeds the threshold runoff) that occurred in conjunction with a negative forecasts (estimated rainfall does not exceed the FFG) (missed events) Z denote the number of positive forecasts (estimated rainfall exceed the FFG) that were not accompanied by an event (the flow at the basin outlet does not exceeds the threshold runoff) (false alarms), and W denote the number of negative forecasts (estimated rainfall does not exceed the FFG) that did not have any associated events (the flow at the basin outlet does not exceeds the threshold runoff) (hits).

Three statistics can be used to summarise the contingency table. The probability of detection (POD) is the ratio of correctly forecasted events to the total number of events:

$$POD = \frac{X}{X + Y} \tag{3}$$

The range of values for POD goes from 0 to 1, the latter value being desirable. A POD of one means that all occurrences of the event were correctly forecast.

The false alarm rate (FAR) is the ratio of the number of false alarms to the total number of predicted events:

$$FAR = \frac{Z}{X + Z} \tag{4}$$

The range of values for FAR goes from 0 to 1, the former value being desirable. A FAR of zero means that in the verification sample, no non-occurrences of the event were forecast to occur.

Neither POD or FAR can give a complete picture of forecasting success; it is therefore desirable to include a statistic depending on both POD and FAR. This is the critical success index (CSI). The CSI is the ratio of correctly forecasted events to the total number of event forecasts that were either made (X+Z) or needed (Y):

$$CSI = \frac{X}{Y + X + Z} = \frac{1}{POD^{-1} + (1 - FAR)^{-1} - 1} \quad (5)$$

For either a zero POD or a unit FAR, the value of CSI is uniquely equal to zero, since there are no hits. The range of values for CSI goes from 0 to 1, the latter value being desirable.

Due to the low number of events in the specific catchments, overall score statistics are computed by combining together all the events from selected catchments. Overall score statistics are computed over Ridanna at Vipiteno and Brenta at Borgo (by using the model locally calibrated) and over the Fleres and Brenta at Levico (by using the model with transposed parameters). In the first case the assessment describes the results over gauged basins, whereas the second case describes the results over ungauged basins. The assessment is carried out by using both observed and model-based threshold flow as a way to evaluate the capability of the method based on use of model-based flow threshold to account inherently for the bias in simulation (Table 6-4 and Table 6-5, respectively). We use here the 0.5-year return time discharge as a threshold to increase the number of flood events available for method analysis. Norbiato et al. (2008) has shown that results from the assessment exercise are only slightly affected by the choice of the threshold.

Table 6-4: Overall score statistics: threshold runoff computed based on observed data

	POD	FAR	CSI
Model with calibrated parameters (basins 1 and 5)	0.90	0.45	0.52
Model with transposed parameters (basins 2 and 6)	0.95	0.65	0.34

Table 6-5: Overall score statistics: threshold runoff computed based on model simulations

	POD	FAR	CSI
Model with calibrated parameters (basins 1 and 5)	0.85	0.35	0.59
Model with transposed parameters (basins 2 and 6)	0.90	0.47	0.50

Comparison of results reported in Table 6-5 with those reported in Table 6-4 shows that the use of model-based threshold leads to improvements in both gauged and ungauged situations. In both cases, the remarkable decrease of FAR is associated to a slight degradation of POD values. This is explained by the general positive bias overestimation associated to the model simulations. This is in general emphasised over ungauged basins (results not reported here for the sake of brevity). Overall, CSI increases by 12% for gauged basins and by 31% for ungauged basins with use of a model-based threshold. As expected, the increase of CSI is more remarkable for ungauged basins, due to lack of local model calibration and the resulting greater likelihood of occurrence of a simulation bias in model application.

6.8 Assessment on three flash flood events

The verification of the performances of the FFG method over gauged and ungauged basins provides only a partial assessment of the method. Since the objective of the method is to diagnose the flash flood susceptibility across a region, we tested the quality of the diagnostic maps provided by the method for three flash flood events. The events occurred on 3-4.10.2006 and 20-21.06.2007 over the upper Isarco river system and on 01.11.2004 over the upper Brenta river system. Rainfall estimates for the three events are obtained by combining weather radar observations and raingauge data with a physically-based scheme for radar error adjustment (Borga et al., 2002; Borga et al., 2007). The rainfall accumulation maps are reported in Figure 6-2, whereas a description of event duration and max point rainfall accumulations are reported in Table 6-6. Basin-averaged rainfall accumulations, peak discharge values and ratios between 2-year peak discharge and observed peak discharge are reported in Table 6-7.

Table 6-6: Storm characteristics of the three flash flood events

Events	Duration (hours)	Max point accumulation (mm)
3-4.10.2006 (Isarco)	12	150
20-21.06.2007 (Isarco)	24	155
01.11.2004 (Brenta)	10	110

Table 6-7: Flood characteristics of the three flash flood events

	Accumulated rainfall (mm)	Peak discharge (Q_p)(m ³ /s)	Q_2/Q_p
3-4.10.2006 (Isarco)			
Ridanna Vipiteno	60.7	80.0	0.78
Racines	54.4	32.0	0.69
Piana	63.4	27.6	0.35
Fleres	62.6	69.4	0.44
20-21.06.2007 (Isarco)			
Ridanna Vipiteno	45.6	60.0	1.05
Racines	72.0	25.5	0.87
Piana	4.8	8.0	1.20
Fleres	60.0	16.8	1.82
01.11.2004 (Brenta)			
Brenta at Borgo	65.0	46.8	0.52
Brenta at Levico	64.0	39.0	0.37

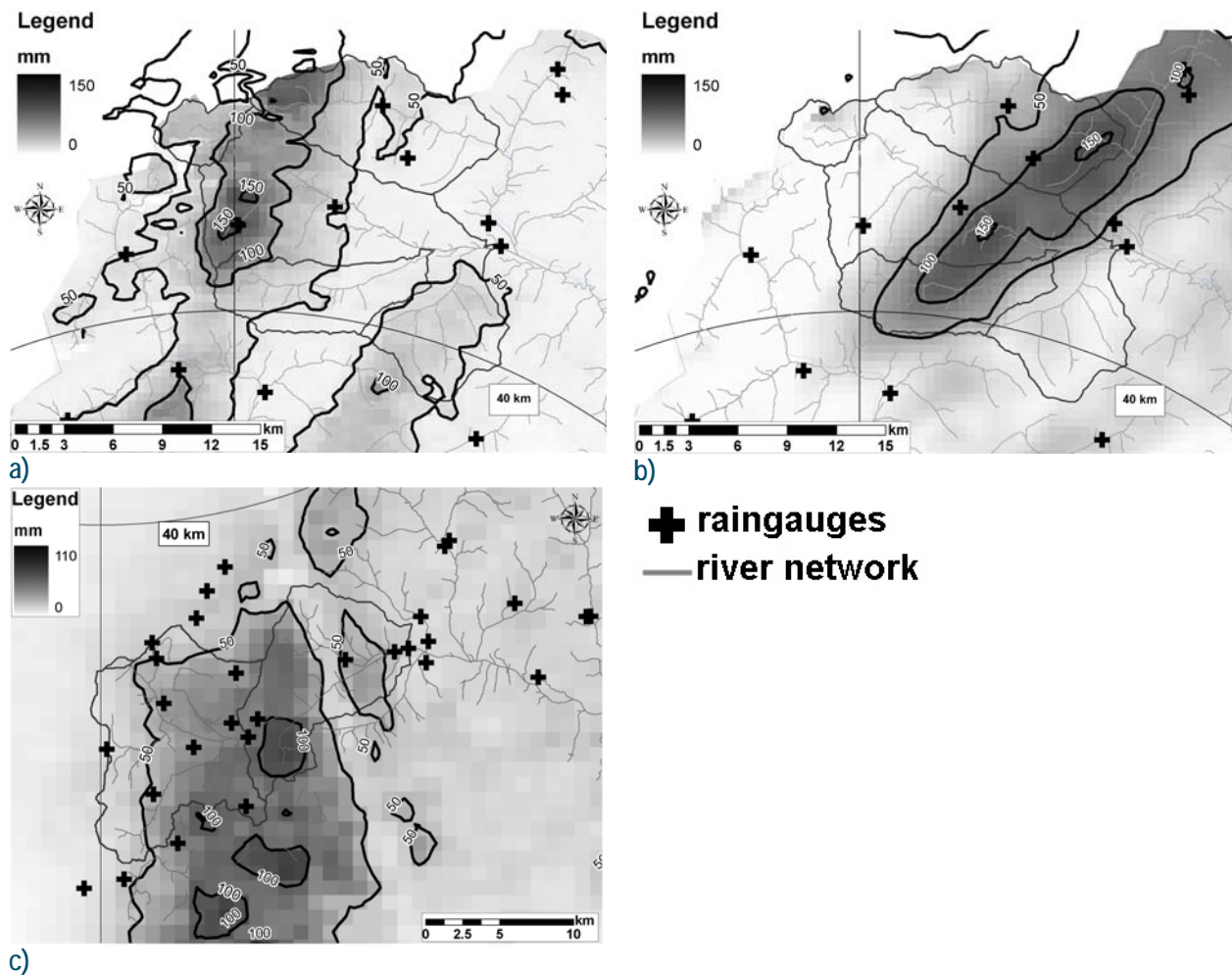


Figure 6-2: Storm total rainfall (mm) for the three flash flood events occurred on: a) 3-4.10.2006; b) 20-21.06.2007; and c) 1.11.2004

The hydrological model and the FFG method were applied in the same way as reported in the previous sections. The model parameters were calibrated over Ridanna at Vipiteno and over Brenta at Borgo. The parameters were transposed respectively to Piana, Fleres and Racines (for the case of the upper Isarco river system) and to Brenta at Levico (for the case of the upper Brenta).

During the event of 3-4.10.2006, the headwater basins of the Fleres and Ridanna river basins had anomalously large rainfall rates for a given rainfall accumulation due to intensification of rainband precipitation in the upper watersheds. In these basins, runoff generation was also associated to intense snow and glacier melt. The event started on October 3, 2006 at 17:00 CET (Central European Time), for a duration of 12 hours and with a rainfall peak on October 4 at 10:00. Significant damages were recorded in the upper portions of the Ridanna basin, where some forest roads were interrupted and the streamgauge station of the Ridanna at Piana was damaged. The initial soil water conditions were relatively dry for this event, due to a long period without significant rain accumulations before the flood.

The storm of 20-21.06.2007 focused on the mid portions of the Ridanna and Fleres basins, whereas the headwater basins were only partially affected by the storm. The event started on June 20, 2007 at 20:00 and lasted for 23 hours with two relatively large rainfall peaks. These peaks occurred in the initial and in the final stages of the event and were associated with embedded convection in rain bands.

Rainfall intensity during the central part of the event was relatively low and of mainly stratiform character. The last rainfall peak was characterised by a persistent convective band which imposed large rainfall gradients and triggered a large number of debris flows. Even though peak discharges were in general lower than for the 2006 flash flood event, total damages were much higher due to the widespread occurrence of debris flows in the mid course of Rio Ridanna and Fleres.

The event occurred on the upper Brenta river system during November 1, 2004 is the most intense among the events examined here. It started on November 1 at 1:00 and lasted for ten hours, with a rainfall peak at 7:00. The storm event led to diffuse flooding in the upper Brenta river basin, and to a critical flooding situation at Borgo, the largest town in this basin.

Results are reported by comparing FFG with estimated rainfall in Figure 6-3 and Figure 6-4. The quality of the predictions may be checked here by paralleling the comparison between FFG and corresponding observed rainfalls at specific durations (Figure 6-3 and Figure 6-4) with the comparison between the 2-yr discharge and the event peak discharge (the comparison is reported in Table 6-7, where the ratios between the two discharges are reported).

Figure 6-3a-d shows that the predictions obtained by means of the FFG are accurate for the four basins. In all these cases the observed peak discharge exceeded the 2-yr discharge; consistently, FFG was equalled or exceeded by the observed rainfall for at least one duration. However, the ratios between FFG and observed rainfall are not consistent with the ratios between the 2-yr discharge and the event peak discharge. The relative patterns of observed rainfall and FFG are similar for Ridanna at Vipiteno, Racines and Fleres, but the ratio between the 2-yr discharge and the event peak discharge ranges from 0.44 to 0.78 on these three basins. This provides an indication that the FFG method is able to capture only a portion of the differences arising in the susceptibility to flash flood across these basins. This is partially due to the simple method used here for parameter transposition to the basins considered as ungauged.

The events of 2006 and 2007 differ by i) initial conditions, ii) spatial location, and iii) temporal structure. In Figure 6-3e-h, relatively wet initial conditions for the 2007 event are reflected in the lower values of FFG with respect to the 2006 event. The temporal structure of the rainfall event, with two peaks at the start and at the end of the event, can be recognised in the convex shape of the observed rainfall patterns in the range of durations between 6 and 24 hours. The larger variability in flash flood response for the 2007 event is well reproduced by the FFG method. However, for the Fleres basin the method suggests that flash flood is likely, when this is not actually the case. This is consistent with observations reported above on the limitations of the regionalisation scheme used here for model application in ungauged basins.

The application of the FFG method to the November 1, 2004 flash flood event suggest that there are striking similarities in the rainfall spatial distribution and in the flood response for the two basins closed at Levico and at Borgo. In spite of the complex hydrological setting in the upper Brenta basin, with the influence of the karstified aquifer and of the natural lakes, the results obtained with the application of the FFG provide a realistic picture of the flash flood susceptibility in the two basins.

Finally, it should be borne in mind that these results were derived based on the assumption of “perfect knowledge” of future rainfall. In other words, the actually observed rainfall is here used as the “forecasted rainfall” and as such the results do not incorporate the “rainfall forecasting uncertainty”. In operational conditions, future rainfall is not known and only quantitative precipitation forecasts originated either by nowcasting techniques or by use of Numerical Weather Prediction models may be available, hence leading to greater uncertainty in real cases of flash flood forecast.

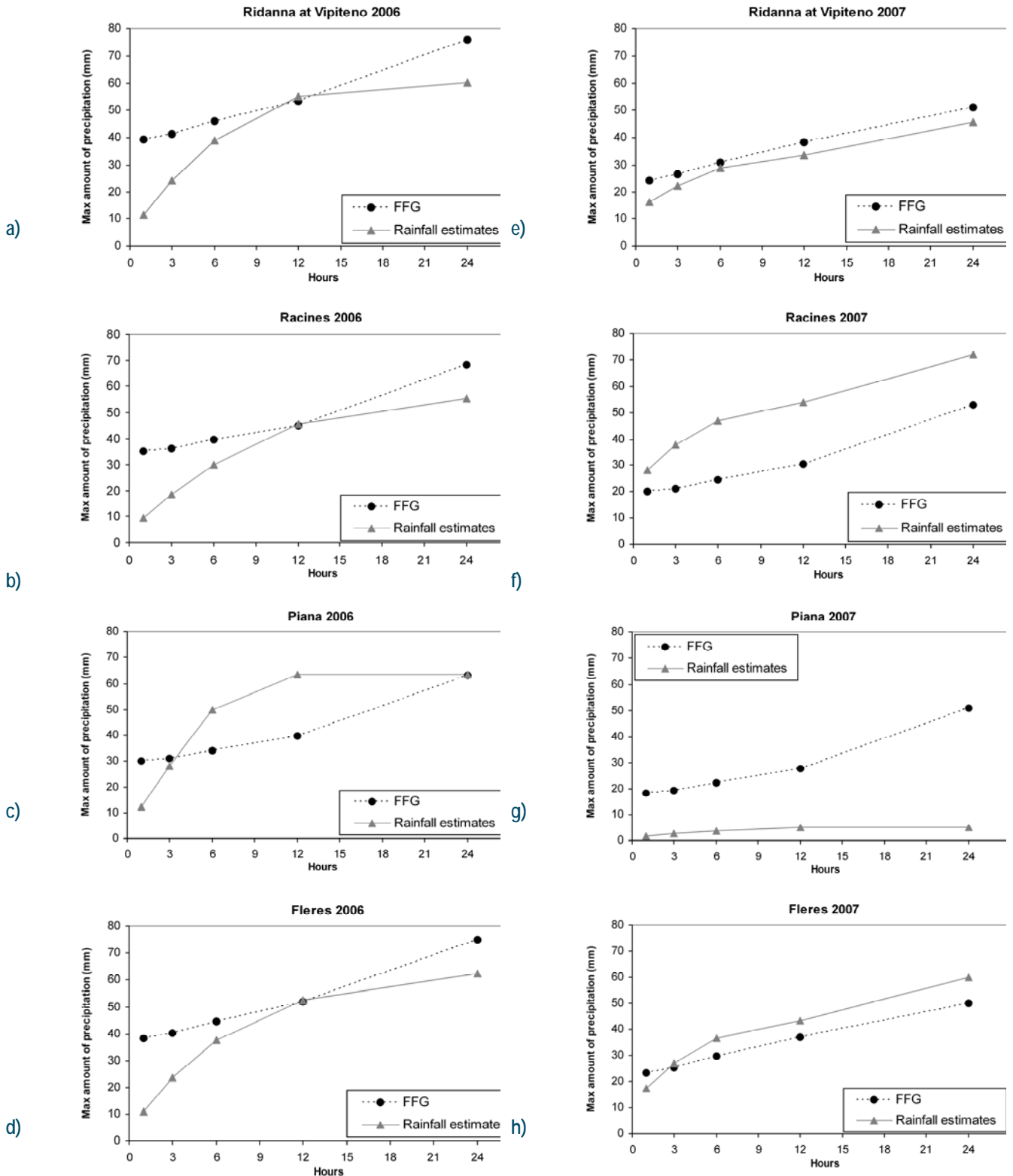


Figure 6-3: Comparison between FFG and rainfall estimates over five rainfall durations (1h, 3h, 6h, 12h and 24h) for four subbasins in the upper Isarco river system and for the two flash flood events occurred on 3-4.10.2006 (a,b,c,d) and on 20-21.06.2007 (e,f,g,h)

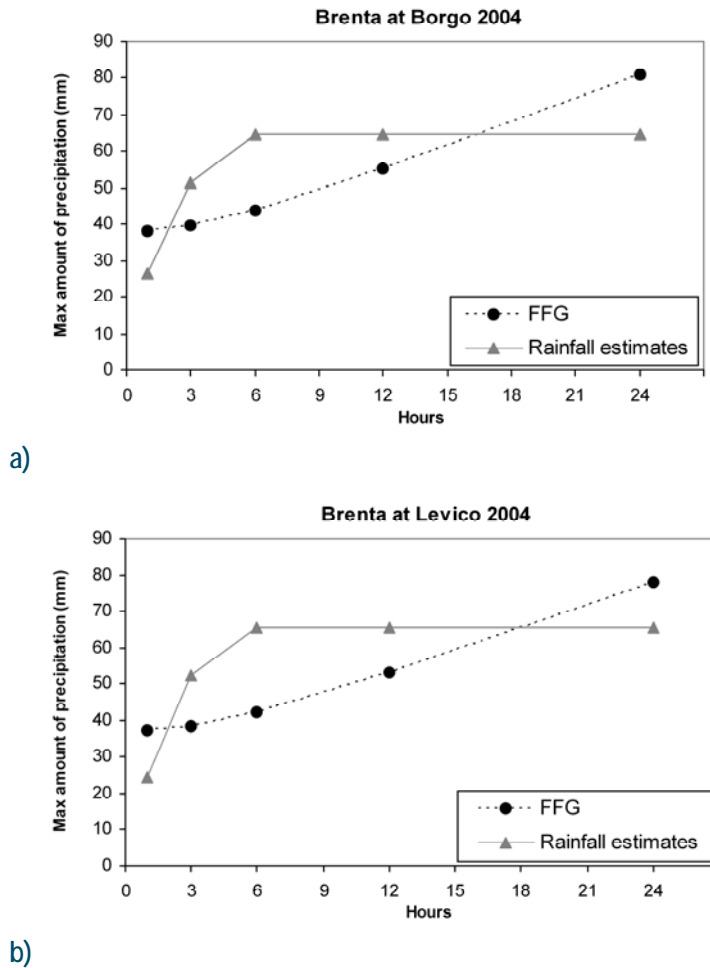


Figure 6-4: Comparison between FFG and rainfall estimates over five rainfall durations (1h, 3h, 6h, 12h and 24h) for two subbasins in the upper Brenta river system and for the flash flood event occurred on 1.11.2004

6.9 Conclusions and future work

We propose using the Flash Flood Guidance (FFG) method and a method of model-based threshold runoff computation to improve the accuracy of flash flood forecasts at ungauged locations. Our approach requires running the lumped hydrological model to derive flood frequencies at the outlet of the ungauged basin under consideration, and then to derive the threshold runoff from these model-based discharges. This model-based threshold runoff is subsequently used in the forecasting phase when running the model to compute the FFG. The approach provides a pragmatic method to characterize flood severity at ungauged locations. The study examines the potential of this method to account for the hydrologic model uncertainty and for biases originated by lack of model calibration on local conditions.

Experiments to validate this approach involved the implementation of a semi-distributed continuous rainfall-runoff model and the operation of the FFG method over four basins located in the central-eastern Italian Alps and ranging in size from 75.2 km² to 213.7 km². Data were available for periods ranging from 11 to 13 years. The model was calibrated on two larger basins and the model parameters were transposed to the other two basins to simulate operations in ungauged basins. The FFG method was applied by using the 2-yr discharge as the threshold runoff. The threshold runoff was derived both by using local discharge statistics and the model-based approach advocated here. Examination of the

results obtained by this comparison shows that the use of model-based threshold leads to improvements in both gauged and ungauged situations. Overall, the Critical Success Index (CSI) increases by 12% for gauged basins and by 31% for ungauged basins by using the model-based threshold with respect to use of local data. As expected, the increase of CSI is more remarkable for ungauged basins, due to lack of local model calibration and the greater likelihood of occurrence of a simulation bias in model application over these basins. This shows that the method of threshold runoff computation provides an inherent bias correction to reduce systematic errors in model applications to ungauged (and gauged) basins.

The method was also applied to simulate FFG operations with three flash flood events and by using additional data from two further basins. This application showed that, even though reasonable results may be obtained by using the FFG to map susceptibility to flash flood across a region, the use of transposed model parameters from gauged to ungauged basins may limit the potential of the method. Improvements could be obtained in this case by using more reliable methods for model parameter regionalisation.

The promising results from these modelling experiments suggest that further work should be devoted to the analysis of the combination of FFG with model-based runoff threshold. In particular, future work should focus on the examination of the influence of spatial and temporal scales on the performances of the method and on the dependence of these scales on the type of rainfall information used to force the model. It is likely that different types of rainfall forcing will translate to different scale-dependence patterns.

Another area where further work is required is the development of more reliable methods for derivation of model parameters. Prior studies (Zhang et al, 2008) have found that the correlations between streamflow characteristics and physical watershed characteristics are often significantly higher than between model parameters and watershed characteristics. Methods based on the regionalization of streamflow characteristics could be tested to improve flash flood forecast in ungauged basins.

Condicio sine qua non for continuing this work in an effective way is the development of a flash flood occurrence database with long term data that would allow reliability analysis (Creutin and Borga, 2005; Gaume et al., 2008). This is a pressing need in the area of flash flood risk management which should receive proper attention from both scientists and policy makers.

7. Catchment dynamics and social response during flash floods: The potential of radar rainfall monitoring for warning procedures

7.1 Introduction

The term “flash flood” identifies a rapid hydrologic response, with water levels reaching a crest within less than one hour to a few hours after the onset of the generating rain event (Creutin and Borga, 2003; Collier, 2007; Younis et al., 2008). The time dimension of the flash flood response is linked, on one side, to the size of the concerned catchments, which is generally less than a few hundred square kilometres and, on the other side, on the activation of surface runoff that becomes the prevailing transfer process. Surface runoff is mainly due to the combination of intense rainfall with steep slopes and/or saturated soils. It also results from anthropogenic forcing such as land use modification, urbanization and fire-induced alteration of the natural drainage system.

Regarding the implementation of risk management measures, the increasing fastness of response of a cascade of medium to very small size nested river catchments has two consequences. Firstly, the people are exposed individually or in small groups in a diffused manner in space (Montz and Grunfest, 2002; Drobot and Parker, 2007). The more we go to small scales, the less they are protected by traditional structural defences that would be too expensive to build. Ruin et al. (2008) show that, during the September 2002 storm in the Gard region, almost half of the casualties occurred on watersheds of ca. 10 km² and concerned drivers on ill-protected secondary roads and campers. In such circumstances, the only way to protect people is to warn them to move to safer areas via secured itineraries. Secondly, this rather complex type of evacuation must be organised before a deadline which becomes shorter and shorter when descending in space scales. Thus, the warning procedure, that transforms perceived or forecasted signals into hazard evaluation and action (Creton-Cazanave et al., 2008), must be carried out within a unusually short delay after the onset of the storm (Montz and Grunfest, 2002).

The current paradigm for flood hazard monitoring and forecasting relies on the relationship between the social response time and the catchment response time: when the social response time is shorter than the catchment response time, purely hydrological-hydraulic models may provide the forecast at the required lead time; on the contrary, when the social response time is larger than the catchment response time, the planning of the event management measures requires use of future rainfall fields from NWP (Numerical Weather Prediction) models (Siccardi et al., 2005). Since the catchment response time gradually varies with the size of the catchment, both space and time considerations govern the adequateness of monitoring and forecasting strategies.

Confronting watershed dynamics to observed social responses about a number of selected flash flood events, this report examines how the current means available for flash-flood monitoring and forecasting can meet the needs of the population at risk to evaluate the flood severity and anticipate its danger. To this end, we identified the chronology of different social actions in the course of the events, and we used well known space-time characteristics of catchment responses.

The report is organised as follows. Section 2 describes the event selection procedure as well as the choice of descriptive parameters, for both geophysical and human aspects. Section 3 quantifies catchment response time under flash flood forcing. Section 4 introduces the characterisation of social response, defining the type of activity and the size of the human groups concerned. Section 5 recalls the current monitoring and forecasting methods that are appropriate to the range of scales considered. The conclusions are reported in Section 6, where we underline the room for adapting the warning process to social scales (individual or organisational scales), introducing more real time information about rainfall accumulations

7.2 Data set used

The data set used combines geophysical and human data that were collected in the framework of recent European research projects (FLOODsite and HYDRATE). These data are somewhat heterogeneous and partial, mainly due to the various difficulties met for observing both geophysical and social processes during extreme events. In this section we define our event selection procedure and the selected descriptive parameters.

7.2.1 Event selection

The selection procedure used is guided by two levels of screening. The first level consists in identifying at the European level a number of "remarkable" flash flood events that caused damages including casualties. Being such, these events are in turn checked to result from a storm that has, for some rainfall durations, a return period of 50 years or more. The second level of screening is related to the availability of social observations that are precise enough to localise and describe the human actions and decisions.

The above described selection led to retain, at the first level, a set of 20 remarkable events that were used for the basic understanding of flash-flood dynamics through scales. At the second level, two storms were selected for which interviews were conducted to document people behaviour. The first storm occurred in the Gard region (France) in September 2002 (Delrieu et al. 2005). This event was one of the most violent observed in this region during the last centuries (Huet et al, 2003). Rainfall accumulations of more than 500 mm in 36 hours covered a rather large area (ca. 5000 km²) giving rise to multiple individual reactions of the tributaries of the rivers Vidourle, Gard and Cèze across a wide range of scales.

The second storm affected the watershed of the Fella River, in the Eastern Italian Alps, where on 29 August 2003 a Mesoscale Convective System hit a 1,500 km² wide area for almost 12 hours, causing loss of lives and substantial disruption of the local economy, with damages close to 1 billion Euro (Borga et al., 2007). The storm total precipitation peak was up to 400 mm and the event rainfall maxima were characterised by return periods in the range of 500-1000 years for 3 to 12-h durations (Norbiato et al., 2007). The flood response in the upper Fella exceeded all the historical records, with unit peak discharges in the order of 20 m³/(s km²) for catchment areas up to 10 km².

7.3 Geophysical parameters

The geophysical description of the selected flash-flood events is based on a minimum number of simple and verifiable hydrological parameters that characterise the time and space scales of the event. It is now well known that flash flood events are difficult to monitor because they develop at space and time scales that conventional measurement networks of rainfall and river discharges are not able to sample effectively (Creutin and Borga, 2003). Rainfall accumulations for each event were carefully evaluated by using both raingauge and bucket data. More detailed rainfall estimates in space and time were obtained by adjusting radar observations accounting for the physics of the radar sensing and incorporating the above accumulation data in the adjustment procedure (Borga et al., 2002). Discharge data were obtained by combining streamgauge measurements when available and reliable, post-event surveys and model simulations to obtain indirect peak discharge estimates and eyewitness interviews to estimate the timing of the peak discharges (see for example Borga et al., 2007 and Marchi et al., 2008).

Given these observations, we used the concept of lag time to characterise the dynamics of the basins of interest. In this study, we defined the lag time as the duration between the time of the centroid of the generating rainfall sequence and the time of the discharge peak. Please note that we used the centroid of rainfall, instead of the more physically sound centroid of the excess rainfall (Morin et al., 2002), due to the difficulties to reconstruct the excess rainfall sequence for each event.

7.4 Human organisation parameters

The parameters pertaining to human response are reported in Appendix 1: (Table 7-1,2,3,4). The data set is organised basically as a series of cases corresponding to the occurrence of a storm event on a particular watershed. For instance, we split the 2002 event that occurred in the Gard region (France), into three distinct cases: the case of the Gard River itself that covers ca 2500 km², the case of the Vidourle River (an adjacent River of ca. 600 km²) and the case of the Valliguières River (a tributary of the Gard River of ca. 100 km²). This distinction was useful to position in scale the different types of human responses documented. For the 2003 event that occurred in the Fella region (Italy), we considered only one case given the less extent of the storm.

Each case is associated to a documented sequence of human actions that are positioned in time and space and that are described in enough detail to be attributed to a type of activity and to a type of human group involved. The position of a given action in time is relative to the time of the flow peak in the concerned river. It is thus an anticipation time in regard to the peak of danger if we assume, as a first guess, a direct linear relationship between the water flow and the danger. The position in space is summarized by the size of the watershed assuming that watersheds of the same size will provide comparable conditions across the considered region.

Human data gathering included different complementary strategies and techniques. In both events, we used existing data from secondary sources, such as municipal and provincial archives, logbooks from rescue brigades, as well as reports from experts (like for instance Huet et al, 2003 for the Gard event; PC- FVG, 2004 for the Fella event).

In complement we used also different types of interviews. For the Fella case fourteen semi-structured interviews were performed with qualified informers, as local authorities, civil servants, community leaders, politicians, scientific and technical experts, members of the local fire brigade corps, etc. In addition, a semi-structured questionnaire survey with 100 residents was used with some open-ended questions about residents' behaviours during the event were included (see De Marchi et al. 2007, for the description of the research design). For the Gard event, we conducted 8 months after the event thirty in depth field interviews inviting people to explain how they lived the event, with their own words and scale of time. For example, a witness on the Valliguières River watershed reported the following: "Our Sunday went as usual until 10:00 or 10:30 in the evening. Then we saw some water entering in the basement. A friend came to help us evacuating packs containing bright new furniture for our kitchen we stored there. My wife injured herself helping us to evacuate the packs. When my friend left I told him as a joke that if we were flooded tonight, we will come to him. [...] I worried. I tried to call the fire brigade in order to evacuate my wife but the road was flooded. One hour after, we decided to leave our home with our child". This example concerns a small group of people (a family). Four activities have been distinguished in this interview and appear as elementary actions in Table 7-3 with the following associated types of activities and social scales: i) identifying water inside the house (information, individual); ii) evacuating goods (protection, individual); iii) requesting help (organisation, individual); iv) evacuating people (protection, individual). The evacuation of the family has been set at 00:30 local time, i.e. 22:30 UTC, assuming that it took them one hour to evacuate the goods from the basement and to request help.

7.5 Rainfall field variability and catchment dynamics

It is well established that atmospheric convection producing flash flood events is either isolated or organised in mesoscale convective systems (MCS) (see for instance Ricard et al., 2007 about the 2002 event). Embedding convective cells with their own life cycle, MCS produce rainfall fields that are highly variable in space and time. The rainfall variability stimulates the nonlinear dynamics of stream flow generation over a wide range of scales (see Menabde and Sivapalan, 2001; Dodov and Foufoula-Georgiou, 2005, among others). In turn, significant differences can be observed between the flood

dynamics of elementary tributaries with respect to the dynamics of the global catchment. The example given in Figure 7-1 illustrates the response of the Fella River (Italy) in August 2003 at three different spatial scales (0.65 km², 24 km² and 165 km²). For a better readability, the figure displays specific discharges i.e., takes the ratio between the discharge values and the catchment area. The response time changes markedly through scales, ranging from less than 1 hour (ca. 40 min.) over the basin of 0.65 km² to 5 hours over the basin of 165 km². Moreover, this example confirms that the different response frequencies are observable within the same flash flood event and produce extreme values at all scales. Similar embedded responses have been observed for other flash flood events (Delrieu et al., 2005).

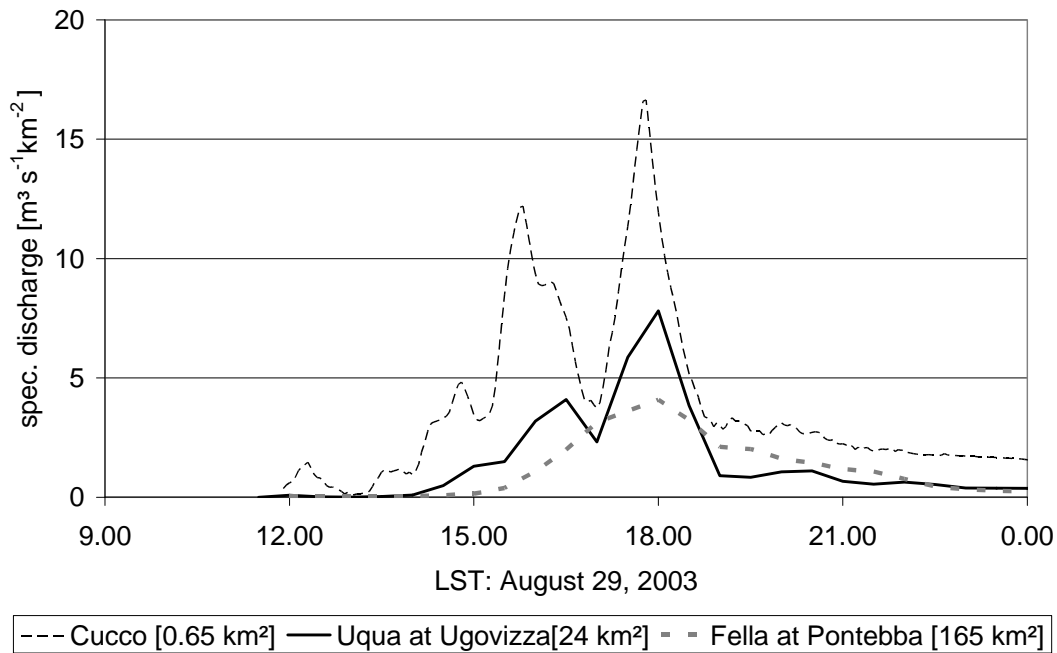


Figure 7-1: Catchment dynamics during the 29 August, 2003 event at three spatial scales: Cucco (0.65 km²), Uqua at Ugovizza (24 km²) and Fella at Pontebba (165 km²).

Having in mind these general hydrometeorological features, on the one hand, and willing a synthetic descriptor of the watershed dynamics to contrast with descriptors of human responses, on the other hand, we used a classical space versus time representation of the response time of a series of watersheds during past flash-floods as the main background of this study (see Orlanski, 1975 in meteorology and Blöschl and Sivapalan, 1995 in hydrology for examples of use of comparable graphs). Figure 7-2 reports the lag time versus the watershed area for a set of flash-flood events recently documented in Austria, France, Greece, Italia, Romania, Slovakia, Spain and the United Kingdom (Gaume et al., 2008). This graph clearly marks a bottom limit of watershed response times increasing as a power function of the watershed size:

$$t = 0.1A^{0.55} \tag{1}$$

with the lag time t in hours and the watershed area A in km².

The line chosen to show this lag-time limit is close to that reported by previous studies (Sivapalan et al., 2002; Berne et al, 2004) and has an exponent close to 0.5, meaning that the water velocity is constant over the considered range of scales. The dispersion of the points above this limit reflects the degree of resonance between the strength, size, duration and position of the generating storms and the size and position of the watersheds.

As far as the events specifically selected for this study are concerned (Gard 2002 and Fella 2003), their position in Figure 7-2 shows that they are representative of the set of events, with some of them rather extreme in term of quickness of response.

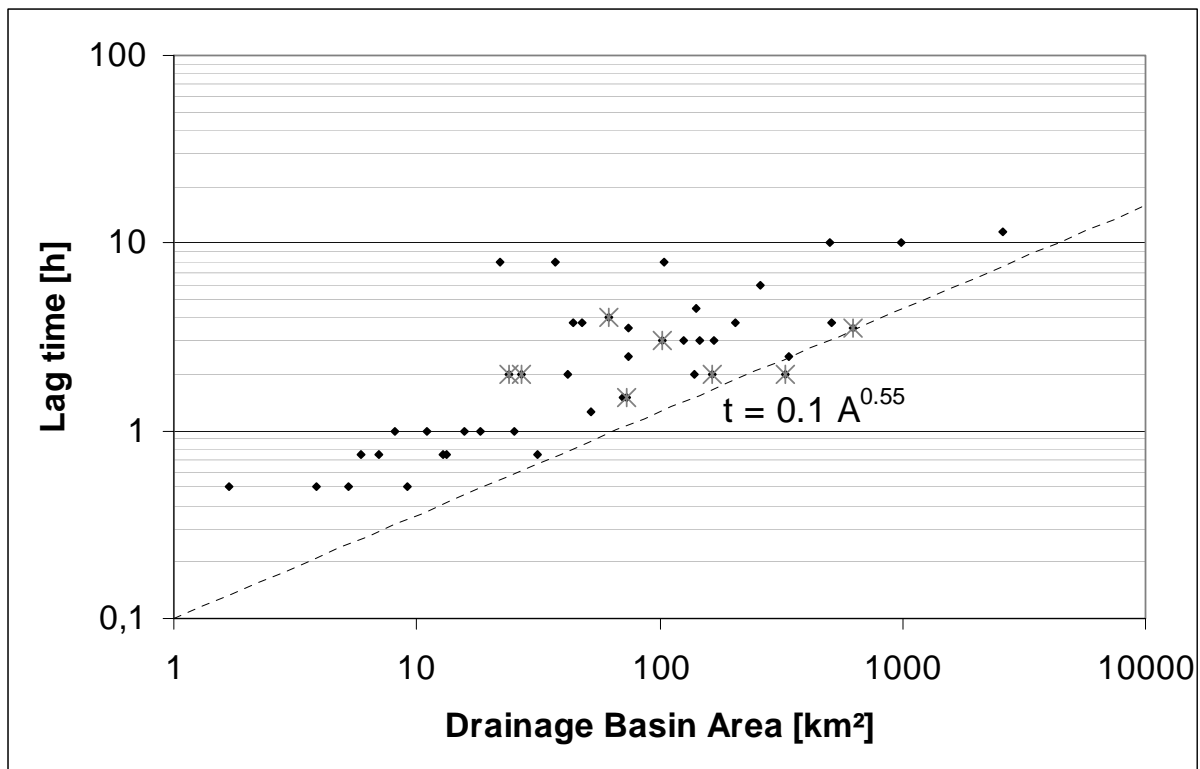


Figure 7-2: Lag time (in hours) versus drainage area (in km²) for the selected events. The model representing the lower envelop is drawn in dashed line. Gard and Fella events are marked with stars.

7.6 Characteristics of the social response

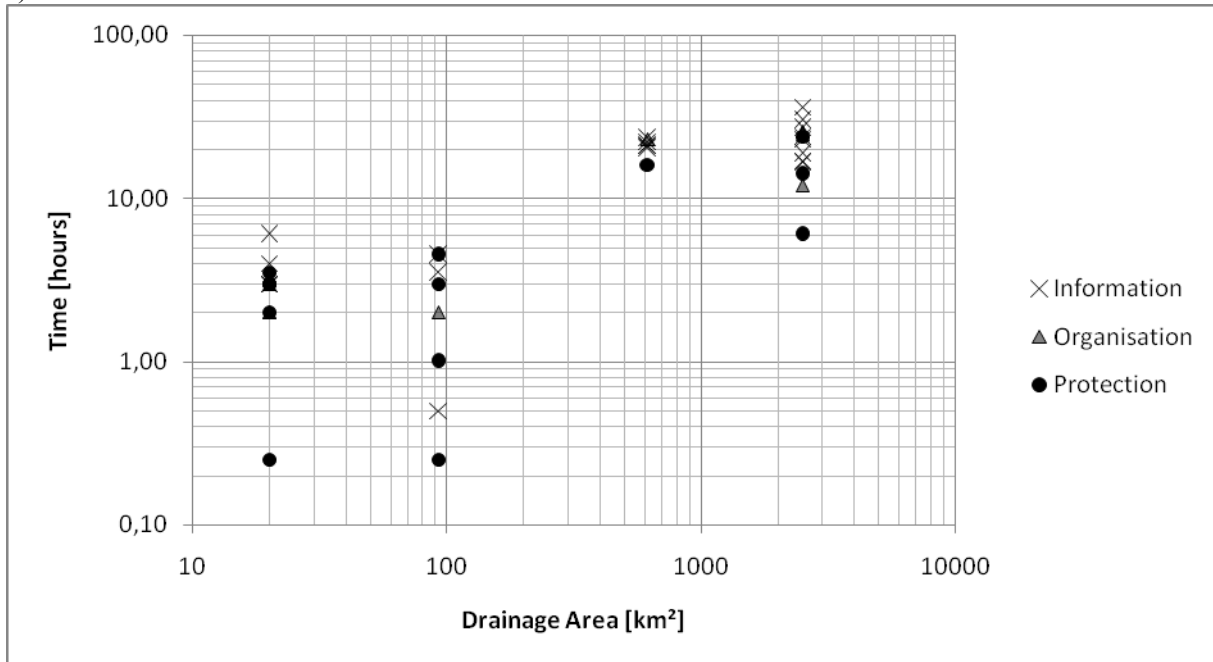
As mentioned in Section 7.1, Table 7-1,2,3,4 describes the chronology of four cases of flash-floods. Each reported action is qualified by the nature of the actors at the origin (initiator) and at the end (receptor), by the type of activity concerned and by the type of human group concerned.

In previous works, we observed that social actions for protecting goods or persons are preceded by a phase of qualification of the situation (Creton-Cazanave et al, 2009). We distinguished three types of actions: information, organisation and protection, that apply . They apply to all the actors, from forecasters to inhabitants and to all social group sizes. The information phase covers the collection of data and its crosscheck with other data or actors to validate the first feeling of danger. It is the first activity of the warning cycle. Organisation synthesises and transforms the above information into a structured response like for instance the mobilisation of human forces or the implementation of a pre-established defence plans. Chronologically and logically organisation takes benefit of the available information and prepares the protection phase which ends the cycle. Protection qualifies efficient actions in terms of security like preventive evacuation of people or goods as well as rescue missions. Human actions are also classified in three types according to the size of the groups concerned. We distinguish individuals, communities and institutions. Individual concerns just one person and by extension a small social entity (a family, for instance). Community pertains to small groups of people which may be more or less organised to deal with emergencies. Neighbourhood groups, voluntary

associations, but also the population of a school or a company as well as of the population of small territorial entities like villages are included in this category.

'Institution' qualifies, on one hand, the public forces like police or civil protection and, on the other hand, the national administration, its local representatives and technical operators like meteorological offices and water management departments.

a)



b)

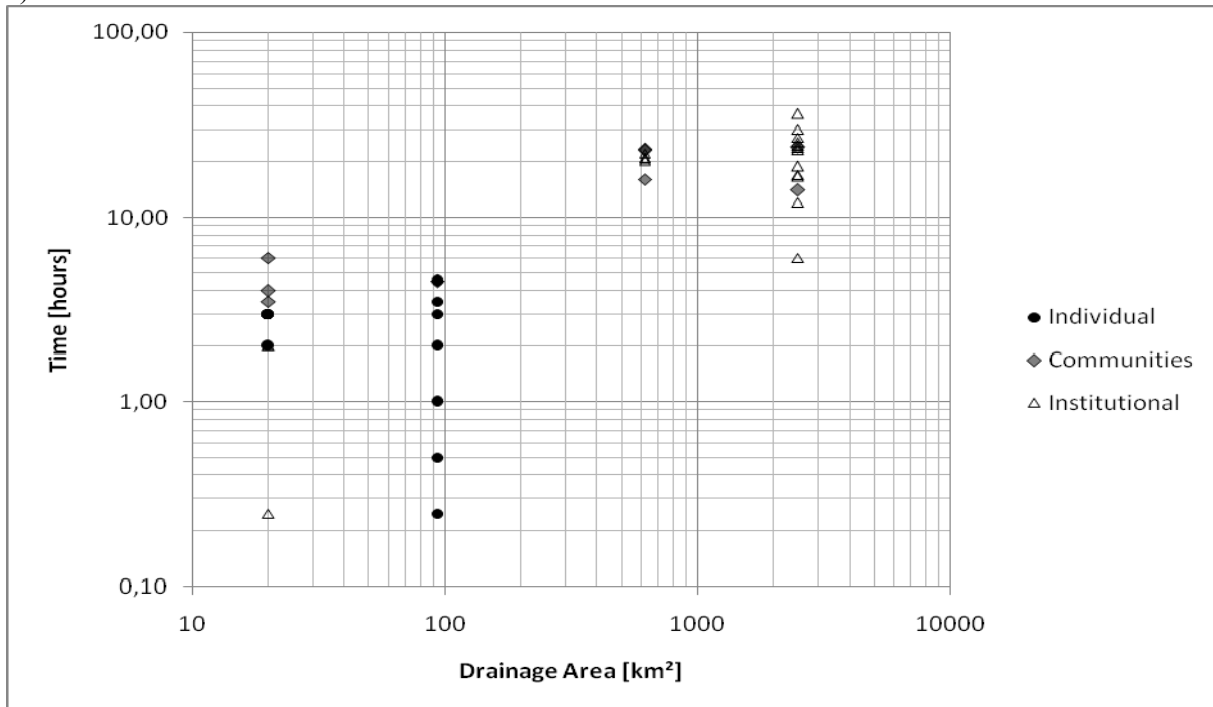


Figure 7-3: Representation of 43 elementary human actions in a logarithmic plot of their anticipation time (i.e. time of action before the flow peak) versus the area of the watershed where they occurred. Three types of actions (Fig. 3a) as well as three types of sizes of human groups (Fig. 3b) are distinguished by the shape of each point representing a elementary action.

Figure 7-3 synthesizes the information contained in Table 7-1,2,3,4 according to the size of the concerned watershed and to the type of action (Figure 7-3a) as well as to the type of group of actors (Figure 7-3b). This Figure calls preliminary remarks about the general organisation of the points from a social point of view and two main comments in relation with the time and space characteristics of flash-floods.

Examination of the different types of activities on Figure 7-3a leads to the pertinence of the logical cycle: information-organisation-protection. Even though the information takes place generally among the first activities (except for one case), it is first noticeable that organisation and protection intervene at different places in the sequences reported for the 4 cases of Figure 7-3a. Different explanations can be given. The evolution of the situation generally induces the need for successive waves of reaction cycles. Missing information in our dataset makes the documentation of the basic cycles seldom complete. Nevertheless, we can notice that complete cycles are present at all scales, confirming that this generic decomposition pertains to all sizes of human groups and is useful at all scales. It is also noticeable that no action is reported after the time of the peak. This is related, in a sense by definition, to the fact that we concentrated our selection of actions on risk prevention, rather than on risk relief. However, given the time needed for these different types of response to be effective, we must also realize that some cycles can potentially fail working properly when the reaction of the watersheds to rain comes before the full implementation of the social response.

Looking at the social scale of the activities on Figure 7-3b, helps to analyze the spatial dimension of the social response. A first twofold comment is that the characteristic time of reaction of the different human groups decreases markedly with their size and that their capacity of anticipation increases with their size. The institutional reaction develops over 30 hours from 36 hours before the flow peak (see Table 7-1). The community reaction appears to be organised in 7 hours, from 23 hours to 6 hours before the peak (according to Table 7-2). The individual reactions appear to be much shorter and to start a few hours before the peak.

A second comment is that the size of the watersheds seems to determine the size of the reacting human groups. Most part of the actions conducted by institutions apply mainly to the largest watersheds (Gard and Vidourle) while, on the smaller ones, communities and individuals are in charge of the response. The dominance of institutional activities on large watersheds hides community and individual actions at those scales that are under-sampled in our dataset. For example, institutional actions have certainly effects on small scales through the broadcast of information but very few elements in interviews of individuals and communities help understanding the use they made of such information. On the other side, it is interesting to consider the cases where the individual response dominates. In the isolated places that are not covered well by the institutional response, individuals have to protect themselves by their own. For example in the Fella river case study, some residents undertook an autonomous evacuation, saving their lives and those of their neighbours. This was decided on the basis of the control and monitoring of the level of the streams and of their possible points of obstruction. In this phase the village was almost isolated due to the obstructions of the roads caused by debris flows and institutional intervention was not possible.

A third comment is that human groups have different capabilities of anticipation based on the nature of information they use. The information available at institutional scale comes mostly from meteorological and water services. In the cases studied here, even when the meteorological information is broadcasted early, at the smallest scales, people appear to rely on their own monitoring of the water levels. In these cases, reliability of the sources of information plays a crucial role. In both the Italian and in the French case, the local voluntary fire brigades groups are considered the main safety catalysts by the residents, possibly due to their local attachment, the deep knowledge of the territory, and training in facing the emergencies. Besides, the hydrological evidence of the flood seems to be a condition for individuals and communities to react. As showed in a parallel study (Creton-Cazanave, 2009) the current meteorological information needs to be adapted at a smaller scale to be used by communities and individuals.

In conclusion, the social response is reasonably described by a generic cycle: information-organisation-prevention across different group sizes. These groups have rather different characteristic temporal behaviours regarding both their capacity of anticipation and response.

7.7 Adequateness of monitoring and forecasting techniques at different scales

Having defined, on one hand, the time and space characteristics of the hydrometeorological response (Figure 7-2) and, on the other hand, the characteristic times of different types of social response (Figure 7-3), we can now integrate these elements in order to appreciate the pertinence of existing monitoring and forecasting tools.

Figure 7-4 integrates, into the same space-time graph used for Figure 7-3 the lag-time limit of Figure 7-2, indicating the relationship between the lower limit of catchment lag time and the corresponding catchment area ($t=0.1A^{0.55}$). In order to account, at least qualitatively, for the minimum duration of the rainfall event generating the catchment response, we have drawn the function $t=2(0.1A^{0.55})$ which in log scale turns to be a parallel line. The obtained transition area divides the time and space scale domain into two areas. Above, the meteorological generation of the rain field is the dominant process. At such space scales and anticipation times, the risk precursors are meteorological factors. Below the transition area, runoff propagation is the dominant process and adapted risk precursors are hydrological factors. The time scale of Figure 7-4 being an anticipation time with respect to the peak discharge, the figure can be used to scrutinise the type of actions according to the anticipation time and the catchment lag time.

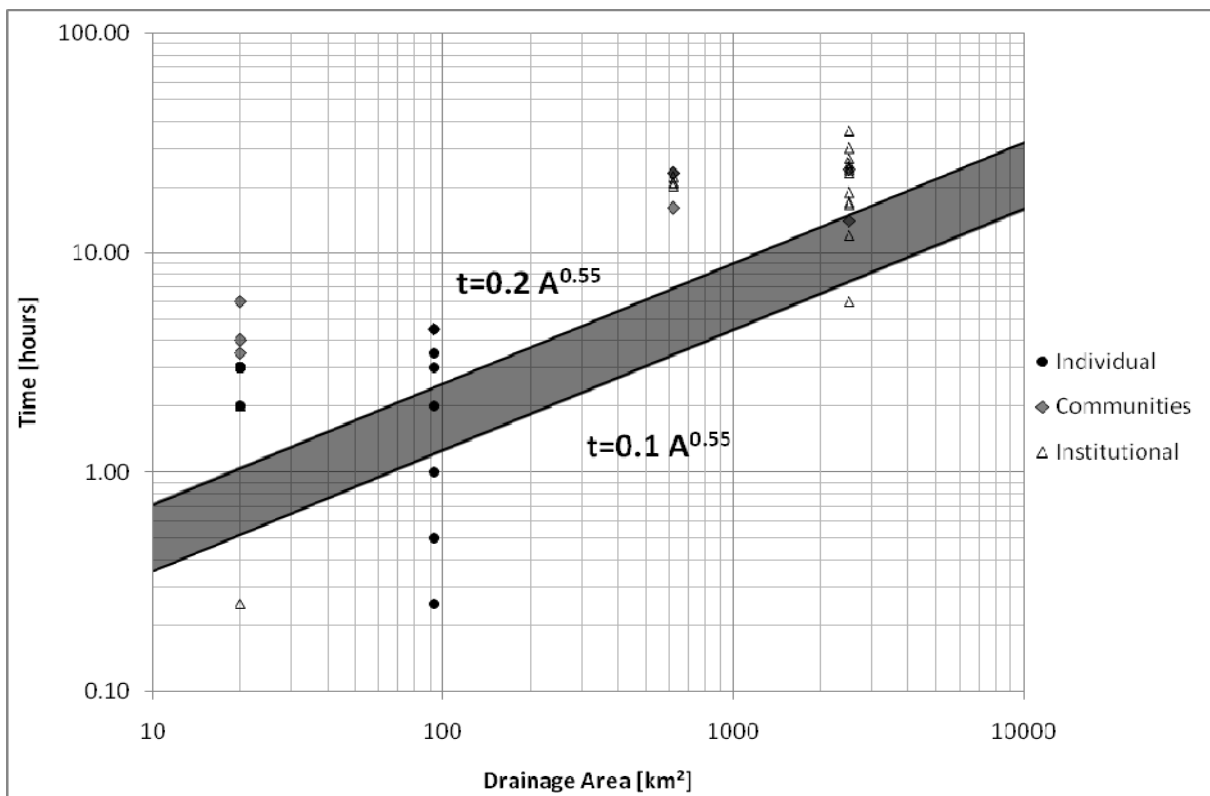


Figure 7-4: Representation of 43 elementary human actions in a logarithmic plot of their anticipation time versus the area of the watershed where they occurred. Three levels of organisation of the actors are distinguished by the different dot shapes. The bottom line of the shaded area represents the relationship between the catchment lag-time and its drainage area.

The upper line is distant of Log 2 from the bottom line and qualitatively indicates the characteristic duration of the generating rain event

The Figure 7-4 globally shows that the position of human responses respect to the flood dynamics is rather homogeneous through scales. Except for the Valliguières case (93 km²) the distribution patterns of human actions relative to the flood dynamics are much similar. They cover a time range equal to 2 to 4 times the reaction time of the catchment and they rarely go beyond the rain peak (i.e. below the lag-time line). As a consequence, most part of the reported human actions develops at periods dominated by the meteorological processes. To that respect additional comments can be made.

The anticipation at the broader scales relies on the use of NWP models for rainfall forecasting and on the generation of relevant flooding scenarios that are behind the official broadcast of the meteorological services. One can note that the largest spatial scale explored in this study is still relatively modest (2.500 km²) compared to the typical surfaces targeted by NWP. At the smaller scales the anticipation time is much shorter (4 or 6 hours) and the question rises about the type of information used. Examination of the responses at the scale less than 100 km² reveals that several organisation and protection actions occurred just before the peak time, and generally at anticipation times less than the catchment response. It is difficult to evaluate how these actions were triggered; however, how reported above, in general it was the raising of water levels in the neighbour rivers, rather than the information received from abroad, that triggered the individual and community actions. Of course, some of the evacuations were organised at these short anticipation times proving that the reactivity of communities and individuals is well adapted. Other actions, equally important, included the decision to stay home and avoid to move. This implies that the information required at these time scales, and for these anticipation times, is a reliable and high-resolution description of the actual rainfall field and of its likely impact on the hydrologic response at very short times. For example, organising the evacuations requires knowledge of how the potential routes can be hit by inundation in the next half hour or less.

Flash flood forecasting tools relying on accurate radar monitoring of the precipitation field and pre-established hydrological scenarios linked to the soil-moisture status of the soils, such as the Flash Flood Guidance method (Georgakakos, 2004, 2006; Martina et al., 2006; Norbiato et al., 2008), may provide enough information for warning at these space and time scales. This real time analysis of radar rainfall accumulations allows forecasting lead times that are at least equal to the response time of the watersheds and allows potentially dealing with basin sizes that match the radar resolution. A key advantage of these methods is that they allow the forecaster to readily ingest local precipitation information and to update warnings without the need to run complex hydrometeorological forecasting chains (Norbiato et al., 2008).

7.8 Conclusions and future research

This report compares watershed dynamics under flash flood forcing to observed social responses for two well studied flash flood events, with the objective of identifying if the current means available for flash-flood monitoring and forecasting can meet the requirements of populations to evaluate the severity of the flood and anticipate its danger. To this end, we identify the social response time for different social actions in the course of the floods, and we compare these to the relevant catchment response time.

In the same manner as the response time of a watershed is linked to its size, we assume that the characteristic time of the above defined warning procedure depends on the number of people concerned and on the level of information available about the hazardous phenomenon.

We introduced a broad characterization of the event management activities into three types according to their main objective (information, organisation and protection). The activities were also characterised into three types according to the scale of human organisation dynamics (individuals, communities and institutions). The simplified schematisation of the human response was necessary

because of the lack of structured observations. We provide so two main parameters to characterize the time schedule of social actions in regard to the storm and flood dynamics: the anticipation time and the reaction time.

Conclusion pertains to i) the characterisation of the social responses according to watershed scale and to the information available, and to ii) the appropriateness of the existing surveillance and forecasting tools to support the social responses identified above.

We observed that the spatial scale seems to determine the size of the reacting human groups, and that there is a link between the spatial scale and the social response time. Most part of the actions conducted by institutions apply mainly to the largest watersheds while on the smaller ones communities and individuals are in charge of the response. The institutional reactions develop in 30 hours when community reactions appear to be concentrated in ca. 6 hours and individual reactions in even less. This suggests that representing the dynamics of the social response with just one number representing the average time for warning a population is an oversimplification. Rather differently, the social response exhibits a parallel with the hydrological response time, by diminishing in time with decreasing the size of the considered watershed.

The second result is that human groups have different capabilities of anticipation apparently based on the nature of information they use. The information available at institutional scale comes mostly from meteorological services, whereas at smaller scales, even when the meteorological information is provided early, people mobilise other types of data, monitoring of the level of water notably. This suggests that, even though at small scales actions are characterised by shorter response times than at larger scales, decisions may be taken with considerable delay with respect to the onset of the precipitation.

These results were confirmed when comparing, on the same graph, watershed response times and social response times. This showed clearly that at scales less than 100 km², a number of actions were taken with response times comparable to the catchment response time. The implications for adapting the warning processes to social scales (individual or organisational scales) are considerable. At small scales and for the implied anticipation times, the reliable and high-resolution description of the actual rainfall field becomes the major source of information for decision-making processes involving evacuations or advising to stay home. Methods like the Flash Flood Guidance (FFG) may provide enough information for warning at these space and time scales. This real time analysis of radar rainfall accumulations allows forecasting lead times that are least equal to the response time of the watersheds and allows potentially dealing with basin sizes that match the radar resolution. Clearly, this leads to stress three major issues: i) the need to obstinately keep improving the accuracy and quality control of real time radar rainfall data, more particularly during extreme flash flood generating storms; ii) the need to introduce more and more accurate real time information about rainfall accumulations during the decision making process; iii) the need to ensure wide access to this information and to products quickly understandable (such as the FFG) among people at risk.

There is clearly a need to confirm these results by means of further studies developed on other events. The observation that a human society is to some extent structured in cascade, with space and time scales of response that are adapted to the disturbing atmospheric and hydrologic processes, may have a wide range of implications. One, among several, may deserve specific attention. The observation may provide a clearer view of the differences among social responses to natural hazards, distinguishing those hazards which are organised according to a natural spatial scale ordering (such as the flood hazard), with respect to those hazards which are not (such as the wildfire hazard). The question of scales, so pervasive in the hydrological science, may be developed further by considering the social scales as well.

7.8.1 Appendix 1:

Table 7-1: Display of the Gard River Case (France). Drainage Area: 2500 km². Peak time : 9/09/2002, 18:00 UTC

Anticipation Time	Type of response	Initiator	Receptor	Type of activity	Social scale
36:00	Meteorological vigilance level 3 (orange) : BRS1 n°1	Météo France	Gard Department	Information	Institutional
29:56	Meteorological vigilance level 3 (orange) : BRS n°2	Météo France	Gard Department	Information	Institutional
27:00	Press release	Préfecture2	Medias and population	Information	Institutional
25:35	Request of heavy means (copters, army means, ...)	Préfecture	National authorities	Organisation	Institutional
24:30	Opening of the cell of operational defence	SIDPC3		Organisation	Institutional
24:00	Warning and organization of the population's evacuation	Mayor of Collias (800 inh.)	Population of Collias	Protection	Communities
23:53	Meteorological vigilance level 3 (orange) : BRS n°3	Météo France	Gard Department	Information	Institutional
23:05	Specialized bulletin (for operators) un-alarmed	Météo France	SIDPC	Information	Institutional
18:48	Météo France Vigilance level 3 (orange) : BRS n°4	Météo France	Gard Department	Information	Institutional
17:00	The threshold of warning fixed by the civil defence plan is attained	Préfecture	Mairie de Collias	Information	Institutional
16:33	Meteorological vigilance level 34 (red) : BRS n°4	Météo France	Gard Department	Information	Institutional
14:00	Preventive evacuation. 200 people refused to leave	Mayor of Comps (1500 inh.)	Population of Comps	Protection	Communities
12:00	Launching of plan ORSEC	Préfecture	Gard Department	Organisation	Institutional
6:00	Rescue by helicopters of 150 people who refused to evacuate	Army	Population of Comps	Protection	Institutional

Table 7-2: Display of the Vidourle Case (France). Drainage Area : 620 km². Peak Time : 9/09/02, 14:00 UTC

Anticipation Time	Type of response	Initiator	Receptor	Type of activity	Social scale
23:15	Information concerning the start of the flooding	Mayor of Sommières (3700 inh.)	Préfecture	Information	Communities
23:00	Help request	Mayor of Aujargues (700 inh.)	SIDPC	Organisation	Communities
22:10	Vigilance thresholds of precipitations reached on the Vidourle catchment	SAC4	Préfecture	Information	Institutional
21:00	Proposal of warning on Vidourle (without previous warning)	SAC	Préfecture	Information	Institutional
20:50	Warning transmission (by phone)	SAC	SIDPC	Information	Institutional
20:11	Reception of warning message	SAC	Defence Ministry	Information	Institutional
16:00	Preventive evacuation of the population	Mayor of Quissac (2300 inh.)	Quissac population	Protection	Communities

Table 7-3: Display of the Valligüères River Case (France). Drainage Area : 93 km². Peak Time : 08/09/2002 23:30 UTC

Anticipation Time	Type of response	Initiator	Receptor	Type of activity	Social scale
4:30	Self warning by inhabitants watching the level of the Gard river	Residents	Neighbours	Information	Individual
4:30	Rescue of people on the roof of their cars	Fire brigade	Residents	Protection	Communities
3:30	Watching water level	Residents		Information	Individual
3:00	Furniture evacuation	Residents		Protection	Individual
2:00	Help request for an injured person	Residents	Fire brigade	Organisation	Individual
1:00	Spontaneous evacuation of a couple with a child	Residents		Protection	Individual
0:30	Watching water level	Residents		Information	Individual
0:15	Furniture evacuation	Residents		Protection	Individual

Table 7-4: Display of the Fella River Case (Italy). Drainage Area : 20 km². Peak time : 29/08/03, 17:00 UTC

Anticipation Time	Type of response	Initiator	Receptor	Type of activity	Social scale
25:30	Alert (via Fax and SMS)	Regional civil protection	Local civil protection	Information	Institutional
6:00	Control and monitoring of the most endangered areas	Local fire brigades corps	Local authorities	Information	Communities
4:00	Warning (sirens)	Local fire brigades corps	Local authorities	Information	Communities
3:30	Protection for the most endangered houses (sandbags, water channels,..)	Local fire brigades corps	Residents	Protection	Communities
3:00	Local vigilance and organization	Residents		Organisation	Individual
3:00	Help brought to neighbours	Residents	Neighbours	Protection	Individual
3:00	Watching of water level	Residents		Information	Individual
3:00	Decision to stay at home and to avoid to move	Residents		Protection	Individual
3:00	Spontaneous individual evacuation	Residents		Protection	Individual
3:00	Went to control house	Residents		Information	Individual
2:00	Road closed to the traffic	Provincial civil protection and prefect		Organisation	Institutional
2:00	Help and support request	National Interior Ministry	Foreign civil protection (Austria, Slovenia, city of Bamberg)	Organisation	Institutional
1:00	Autonomous evacuation	Residents		Protection	Individual
0:15	Compulsory evacuation	Provincial civil protection, mayor, residents		Protection	Institutional

8. Conclusions and recommendations

8.1 *The flash flood observational system*

8.1.1 *Post event surveys*

Traces left by water and sediments during flash floods provide an opportunity for developing spatially detailed post-event surveys of flash flood response along the stream network. Indirect methods such as slope-area, contracted opening, flow-over-dam, or flow-through-culvert are often used for this purpose. However, the important thing here is that the survey needs to capture not only the maxima of peak discharges: less intense responses within the impacted region are important as well. These can be contrasted with the corresponding generating rainfall intensities and depths obtained by weather radar re-analysis, thus permitting identification of the catchment properties controlling the rate-limiting processes. Collection of eyewitness accounts and observations represents an integral part of the flash flood response survey. It should be noted that these 'observations' may be currently collected as digital imagery from movies and pictures. These represent an extremely important information source to refine the assessment of flow type/depth, the estimates of flow velocity and discharge, and for the evaluation of flooding extent. For instance, digital imagery from movies may afford use of advanced techniques for discharge estimation, such as the Particle Image Velocimetry (PIV) technique. Interviews with eyewitnesses provide information and anecdotal evidence on the time sequence and dynamics of the flood, and as such they add a time dimension to the spatial patterns of flash flood response. It should be recognised that accuracy of the witnesses accounts is limited (up to ± 15 min, according to Borga et al., 2007). Consequently, when these observations are used to estimate the timing of the flood peaks, their information content should be related to the catchment response time, and therefore with the catchment scale.

8.1.2 *Integration of the survey observations by means of hydrological modelling*

The utility of the individual observations gathered by means of the flash flood survey needs to be extended by use of hydrological models driven by the space-time estimates of rainfall obtained by means of radar re-analysis. The multiple simulations obtained in this way ensure closure of the water balance at the event scale and consistent dynamics of the rainfall-runoff sequence. The simulations may be compared with the spatially-detailed response observations with the objective of evaluating the consistency between the various sources of information within a framework for uncertainty analysis. It is likely that non-probabilistic approaches, including sensitivity-analyses, convey the most promising perspectives (Montanari, 2007) for this purpose.

Flash flood events are usually characterised by extensive flooding. More insight into the flash flood dynamics may be obtained by integrating hydrological models with 1D and 2D hydraulic models. The relevant simulations could be compared with the inundation maps made available for these events. Data concerning flooded bridges and damaged structures could also be exploited to evaluate the consistency of the hydraulic description of the events.

The final outcomes of the integrated survey methodology are represented by the data themselves, characterised by uncertainty assessment, and by the increased capability to examine the terms of the hydrological balance at the event scale. This affords examination of key hypotheses concerning the hydrology and hydraulics of catchment response under flash flood conditions. Examples include i) the role of antecedent soil moisture conditions on flood magnitude; ii) the role of land use and catchment properties on runoff generation; and iii) dependence of flood properties on basin scale by means of space-time scaling properties of rainfall.

Surveying flash flood response may therefore provide valuable insight; however, generalizing the findings beyond the areas of interest may prove to be difficult. Each episode seems to have particularities that cannot be specified in full detail. Advancing understanding in the context of flash

flood studies, which are by necessity opportunistic and event-based, requires the development of a parsimonious avenue to synthesis. This may be based on classification and similarity concepts which can be profitably used when the processes are not fully understood. Contrasting different case studies and learning from the similarities and dissimilarities may help to find an explanation or description of the underlying patterns.

8.1.3 Requirements for space-time rainfall observations

The literature on the significance of aggregation of rainfall for runoff estimation is complex and sometimes contradictory. Effects can be expected to vary depending on the characteristic of the rainfall, the nature of the catchment, and the spatial scale of the catchment and rainfall. The mountainous region on the north-eastern border of the Friuli region in Italy produces some of largest unit discharge peaks in the northern Mediterranean basin and is monitored with a dense network of weather radar and raingauge stations. This offered an opportunity to examine the impact of spatial aggregation of rainfall on extreme flood modelling.

Flood response to an extreme storm events, occurred on the Fella River basin, at various catchment scales ranging from 10 km² to 600 km², were reproduced by using high resolution radar rainfall estimates and a distributed hydrologic model, based on a Hortonian infiltration model and a network-based representation of hillslope and channel flow. Four input spatial resolutions were considered, with grid size equal to 1-, 4-, 8- and 16- km, for rainfall properties representation. A dimensionless parameter given by the ratio between input length aggregation and the square root of the watershed area (L_R/L_W) was used to describe the sensitivity of the runoff model. Given the focus on Hortonian runoff generation mechanism and surface runoff propagation through hillslopes and branched channel networks, we examined the role of runoff transport geometry in the coarsening of spatial rainfall representation and on simulated runoff volumes and peak discharges.

The rainfall spatial variability play an important role when rainfall fields are systematically structured across locations with equal flow distance coordinates, as it occurs in the case of orographic effect and when catchments are elongated in the direction perpendicular to the mountainous range. When heavy rainfall lies on a sufficiently narrow range of isochrones, the smoothing effect due to increasing the rainfall aggregation length may result in a significant distorsion of the rainfall field geometry with respect to the river network. In these cases, the increase of the spatial rainfall aggregation length leads to a significant deformation of the flood shape, with an anticipation of the simulated flood peak when the precipitation is concentrated towards the periphery of the catchment, and a delay of the simulated flood peak when the precipitation is concentrated towards the outlet of the catchment. These effects are negligible at the small catchment scale and become significant with increasing the catchment size. When infiltration is 'switched off' in the runoff model and all the variability arises due to runoff transport processes, the distorsion of the rainfall field geometry with respect to river network may be an important control on peak discharge error, even at catchment scales less than 500 km². Obviously, this distorsion has no impact on the runoff volume error, which is in this case completely determined by the rainfall volume error. This volume error arises when rainfall values pertaining to areas just outside the catchment enter the computation of the average rainfall over the basin by increasing the aggregation length. The rainfall volume error is controlled mainly by the ratio L_r/L_w and by the rainfall integral scale; it exerts a dominant impact on peak discharges at small catchment scales (75 km²), and becomes less significant by increasing the catchment dimension.

Errors on both runoff volumes and peak discharges increase when infiltration is taken into account in the runoff model. This is expected, since the infiltration process injects further spatial variability, both random and structured, into the rainfall-runoff process. Effects are particularly remarkable when significant structured rainfall variability combines with relatively important infiltration rates due to dry initial conditions, as this emphasises the non linear character of the rainfall-runoff relationship. In general, these results confirm that the correct estimate of rainfall volume is not enough for the accurate reproduction of flash flood events characterised by large and structured rainfall spatial variability, even at catchment scales around 250 km². However, accurate rainfall volume estimation may suffice

for less spatially variable flood events. The results shows also that the rainfall volume errors generally magnify through the rainfall-runoff modelling, at least for the runoff model considered here.

This investigation has documented how input variability, as filtered by using different spatial aggregation lengths, feeds through to variability in modelled runoff response at the catchment scale. More extensive investigations would strengthen this understanding and provide additional guidance on the design of radar/raingauge networks for flow forecasting and the spatial resolution requirements for rainfall and soil properties at different catchment scales. Further work might determine whether the results obtained in this investigation apply to other model formulations and may be generalised to other hydroclimatic environments. In this framework, future investigations should focus on the sensitivity of the averaging of space-time rainfall fields across locations with equal flow distance coordinates to the rainfall aggregation length and to river network geometry. As shown here, this is a significant and relatively unexplored feature of catchments where rain exhibits significant spatial variability and linear routing through branched channel networks plays a significant role.

8.2 Assessment of the FFG approach for flash flood forecasting and warning

In this section, we propose using the Flash Flood Guidance (FFG) method and a method of model-based threshold runoff computation to improve the accuracy of flash flood forecasts at ungauged locations. Our approach requires running the lumped hydrological model to derive flood frequencies at the outlet of the ungauged basin under consideration, and then to derive the threshold runoff from these model-based discharges. This model-based threshold runoff is subsequently used in the forecasting phase when running the model to compute the FFG. The approach provides a pragmatic method to characterize flood severity at ungauged locations. The study examines the potential of this method to account for the hydrologic model uncertainty and for biases originated by lack of model calibration on local conditions.

Experiments to validate this approach involved the implementation of a semi-distributed continuous rainfall-runoff model and the operation of the FFG method over four basins located in the central-eastern Italian Alps and ranging in size from 75.2 km² to 213.7 km². Data were available for periods ranging from 11 to 13 years. The model was calibrated on two larger basins and the model parameters were transposed to the other two basins to simulate operations in ungauged basins. The FFG method was applied by using the 2-yr discharge as the threshold runoff. The threshold runoff was derived both by using local discharge statistics and the model-based approach advocated here. Examination of the results obtained by this comparison shows that the use of model-based threshold leads to improvements in both gauged and ungauged situations. Overall, the Critical Success Index (CSI) increases by 12% for gauged basins and by 31% for ungauged basins by using the model-based threshold with respect to use of local data. As expected, the increase of CSI is more remarkable for ungauged basins, due to lack of local model calibration and the greater likelihood of occurrence of a simulation bias in model application over these basins. This shows that the method of threshold runoff computation provides an inherent bias correction to reduce systematic errors in model applications to ungauged (and gauged) basins.

The method was also applied to simulate FFG operations with three flash flood events and by using additional data from two further basins. This application showed that, even though reasonable results may be obtained by using the FFG to map susceptibility to flash flood across a region, the use of transposed model parameters from gauged to ungauged basins may limit the potential of the method. Improvements could be obtained in this case by using more reliable methods for model parameter regionalisation.

The promising results from these modelling experiments suggest that further work should be devoted to the analysis of the combination of FFG with model-based runoff threshold. In particular, future work should focus on the examination of the influence of spatial and temporal scales on the performances of the method and on the dependence of these scales on the type of rainfall information

used to force the model. It is likely that different types of rainfall forcing will translate to different scale-dependence patterns.

Another area where further work is required is the development of more reliable methods for derivation of model parameters. Prior studies (Zhang et al, 2008) have found that the correlations between streamflow characteristics and physical watershed characteristics are often significantly higher than between model parameters and watershed characteristics. Methods based on the regionalization of streamflow characteristics could be tested to improve flash flood forecast in ungauged basins.

Conditio sine qua non for continuing this work in an effective way is the development of a flash flood occurrence database with long term data that would allow reliability analysis (Creutin and Borga, 2005; Gaume et al., 2008). This is a pressing need in the area of flash flood risk management which should receive proper attention from both scientists and policy makers.

8.3 Catchment dynamics and social response during flash floods

This Section aims to identify if the current means available for flash-flood monitoring and forecasting can meet the requirements of populations to evaluate the severity of the flood and anticipate its danger. To this end, we identify the social response time for different social actions for two well studied flash flood events in the course of the floods, and we compare these to the relevant catchment response time.

In the same manner as the response time of a watershed is linked to its size, we assumed that the characteristic time of the above defined warning procedure depends on the number of people concerned and on the level of information available about the hazardous phenomenon. We introduced a broad characterization of the event management activities into three types according to their main objective (information, organisation and protection). The activities were also characterised into three types according to the scale of human organisation dynamics (individuals, communities and institutions). The simplified schematisation of the human response was necessary because of the lack of structured observations. We provide so two main parameters to characterize the time schedule of social actions in regard to the storm and flood dynamics: the anticipation time and the reaction time. Conclusion pertains to i) the characterisation of the social responses according to watershed scale and to the information available, and to ii) the appropriateness of the existing surveillance and forecasting tools to support the social responses identified above.

We observed that the spatial scale seems to determine the size of the reacting human groups, and that there is a link between the spatial scale and the social response time. Most part of the actions conducted by institutions apply mainly to the largest watersheds while on the smaller ones communities and individuals are in charge of the response. The institutional reactions develop in 30 hours when community reactions appear to be concentrated in ca. 6 hours and individual reactions in even less. This suggests that representing the dynamics of the social response with just one number representing the average time for warning a population is an oversimplification. Rather differently, the social response exhibits a parallel with the hydrological response time, by diminishing in time with decreasing the size of the considered watershed

The second result is that human groups have different capabilities of anticipation apparently based on the nature of information they use. The information available at institutional scale comes mostly from meteorological services, whereas at smaller scales, even when the meteorological information is provided early, people mobilise other types of data, monitoring of the level of water notably. This suggests that, even though at small scales actions are characterised by shorter response times than at larger scales, decisions may be taken with considerable delay with respect to the onset of the precipitation.

These results were confirmed when comparing, on the same graph, watershed response times and social response times. This showed clearly that at scales less than 100 km², a number of actions were

taken with response times comparable to the catchment response time. The implications for adapting the warning processes to social scales (individual or organisational scales) are considerable. At small scales and for the implied anticipation times, the reliable and high-resolution description of the actual rainfall field becomes the major source of information for decision-making processes involving evacuations or advising to stay home. Methods like the Flash Flood Guidance (FFG) may provide enough information for warning at these space and time scales. This real time analysis of radar rainfall accumulations allows forecasting lead times that are least equal to the response time of the watersheds and allows potentially dealing with basin sizes that match the radar resolution. Clearly, this leads to stress three major issues: i) the need to obstinately keep improving the accuracy and quality control of real time radar rainfall data, more particularly during extreme flash flood generating storms; ii) the need to introduce more and more accurate real time information about rainfall accumulations during the decision making process; iii) the need to ensure wide access to this information and to products quickly understandable (such as the FFG) among people at risk.

There is clearly a need to confirm these results by means of further studies developed on other events. The observation that a human society is to some extent structured in cascade, with space and time scales of response that are adapted to the disturbing atmospheric and hydrologic processes, may have a wide range of implications. One, among several, may deserve specific attention. The observation may provide a clearer view of the differences among social responses to natural hazards, distinguishing those hazards which are organised according to a natural spatial scale ordering (such as the flood hazard), with respect to those hazards which are not (such as the wildfire hazard). The question of scales, so pervasive in the hydrological science, may be developed further by considering the social scales as well.

9. References

1. Alcoverro J., Corominas J. and Gomez M. (1999) *The barranco de Aras flood of 7 August 1996 (Biescas, Central Pyrenees, Spain)*, Engineering Geology, 51, 237-255.
2. Andréassian V., Perrin C., Michel C., Usart-Sanchez I. and Lavabre J. (2001) *Impact of imperfect rainfall knowledge on the efficiency and the parameters of watershed models*, Journal of Hydrology, 250, 206-223.
3. Ayral P-A. (2005) *Contribution à la spatialisation du modèle opérationnel de prévision des crues éclair ALHTAÏR – Approches spatiale et expérimentale – Application au bassin versant du Gardon d'Anduze (Gard – France)*, PhD, Université d'Aix-Marseille I, France.
4. Barancourt C., Creutin J. D., and Rivoirard J. (1992) *A Method for Delineating and Estimating Rainfall Fields*, Water Resour. Res., 28(4), 1133–1144.
5. Bell V.A. and Moore R.J. (2000) *The sensitivity of catchment runoff models to rainfall data at different spatial scales*, Hydrology and Earth System Sciences, 4(4), 653-667.
6. Belmonte A.C. and Beltran F.S. (2001) *Flood events in Mediterranean ephemeral streams (ramblas) in Valencia region, Spain*, Catena, 45, 229-249.
7. Benson M.A. and Dalrymple T. (1967) *General field and office procedures for indirect discharge measurements*, U.S. Geological Survey Tech. Water Resour. Invest., Book 3, Chapter A-1.
8. Berenguer M., Corral C., Sánchez-Diezma R. and Sempere-Torres D. (2005) *Hydrological Validation of a Radar-Based Nowcasting Technique*. Journal of Hydrometeorology , Vol: 6 , No: 4 pp: 532-549.
9. Berenguer M., Sempere-Torres D., Corral C. and Sánchez-Diezma R. (2006) *A fuzzy logic technique for identifying nonprecipitating echoes in radar scans*, Journal of Atmospheric and Oceanic Technology , Vol: 23, pp: 1157-1180.
10. Berne A., Delrieu G., Creutin J.D and Obled C. (2004) *Temporal and spatial resolution of rainfall measurements required for urban hydrology*, Journal of Hydrology, 299, 166–179.
11. Blöschl G. (2005) *Rainfall-runoff modelling of ungauged catchments*, Article 133 in: Encyclopedia of Hydrological Sciences, M. G. Anderson (Managing Editor), J. Wiley and Sons, Chichester, pp. 2061-2080.
12. Blöschl G. and Sivapalan M. (1995) *Scale issues in hydrological modelling: a review*, Hydrological Processes 9: 251-290.
13. Borga M., Boscolo P., Zanon F. and Sangati M. (2007) *Hydrometeorological analysis of the August 29, 2003 flash flood in the eastern Italian Alps*, J. Hydrometeorology, 8(5), 1049-1067.
14. Borga M., F. Tonelli, Moore R.J. and Andrieu H. (2002) *Long-term assessment of bias adjustment in radar rainfall estimation*, Water Resources Research, 38(11), 1226, doi:10.1029/2001WR000555.
15. Borga M., Gaume E. Creutin J.D. and L. Marchi (2008) *Surveying flash flood response: gauging the ungauged extremes*. 10.1002/hyp.7111, Hydrological Processes, 22(18), 3883-3885.
16. Borga, M., Dalla Fontana G. and Vezzani C. (2005) *Regional rainfall depth-duration-frequency equations for an alpine region*, Natural Hazards, 36, 221-235.

17. Borga, M., S. Degli Esposti and D. Norbiato, (2006) *Influence of errors in radar rainfall estimates on hydrological modelling prediction uncertainty*. Water Resources Research, 42, W08409, doi:10.1029/2005WR004559, 2006.
18. Bowers J.C. (2001) *Floods in Cuyama valley, California*, February 1998, U.S. geological survey Fact sheet FS-162-01.
19. Bundesamt für Wasserwirtschaft (1991) *Ursachenanalyse der Hochwasser 1987, Ergebnisse der Untersuchungen, Bundesamt für Wasserwirtschaft, Mitteilung des Landeshydrologie und -geologie Nr.14, Bern, Switzerland*.
20. Caredio F., D'Amato Avanzi G., Puccinelli A., Trivellini A., Venetutelli M. and Verani M. (1998) *La catastrofe idrogeologica del 19/6/1996 in Versilia e Garfagnana (Toscana, Italia): aspetti geomorfologici e valutazioni idrauliche*, Alba, 2, 75-88,
21. Carpenter T.M., Sperflage J.A., Georgakakos K.P., Sweeney T. and Fread D.L. (1999) *National threshold runoff estimation utilizing GIS in support of operational flash flood warning systems*, Journal of Hydrology, 224, 21–44.
22. Carter J.M., Williamson J.E. and Teller R.W. (2002) *The 1972 Black Hills-Rapid City flood revisited*, U.S. geological survey Fact sheet FS-037-02.
23. Chow V.T. (1959) *Open-channel hydraulics*, McGraw-Hill Book Company.
24. Collier C. (2007) *Flash flood forecasting: What are the limits of predictability?* Q. J. R. Meteorol. Soc. 133, 622A, 3-23.
25. Corral C., Berenguer M., Sánchez-Diezma R. and Sempere-Torres D. (2005) *The use of radar data for hydrological purposes in the Besòs catchment*, EGU General Assembly 2005, Vienna, Austria, 24-29 April 2005. Geophysical Research Abstracts, Vol. 7, 09763, 2005. SRef-ID: 1607-7962/gra/EGU05-A-09763.
26. Cosandey C. (1993) *La crue du 22 septembre 1992 sur le Mont Lozère*, Revue de géomorphologie dynamique, 2, 49-56.
27. Costa J.E. (1987) *Hydraulics and basin morphometry of the largest flash-floods in the conterminous United States*, Journal of Hydrology, 93, 313-338.
28. Costa J.E. (1987b) *A comparison of the largest rainfall-runoff floods in the united states with those of the people's republic of China and the world*, Journal of Hydrology, 96, 101-115.
29. Créton-Cazanave L., Lutoff C., Soubeyran O. (2008) *Alerte aux crues rapides : de l'utilité d'une nouvelle approche. Colloque « Vulnérabilités sociétales, risques et environnement : comprendre et évaluer », mai 2008 – L'Harmattan – à paraître*.
30. Creutin J.D., Muste M., Bradley A.A., Kim S.C. and Kruger A. (2003) *River gauging using PIV techniques: a proof of concept experiment on the Iowa River*, Journal of Hydrology, 227, doi:10.1016/S0022-1694(03)00081-7 .
31. Creutin, J.D. and Borga M. (2003) *Radar hydrology modifies the monitoring of flash flood hazard*, Hydrological Processes, 17, 7, 1453-1456, doi 10.1002/hyp.5122.
32. Creutin, J.D., M. Borga, C. Lutoff, A. Scolobig, I. Ruin and Creton-Cazanave, (2009) *Catchment dynamics and social response during flash floods: The potential of radar rainfall monitoring for warning procedures*. Meteorological Applications, in print.
33. Da Ros D. and Borga M. (1997) *Use of digital elevation model data for the derivation of the geomorphologic instantaneous unit hydrograph*, Hydrological Processes, 11, 13-33, 1997.
34. De Marchi B., Scolobig A., Delli Zotti G. and Del Zotto M. (2007) *Risk construction and social vulnerability in an Italian Alpine Region*. Report T11-07-12 of FLOODsite Project, <http://www.floodsite.net/html/publications2.asp?ALLdocs=on&Submit=View>.

35. Delrieu G., Ducrocq V., Gaume E., Nicol J., Payrastra O., Yates E., Andrieu H., Ayrat P-A., Bouvier C., Creutin J-D., Livet M., Anquetin S., Lang M., Neppel L., Obled C, Parent-du-Châtelet J., Saulnier G-M., Walpersdorf A. and Wobrock W. (2004) *The catastrophic flash-flood event of 8-9 September 2002 in the Gard region, France: a first case study for the Cévennes-Vivarais Mediterranean Hydro-meteorological Observatory*, Journal of Hydrometeorology, 6, 34-52.
36. Delrieu G., I. Braud, A. Berne, M. Borga, B. Boudevillain, F. Fabry, J. Freer, E. Gaume, E. Nakakita, A. Seed, P. Tabary and R. Uijlenhoet (2009) *Weather Radar and Hydrology*. Advances in Water Resources, 2009, in print
37. Denlinger R.P., O'Connell D.R.H. and House K.P. (2001) *Robust determination of stage and discharge: an example from an extreme flood on the Verde River, Arizona*, in *Ancient Floods modern hazard*, P.K. House, R.H. Webb, V.R. Baker and D.R. Levish editors, American geophysical union, Water science and application volume 5, 127-146.
38. Dodov, B. and Foufoula-Georgiou E. (2005) *Incorporating the spatio-temporal distribution of rainfall and basin geomorphology into nonlinear analyses of streamflow dynamics*, Advances in Water Resources, 28, 711-728.
39. Drobot S. and Parker D.J. (2007) *Advances and challenges in flash flood warnings*, Environmental Hazards 7, 173-178.
40. Duan, Q., Sorooshian S. and Gupta V.K. (1992) *Effective and efficient global optimization for conceptual rainfall-runoff models*, Water Resources Research 28(4), 265–284.
41. Fourquet G. (2005) *Développement d'un système hydrométrique par analyse d'images numériques, Evaluation d'une année de fonctionnement continu sur l'Isère à Saint Martin d'Hères*, Phd Thesis, INPG, Grenoble, France.
42. Franco M., Sánchez-Diezma R. and Sempere-Torres D. (2006) *Correction of the error related to the vertical profile of reflectivity: previous partitioning of precipitation types*. Fourth European Conference on Radar in Meteorology and Hydrology (ERAD), Barcelona.
43. Gaume E. (2006) *Post flash-flood investigations, methodological note*, FLOODsite report T23-06-02, available from <http://www.floodsite.net/html/publications2.asp?documentType=1>
44. Gaume E., Livet M., Desbordes M. and Villeneuve J-P. (2003a) *Hydrological analysis of the Avene river (France) extraordinary flood, 6 and 7 October 1997*, Physics and chemistry of the Earth, 28 (6-7), 263 - 267.
45. Gaume E., Ayrat P-A., Bouvier C., Creutin J-D, Delrieu G., Livet M. and O. Payrastra (2003b) *Hydrological analysis of the Gard river (France) extraordinary flood, 8 and 9 September 2002*, Proceedings of the 5rd EGS Plinius Conference, Ajaccio, France, Editrice 2003.
46. Gaume E., Livet M., Desbordes M. and Villeneuve J-P. (2004) *Hydrologic analysis of the Aude, France, flash-flood 12 and 13 november 1999*, Journal of Hydrology, 286, 135-154.
47. Gaume, E. and M. Borga (2008) *Post-flood field investigations in upland catchments after major flash floods: proposal of a methodology and illustrations*. J. Flood Risk Management, 1(4), 175-189, DOI: 10.1111/j.1753-318X.2008.00023.x; <http://dx.doi.org/10.1111/j.1753-318X.2008.00023.x>.
48. Gaume, E., Bain V., Bernardara P., Newinger O., Barbuc M., Bateman A., Blaškovičová L., Blöschl G., Borga M., Dumitrescu A., Daliakopoulos I., Garcia J., Irimescu A, Kohnova S., Koutroulis A., Marchi L., Matreata S., Medina V., Preciso E., Sempere-Torres D., Stancalie G., Szolgay J., Tsanis I., Velasco D. and Viglione A. (2008) *A collation of data on European flash floods*, Journal of Hydrology, conditionally accepted.
49. Georgakakos K. P. (1992) *Advances in forecasting flash floods*. In Proceedings of the CCNAA-AIT Joint Seminar on Prediction and Damage Mitigation of Meteorologically

- Induced Natural Disasters, 21-24 May 1992, National Taiwan University, Taipei, Taiwan, 280-293.
50. Georgakakos K. P. (2004) *Mitigating adverse hydrological impacts of storms on a global scale with high resolution, global flash flood guidance*, Abstracts Volume of International Conference on Storms/AMOS-MSNZ National Conference, 5–9 July. Australian Meteorological Society, Brisbane, Australia pp. 23-30.
 51. Georgakakos K. P. (2006) *Analytical results for operational flash flood guidance*, *Journal of Hydrology*, Vol 317 (1-2), 81-103, doi:10.1016/j.jhydrol.2005.05.009.
 52. Gilard O. and Mesnil J-J. (1995) *La crue de Vaison-la-Romaine du 22 septembre 1992*, Informations Techniques du CEMAGREF, 95, 1-8.
 53. Gutknecht D. (1994) *Extremhochwasser in kleinen Einzugsgebieten*, Österreichische Wasser und Abfallwirtschaft, 46 (3/4), 50-57.
 54. Hargreaves, G. H., and Samani, Z. A. (1982) *Estimating potential evapotranspiration*. J. Irrig. Drain. Div., 108, 225–230.
 55. Hemain J-C. and Dourlens C. (1989) *A propos des inondations catastrophiques de Nîmes*, La Houille Blanche, 6, 421-433.
 56. House P.K. and Pearthree P.A. (1995) *A geomorphologic and hydrologic evaluation of an extraordinary flood discharge estimate: Bronco Creek, Arizona*, Water Resources Research, 31 (12), 3059-3073.
 57. Huet P., Martin X., Prime J.L., Foin P., Laurain C. and Cannard P. (2003) *Retour d'expérience des Crues de Septembre 2002 dans les départements du Gard, de l'Hérault, du Vaucluse, des Bouches du Rhône, de l'Ardèche et de la Drôme.*, Rapport d'expertise, Ministère de l'environnement, 130p.
 58. Huet Ph. (2005) *La méthodologie des retours d'expériences après les accidents naturels, première tentative de codification, Rapport de l'inspection générale de l'environnement*, Ministère de l'écologie et du développement durable, Paris, France.
 59. International association for hydrological sciences (1974) *Flash-floods, proceedings of the Paris symposium*, September 1974, IAHS-UNESCO-WMO, Publication 112.
 60. Jarrett R.D. (1987) *Errors in slope-area computations of peak discharges in mountain streams*, Journal of Hydrology, 96, 53-67.
 61. Jarrett R.D. (1990) *Hydrologic and Hydraulic Research in Mountain Rivers*, Water Resources Bulletin, 26 (3), 419-429.
 62. Journel, A. G. (1983) *Non parametric estimation of spatial distributions*. Math. Geol., 15(3), 445-467, 1983.
 63. Juracek K.E., Perry Ch. A. and Putnam J.E. (2001) *The 1951 floods in Kansas revisited*, U.S. geological survey Fact sheet FS-041-01.
 64. Klemes V. (1986) *Operational testing of hydrological simulation models*, Hydrol. Sci. J., 31, 13-24.
 65. Kouwen, N. and Garland G. (1989) *Resolution considerations in using radar rainfall data for flood forecasting*, Can. J. Civ. Eng., 16, 279-289.
 66. Lebel, T., Bastin G., Obled C. and Creutin J. (1987) *On the Accuracy of Areal Rainfall Estimation: A Case Study*, Water Resour. Res., 23(11), 2123-2134.
 67. Lefrou C., Martin X., Labarthe J-P., Varret J., Mazière B., Tordjeman R. and Feunteun R. (2000) *Les crues des 12, 13 et 14 novembre 1999 dans les départements de l'Aude, de l'Hérault, des Pyrénées-Orientales et du Tarn, rapport de l'inspection générale de l'environnement*, Ministère de l'écologie et du développement durable, Paris, France.

68. Marchi, L., Cavalli M., Sangati M. and Borga M. (2009) *Hydrological controls and erosive response of a major debris flows triggered during a flash flood event*. Hydrological Processes, in print.
69. Martina M.L.V., Todini E. and Libralon A. (2006) *A Bayesian decision approach to rainfall thresholds based flood warning*, Hydrol. Earth Syst. Sci., 10, 413–426.
70. Menabde, M. and Sivapalan M. (2001) *Linking space–time variability of river runoff and rainfall fields: a dynamic approach*, Adv Water Resour.; 24:1001–14.
71. Meunier M. (1991) *Elements d'hydraulique torrentielle, Etudes Montagne n.1*, Cemagref, Antony, France.
72. Mogil H. M., Monro J. C. and Groper H. S. (1978) *NWS's flash flood warning and disaster preparedness programs*, Bulletin of the American Meteorological Society 59, 690-699.
73. Montz B.E. and Grunfest E. (2002) *Flash flood mitigation: recommendations for research and applications*, Environmental Hazards 4, 15–22.
74. Moore R.J. (1985) *The probability-distributed principle and runoff production at point and basin scales*, Hydrol. Sci. J., 30, 273-297.
75. Morin E., Georgakakos K. P., Shamir U., Garti R. and Enzel Y. (2002) *Objective, observations-based, automatic estimation of the catchment response timescale*. Water Resour. Res., 38 (10), 1212, doi:10.1029/2001WR000808.
76. Naden P.S. (1992) *Spatial variability in flood estimation for large catchments: the exploitation of channel network structure*, Hydrol. Sci. J, 37, 53-71.
77. Nash J.E. and Sutcliffe J.E. (1970) *River flow forecasting through conceptual models, Part I: a discussion of principles*, Journal of Hydrology 10, 282–290.
78. Naulet R. (2002) *Utilisation de l'information des crues historiques pour une meilleure prédétermination du risque d'inondation. Application au bassin de l'Ardèche à Vallon Pont-d'Arc et St-Martin d'Ardèche*, Thèse de l'Université Joseph Fourier, Grenoble, France.
79. Nicotina L., Alessi-Celegon E., Rinaldo A. and Marani M. (2008) *On the impact of rainfall patterns on the hydrologic response*, Water Resour. Res., in press.
80. Norbiato D., Borga M., Degli Esposti S., Gaume E. and Anquetin S. (2008) *Flash flood warning based on rainfall depth-duration thresholds and soil moisture conditions: An assessment for gauged and ungauged basins*. J. Hydrology, 274-290, 10.1016/j.jhydrol.2008.08.023.
81. Norbiato D., Borga M., Sangati M. and Zanon F. (2007) *Regional Frequency Analysis of Extreme Precipitation in the eastern Italian Alps and the August 29, 2003 Flash Flood*, J. Hydrology, 345, 3-4, 149-166, 2007.
82. Norbiato, D., M. Borga and R. Dinale, (2009) *Flash flood warning in ungauged basins by use of the Flash Flood Guidance and model-based runoff thresholds*. Meteorological Applications, in print.
83. Norbiato, D., M. Borga, R. Merz, G. Blöschl and A. Carton (2009) *Controls on event runoff coefficients in the eastern Italian Alps*. J. Hydrology, conditionally accepted.
84. Ntekos A. A., Krajewski W. F. and Georgakakos K. P. (2006) *On the uncertainties of flash flood guidance: Towards probabilistic forecasting of flash floods*, *Journal of Hydrometeorology*, 896–915.
85. O' Connor J.E. and Costa J.E. (2003) *Large floods in the United States: where they happen and why*, U.S. geological survey circular 1245.
86. Obled C., Wendling J. and Beven K. (1994) *Sensitivity of hydrological models to spatial rainfall patterns: An evaluation using observed data*, Journal of Hydrology, 159, 305-333.

87. Ogden F.L., Sharif H.O., Senarath S.U.S., Smith J.A., Baeck M.L. and Richardson J.R. (2000) *Hydrologic analysis of the Fort Collins, Colorado flash-flood of 1997*, Journal of Hydrology, 228, 82-100.
88. Ogden F.L. and Julien P.Y. (1994) Runoff model sensitivity to radar rainfall resolution, *Journal of Hydrology*, 158, 1-18.
89. Orlanski I. (1975) *A rational subdivision of scales for atmospheric processes*, Bull. Am. Meteorol. Soc., 56(5), 527-530.
90. Pardé M. (1961) *Sur la puissance des crues en diverses parties du monde*, Geographica, Zaragoza, Spain.
91. Payrastre O., Gaume E. and Andrieu H. (2005) *Use of historical data to assess the occurrence of floods in small watersheds in the French Mediterranean area*, Advances in Geosciences, 2, 313-320.
92. PC FVG - PROTEZIONE CIVILE DELLA REGIONE AUTONOMA FRIULI VENEZIA GIULIA (2004) *Alluvione 29 agosto 2003: Stato degli interventi*, IV Commissione Protezione Civile.
93. Pegram G.G.S. and Clothier A.N. (2001) *High Resolution Space-Time Modelling of Rainfall: The "String of Beads" Model*. Journal of Hydrology, Vol 241. pp: 26-41.
94. Perry C. A. (2000) *Significant floods in the united states during the 20th century - USGS measures a century of floods*, USGS Fact sheet FS-024-00.
95. Reed S., Schaake J. and Zhang Z. (2007) *A distributed hydrologic model and threshold frequency-based method for flash flood forecasting at ungauged locations*, Journal of Hydrology, 337 (3), p.402-420.
96. Ricard D., Ducrocq V., Bresson R. and Auger L. (2007) *Mesoscale environment associated with mediterranean heavy precipitating events*. 12th Conference on Mesoscale Processes, 7p.
97. Rico M., Benito G. and A. Barnolas (2001) *Combined paleoflood and rainfall-runoff assessment of mountain floods (Spanish Pyrenees)*, Journal of Hydrology, 245, 59-72.
98. Ruin I., Creutin J.-D., Anquetin, S. and C. Lutoff (2008) *Human exposure to flash-floods – relation between flood parameters and human vulnerability during a storm of September 2002 in Southern France*, Journal of Hydrology, doi: 10.1016/j.jhydrol.2008.07.044
99. Sächsisches Landesamt für Umwelt und Geologie (2004) *Hochwasser August 2002 in den Osterzgebirgsflüssen, Ereignisanalyse*, Technical report, Dresden, Germany.
100. Sangati M. and Borga M., (2009) *Influence of rainfall spatial resolution on flash flood modelling*. Natural hazards and Earth System Sciences, conditionally accepted.
101. Sangati M., Borga M., Rabuffetti D. and R. Bechini, (2009) *Influence of rainfall and soil properties spatial aggregation on extreme flash flood response modelling: an evaluation based on the Sesia river basin, North Western Italy*. Advances Water Resources, in print.
102. Segond M.L., Wheeler H.S. and Onof C., (2007) *The significance of spatial rainfall representation for flood runoff estimation: A numerical evaluation based on the Lee catchment*, UK. Journal of Hydrology, 347, 116-131.
103. Siccardi F., Boni G., Ferraris L. and Rudari R. (2005) *A hydrometeorological approach for probabilistic flood forecast*, J. Geophys. Res., 110, D05101, doi:10.1029/2004JD005314.
104. Sivapalan M., Jothityangkoon C. and Menabde M. (2002) *Linearity and nonlinearity of basin response as a function of scale: Discussion of alternative definitions*, Water Resour. Res., 38(2), 10.1029/2001WR000482.
105. Smith J.A., Baeck M.L., Steiner M. and Miller A.J. (1996) *Catastrophic rainfall from an upslope thunderstorm in the central Appalachians: the Rapidan storm of June 27, 1995*, Water Resources Research, 32 (10), 3099-3113.

106. Smith M.B., Seo D.J., Koren V.I., Reed S.M., Zhang Z., Duan Q., Moreda F. and Cong S., (2004) *The distributed model intercomparison project (DMIP): motivation and experiment design*, Journal of Hydrology, 298, 4-26.
107. Soil Conservation Service (1973) *A method for estimating volume and rate of runoff in small watersheds*, Technical paper 149. Washington.
108. U.S. Department of Agriculture (1986) *Urban hydrology for small watersheds*, U.S. Department of Agriculture Tech. Release 55, 164 pp.
109. Velasco-Forero C., Sempere-Torres D., Sánchez-Diezma D., Cassiraga E., Gómez-Hernández J. J. (2007) *Blending radar and raingauge data in real time: effects of the raingauge network density on the quality of estimates*. 33rd Conference on Radar Meteorology, AMS, Cairns, Australia, 6-10 August 2007.
110. Velasco-Forero C., Schröter K., Sempere-Torres D. and Ostrowski M. (2007a) *Effects of rainfall-runoff model structure and rainfall spatial model on hydrological flood forecasting*. EGU General Assembly 2007, Vienna, Austria, 15-20 April 2007. Geophysical Research Abstracts, Vol. 9, 10303, 2007, SRef-ID: 1607-7962/gra/EGU2007-A-10303.
111. Webb R.H. and Jarrett R.D. (2002) *One-dimensional estimation techniques for discharges of paleoflood and historical floods*, in *Ancient floods modern hazards, Principles and application of paleoflood hydrology*, American Geophysical Union, Water science and application 5.
112. Winchell M., Gupta H. and Sorooshian S. (1998) *On the Simulation of Infiltration- and Saturation-Excess Runoff Using Radar-Based Rainfall Estimates: Effects of Algorithm Uncertainty and Pixel Aggregation*, Water Resour. Res., 34(10), 2655-2670.
113. Winston W.E. and Criss R.E. (2002) *Geochemical variations during flash-flooding, Meramec River basin, May 2000*, Journal of hydrology, 265, 149-163.
114. Woods R.A. and Sivapalan M. (1999) *A synthesis of space-time variability in storm response: Rainfall, runoff generation and routing*, Water Resour. Res. , 35(8), 2469-2485.
115. Younis, J., Anquetin S. and Thielen J. (2008) *The benefit of high-resolution operational weather forecasts for flash-flood warning*, Hydrology and Earth System Sciences and Discussion, 5, 345-377.
116. Zhang Y., Smith J. A. and Baeck M. L. (2001) *The hydrology and hydrometeorology of extreme floods in the Great Plains of eastern Nebraska*, Adv. Water Resour., 24, 1037-1050.
117. Zhang Z., Wagener T., Reed P. and Bhushan R. (2008) *Reducing uncertainty in predictions in ungauged basins by combining hydrologic indices regionalization and multiobjective optimization*. Water Resour. Res., 44, W00B04, doi:10.1029/2008WR006833.